Role of G-protein $G_{12/13}$ signaling in angiogenesis

Dissertation for attaining

the PhD degree of Natural Sciences

submitted to the Faculty 15

of the Johann Wolfgang Goethe University

in Frankfurt am Main

by

Kishor Kumar Sivaraj

from The Nilgiris, INDIA

Max-Planck-Institute for Heart and Lung Research

Bad Nauheim (2013)

(D 30)

accepted by the Faculty 15 of the

Johann Wolfgang Goethe University as a dissertation.

Dean: Prof. Dr. Anna Starzinski-Powitz

Expert assessor: Prof. Dr. Nina Wettschureck, Prof Dr. Amparo Acker-Palmer

Date of the disputation:

Acknowledgements

Apart from the efforts of myself, the success of my thesis depends largely on the encouragement and guidelines of many others. I take this opportunity to express my gratitude to the people who have been instrumental in the successful completion of my thesis.

First and foremost, I would like to show my greatest appreciation to Prof. Dr. Nina Wettschureck and Prof. Dr. Stefan Offermanns. I can't thank enough for their tremendous support and help they have given right from the beginning till date. I feel motivated and encouraged every time I attend the meeting. Without their encouragement and guidance this project would not have materialized.

I would like to express my deepest appreciation to my PhD thesis committee chair Prof. Dr. Amparo Acker-Palmer and the Dean Prof. Dr. Anna Starzinski-Powitz, Department of Biological Sciences (F15), Goethe university, Frankfurt am main, Germany.

I consider it an honor to work with Dr. Mikito Takefuji, Dr. Till Althoff and Myriam Grimm, who gave healthy scientific discussions and suggestions in the initial days.

I would also like to extend my thanks to the technicians of the laboratory for their help rendered to me in appropriate time.

The guidance and support received from all my lab members, this was vital for the success of the thesis. I am grateful for their constant support and help.

I owe my deepest gratitude to thank my parents, sister and friends for having given me constant mental support and confidence to achieve this level.

CONTENTS

Contents

1. ABBREVIATIONS

°C	Degree celsius
µ	Micro
bFGF	Basic fibroblast growth factor
B16	B16/F10 Mouse Melanoma cell line
Cdc42	Cell division cycle 42
CXCR4	CXC-motif chemokine receptor-4
Dll4	Delta-like 4
DMEM	Dulbecco's modified Eagle's medium
D-PBS	Dulbecco's phosphate buffer saline
E	Embryonic day
EC	Endothelial cell
EGFR	Epidermal growth factor receptor
Eph	Erythropoietin-producing hepatocellular
Ephrin	Eph family receptor interacting protein
eNOS	Endothelial nitric oxide synthase
ERK1/2	Extracellular-signal-regulated kinase-1/2
FAK	Focal adhesion kinase
FBS	Fetal bovine serum
Flt-1	Fms-related tyrosine kinase 1
Gα	G-protein α subunit
Gβγ	G-protein βγ subunit
GAP	GTPase-activating proteins
GEF	Guanine nucleotide exchange factor

1.Abbreviations

GPCR	G-protein coupled receptors
GPI	Glycosylphosphatidylinositol
H	Hour
HBSS	Hank's buffered salt solution
HEK	Human embryonic kidney
HIF1α	Hypoxia-inducible factor 1, alpha subunit
HUVEC	Human umbilical vein endothelial cells
Ig	Immunoglobulin
KO	Knockout
Kd	Knockdown
LB	Luria-Bertani
LLC1	Lewis lung carcinoma
LPA	Lysophosphatidic acid
M	Molar
m	Milli
MAPK	Mitogen-activated protein kinase
Min	Minute
N	Nano
NF-κB	Nuclear factor kappa B
NO	Nitric oxide
NICD	Notch intracellular domain
Nrp	Neuropilin
P	Postnatal day
PAK	p21-activated kinase
PAR	Protease-activated receptor

PCR	Polymerase chain reaction
PDGFβ	Platelet-derived growth factor beta
PFA	Paraformaldehyde
pH	Potential hydrogenii
PI3K	Phosphoinositol 3-kinase
PKC	Protein kinase C
PLC-γ	Phospholipase C-γ
PlGF	Placenta growth factor
Plxn	Plexin
PtdIn	Phosphatidylinositol
Rac1	RAS-related C3 botulinum substrate-1
RhoA	Ras homolog gene family: member-A
RTK	Receptor tyrosine kinase
S1P	Sphinogosine-1-phosphate
SDF1	Stromal-derived factor-1
Sema	Semaphorin
SRF	Serum response factor
TGFβ	Transforming growth factor-beta
TIE2	Tunica internal endothelial cell kinase-2
TNFα	Tumor necrosis factor alpha
TSP1	Thrombospondin-1
Tyr	Tyrosine
Unc5b	Uncoordinated-5 homolog-B
VEC	Vascular endothelial cadherin
VEGF	Vascular endothelial growth factor

VEGFR Vascular endothelial growth factor receptor

2. SUMMARY

Angiogenesis, the formation of new blood vessels from existing ones, is a fundamental biological process required for embryonic development; it also plays an important role during postnatal organ development and various physiological and pathological remodeling processes in the adult organism. Vascular endothelial growth factor (VEGF) and its main receptor, VEGF receptor-2 (VEGFR-2), play a central role in angiogenesis. VEGFR-2 expression is strongly upregulated in angiogenic vessels, but the mechanisms regulating VEGFR-2 expression are not well understood. We found in this study that the G-protein α subunit $G\alpha_{13}$ plays an important role in the regulation of VEGFR-2 expression. In vitro, we found that knockdown of $G\alpha_{13}$ reduced VEGFR-2 expression in human umbilical vein endothelial cells and impaired responsiveness to VEGF-A. This phenotype was rescued by adenoviral normalization of VEGFR-2 expression. $G\alpha_{13}$-dependent VEGFR-2 expression involved activation of the small GTPase RhoA and transcription factor NF-κB; it was abrogated by deletion of the NF-κB binding site at position -84 of the VEGFR-2 promoter. In vivo, endothelial cell-specific loss of $G\alpha_{13}$ resulted in reduced VEGFR-2 expression, impaired responsiveness towards VEGF-A in Matrigel assays, and reduced retinal angiogenesis. Importantly, also tumor vascularization was diminished in the absence of endothelial $G\alpha_{13}$, resulting in reduced tumor growth. Taken together, we identified $G\alpha_{13}$-dependent NF-κB activation as a new pathway underlying the transcriptional regulation of VEGFR-2 during retinal and tumor angiogenesis.

3. INTRODUCTION

3.1 Vasculogenesis and angiogenesis

Blood vessels provide organs with oxygen and nutrients and support tissue growth and repair. Blood vessels can be devided into three functional groups: Arteries and arterioles transport blood from the heart to the periphery, capillaries allow the exchange of water and chemicals between blood and tissues, venules and veins carry blood back to the heart. During embryonic development blood vessels are generated de novo ("vasculogenesis") or by sprouting from existing vessels ("angiogenesis"). Also during postnatal life the generation of new vessels is of crucial importance, for example in organ growth or wound healing. Imbalances in angiogenesis contribute to the pathogenesis of numerous disease states, for example ischemic diseases and cancer. Both under physiological and pathological conditions the major driving force of angiogenesis are the endothelial cells (ECs), which line the inner surface all types of vessels.

3.1.1 Vessel formation

The de novo formation of embryonic blood vessels is one of the earliest events in organogenesis. In the mammalian embryo, the yolk sac develops by aggregation, differentiation and migration of angioblasts (mesodermal–derived endothelial progenitors) into a primitive capillary plexus by a process called "vasculogenesis". From this primitive plexus, new blood vessels form by angiogenesis, a process that involves

ECs sprouting, migration, and proliferation and leads to the formation of a functional vascular system (Coultas et al., 2005). The vascular system is a hierarchically organized structure consisting of arteries, veins, and capillaries (Adams and Alitalo, 2007; Gaengel et al., 2009). ECs undergo either arterial or venous fate in response to a combination of different cellular and molecular mechanisms **(Figure 3-1)**, and some of the ECs in emryonic veins further differentiate into lymphatic vessels. EC proliferation, lumen formation and the recruitment of mural cells such as pericytes and smooth muscle cells are further steps required for vessel remodeling and maturation.

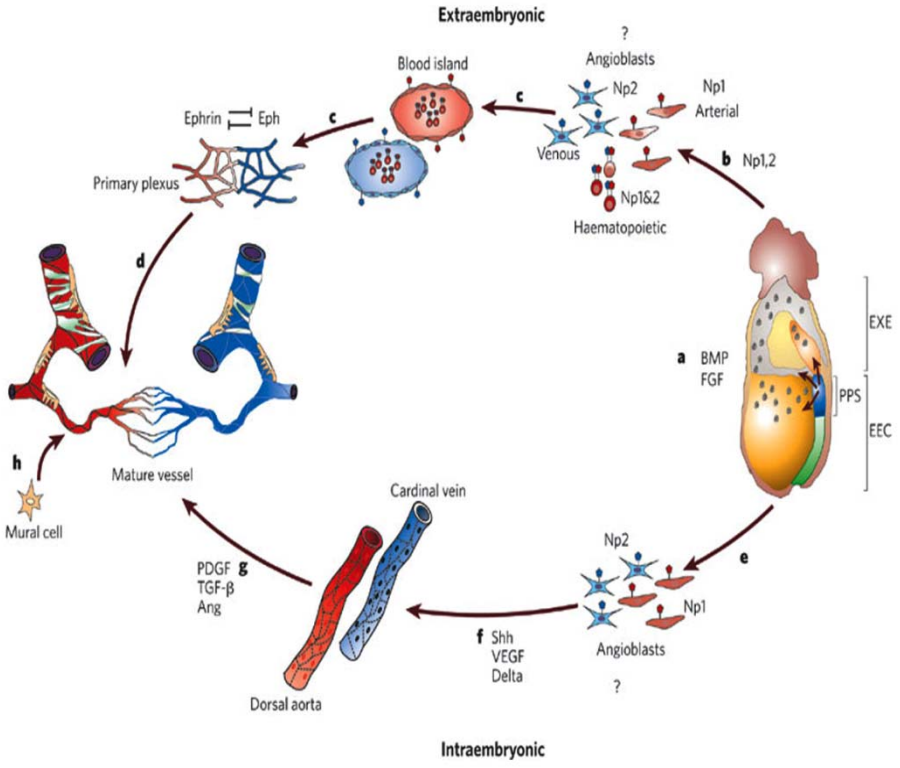

Figure 3-1: Formation of vascular system.

a, Vascular progenitors appear in the posterior primitive streak (PPS). **b**, Vascular progenitors (Flk1-positive) cells in the primitive streak give rise to both blood and endothelium (haemangioblasts), but are restricted to haematopoietic or angiogenic fate after emigrating into extra-embryonic sites (extra-embryonic ectoderm (EXE), yolk sac and allantois) and intra-embryonic sites (embryonic ectoderm (EEC)). **c**, In the yolk sac, these progenitors aggregate into endothelial-lined blood islands that then fuse to

generate a primary capillary plexus. **d**, The primary capillary plexus undergoes remodelling along with intra-embryonic vessels to form a mature circulation. **e**, Intra-embryonic angioblasts migrate along distinct pathways before (**f**) aggregating directly into the dorsal aorta or cardinal vein, without a plexus intermediate. **g**, The primary vessels (capillary plexus, dorsal aorta and cardinal vein) then remodel, together with the extra-embryonic plexus, to form a mature vasculature **h**, Mural cells (pericytes and smooth-muscle cells) proliferate and differentiate and are recruited to vessels. Ang, angiopoietin; Eph, Eph receptor family; Shh, sonic hedgehog; Np, neuropilin. Model is adapted from (Coultas et al., 2005).

3.1.2 Cellular and molecular mechanisms of angiogenesis

Angiogenesis is a complex process that requires sequential steps of EC behavior. In normal vessels, ECs form a quiescent monolayer that lines the inner surface of the blood vessel. In response to an angiogenic stimulus, ECs switch their behavior from quiescent to angiogenic (Coultas et al., 2005). This transition involves the following steps: First, ECs lose their adhesion junctions and sprout towards to the angiogenic stimulus. Second, ECs and tissue microenvironment release proteases that degrade the surrounding basement membrane. Third, EC proliferation, lumen formation and remodeling leads to the formation of a functional blood vessel. Each of these phases is controlled by different cellular and molecular mechanisms **(Figure 3-2)** (Adams and Alitalo, 2007; Carmeliet, 2003; Cleaver and Melton, 2003; Potente et al., 2011).

Numerous studies in fish and mice revealed the central importance of EC-specific signaling cascades in angiogenesis, for example of vascular endothelial growth factors (Vegfs), Vegf receptors (Vegfrs) or components of the angiopoietin/Tie signaling cascde (Maisonpierre et al., 1997). In addition also other, more widely used signaling pathways have been implicated in angiogenesis, such as platelet-derived growth factor (Pdgf)

(Lindahl et al., 1997), transforming growth factor-β (Tgf-β)(Chen and Lechleider, 2004), G-protein coupled receptors (GPCRs) (Kuhnert et al., 2010; Liu et al., 2000), Integrin (Reynolds et al., 2009; Zovein et al., 2010) and Notch signaling (Lawson et al., 2001).

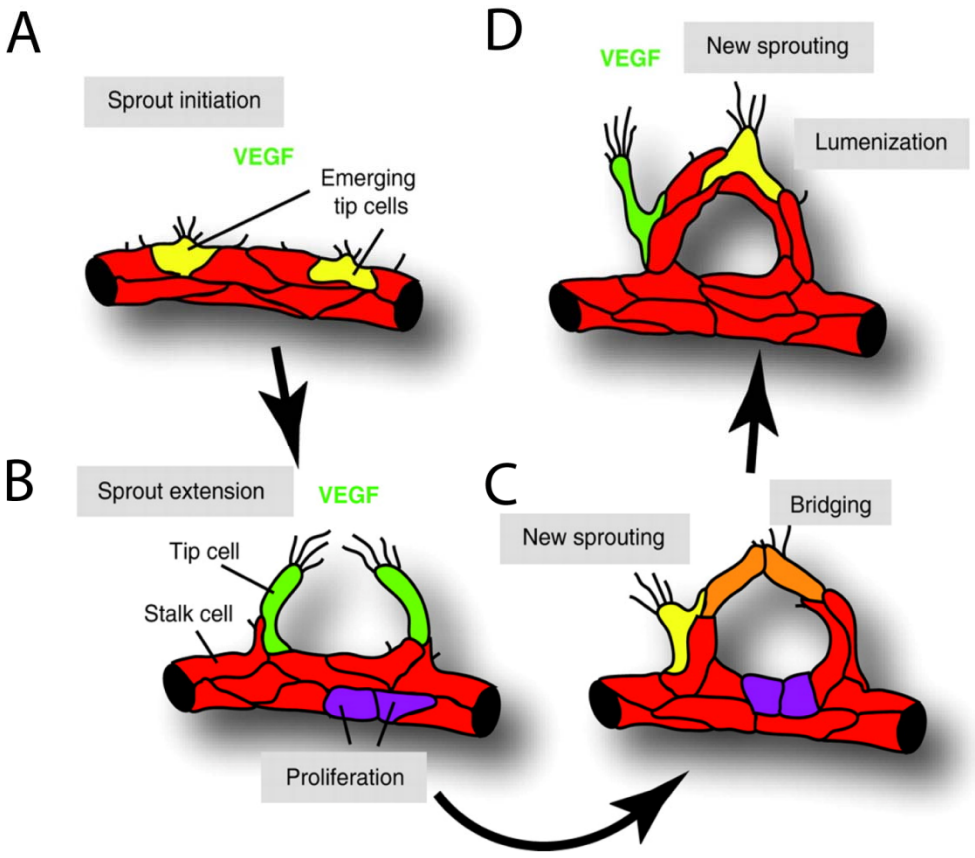

Figure 3-2: Angiogenic sprouting and blood vessel growth.

A, ECs initiate sprouting in response to tissue-derived angiogenic signals such as VEGF. **B,** A fraction of cells (shown in yellow and green) extends long filopodia and acquires motile and invasive behavior. These tip cells lead and guide new sprouts, whereas other ECs (shown in red) form the sprout stalk or stay behind to maintain tissue perfusion. **C,** At some point during sprout extension, tip cells will contact other tip cells or vessels to establish new connections. These cell bridges (orange) are converted into new blood-carrying vessels. **D,** Simultaneously, new sprouting is initiated at other sites (yellow and green cells) and additional ECs are generated by proliferation (purple). Scheme is adapted from (Adams and Eichmann, 2010).

3.1.3 Vascular endothelial growth factors and their receptors

Vascular endothelial growth factors (VEGFs) and their receptors are essential regulators of vascular development during vasculogenesis and angiogenesis, and also were identified as vascular permeability factors (VPF). The VEGFs bind to three tyrosine kinase receptor (RTKs), known as VEGF receptor-1 (VEGFR-1/Flt-1), VEGFR-2/KDR/Flk-1 and VEGFR-3/Flt-4 (**Figure 3-3)**.

VEGF-A can act on endothelial cells in both an autocrine and paracrine manner. Under homeostatic conditions, Vegf is released from ECs themselves and contributes to EC survival (Coultas et al., 2005). Under conditions of hypoxia or low pH, VEGF is upregulated in non-endothelial cells (e.g., myeloid cells, stromal cells, or tumor cells) and acts on ECs to induce the angiogenic switch. The expression of VEGF-A is regulated by hypoxia-inducible factor (HIF) (Germain et al., 2010) leading to increased expression during tissue growth both in physiological (wound healing, embryonic development) and in pathological (cancer) process. Disruption of even a single allele of the VEGF-A gene in mice results in embryonic lethality due to severe vascular defects (Ferrara et al., 1996).

VEGF-C is a ligand of the receptors VEGFR-2 and VEGFR-3. While VEGFR-2 is the key regulator of both pre- and postnatal angiogenesis, VEGFR-3 is necessary for the formation of the blood vasculature during early embryogenesis (Tammela et al., 2008), but later becomes a key regulator of lymphangiogenesis (Alitalo, 2011). PlGF is homologous to VEGF and also acts as an angiogenic factor (Fischer et al., 2008).

Deficiency of VEGF-B in mice does not impair angiogenesis in normal development. VEGF-B has only restricted angiogenic activity in certain tissues such as the heart, yet it promotes neuronal survival and induces metabolic effects (Fischer et al., 2008).

The VEGFR-1 (Flt-1) receptor is widely expressed, but its role in angiogenesis remains elusive. VEGFR-1 kinase activity is poor and not required for endothelial cell function. VEGFR-1 exists both as a membrane-anchored form and as a soluble secreted form (sFlt-1). sFlt-1 acts as a decoy for VEGF, thereby reducing the amount of free VEGF available for VEGFR-2 activation; loss of VEGFR-1 therefore results in vessel overgrowth (Fischer et al., 2008).

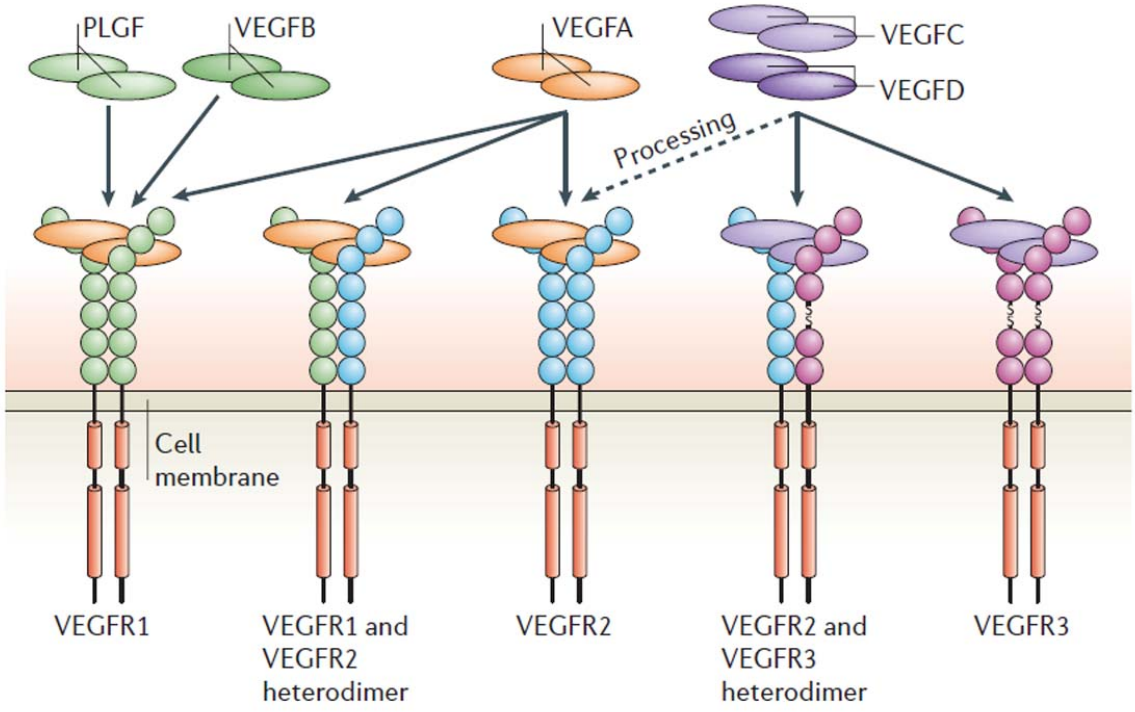

Figure 3-3: vascular endothelial growth factors (VEGFs) and receptors (VEGFR)

Vascular endothelial growth factors (VEGFs) bind to the three VEGF receptor (VEGFR) tyrosine kinases, leading to the formation of VEGFR homodimers and heterodimers.

Proteolytic processing of VEGF-C and -D allows for binding to VEGFR-2. From (Olsson et al., 2006).

VEGFR-2, also known as KDR (kinase insert domain receptor) in humans or Flk-1 (fetal liver kinase-1) in mice, is the main receptor for VEGF-A; its signaling induces endothelial cell sprouting, proliferation and migration during angiogenesis (Coultas et al., 2005). VEGFR-2 is expressed most prominently in vascular endothelial cells and their embryonic precursors, with highest expression levels during embryonic vasculogenesis and angiogenesis (Millauer et al., 1993; Oelrichs et al., 1993; Quinn et al., 1993), and also during pathological processes such as tumor angiogenesis (Millauer et al., 1994; Plate et al., 1993). VEGF signaling promotes VEGFR-2 receptor dimerization, which in turn allows trans/autophosphorylation of intracellular tyrosine residues. VEGF-A induced VEGFR-2 activation leads to the phosphorylation of several proteins like phospholipase C-γ (PLC-γ), PI-3 kinase (PI3K), Ras GTPase-activating protein and the Src family. VEGF induced EC growth and survival is controlled by the Raf-Erk and PI3K–Akt pathway signaling cascades (Cleaver and Melton, 2003; Coultas et al., 2005; Herbert and Stainier, 2011). VEGF-A can induce VEGFR-2 endocytosis, this process can activate several downstream signaling such as ERK1/2, Rac and Akt (Eichmann and Simons, 2012). High levels of VEGFR-2 endocytosis were observed at the angiogenic front ECs (tip and stalk cells), this process is controlled by ephrin-B2, Dab-2 and the PAR-3 protein complex. In mice, loss of VEGFR-2 causes lethality of the knockout embryo at E8.5 to 9.0 due to a defect in the formation of blood islands (Carmeliet et al., 1996; Ferrara et al., 1996; Shalaby et al., 1995), a phenotype similar to that of VEGF-A-deficient mice.

The VEGFR-3 (Flt4) receptor is activated by VEGF-C and VEGF-D. VEGFR-3 is a critical regulator of lymphogenesis. VEGFR-3 is expressed both in lymph ECs in the adult and in vascular ECs during development. In addition, VEGFR-3 is upregulated during developmental and tumor angiogenesis. VEGFR-3 knockout mice die at E10.0-11.0 because of cardiovascular remodeling defects (Dumont et al., 1998). Selective blockade of VEGFR-3 signaling in endothelial cells affected retina and tumor angiogenesis (Tammela et al., 2008). Functional loss of VEGFR-3 in humans causes lymphedema.

3.1.4 Retinal for angiogenesis model

At birth, the murine retina is avascular and receives oxygen and nutrients from adjacent hyaloid vessels. During the early postnatal period a highly organized retinal vasculature develops: From postnatal days P1 to P7 a single superficial layer of vessels grows from the center towards the periphery (the superficial layer), followed by the formation of the deep retinal plexus and vessel remodeling (Gariano and Gardner, 2005).

During retinal sprouting angiogenesis, specialized ECs called tip cells extended filopodia towards to angiogenic signal. EC sprouting is regulated by Notch and VEGF signaling pathways. High levels of VEGF signaling in tip cells, induced expression of Notch ligand Dll4. This leads to Notch activation in adjacent stak cell and the supression of VEGFR-2/VEGFR-3 expression (Roca and Adams, 2007).

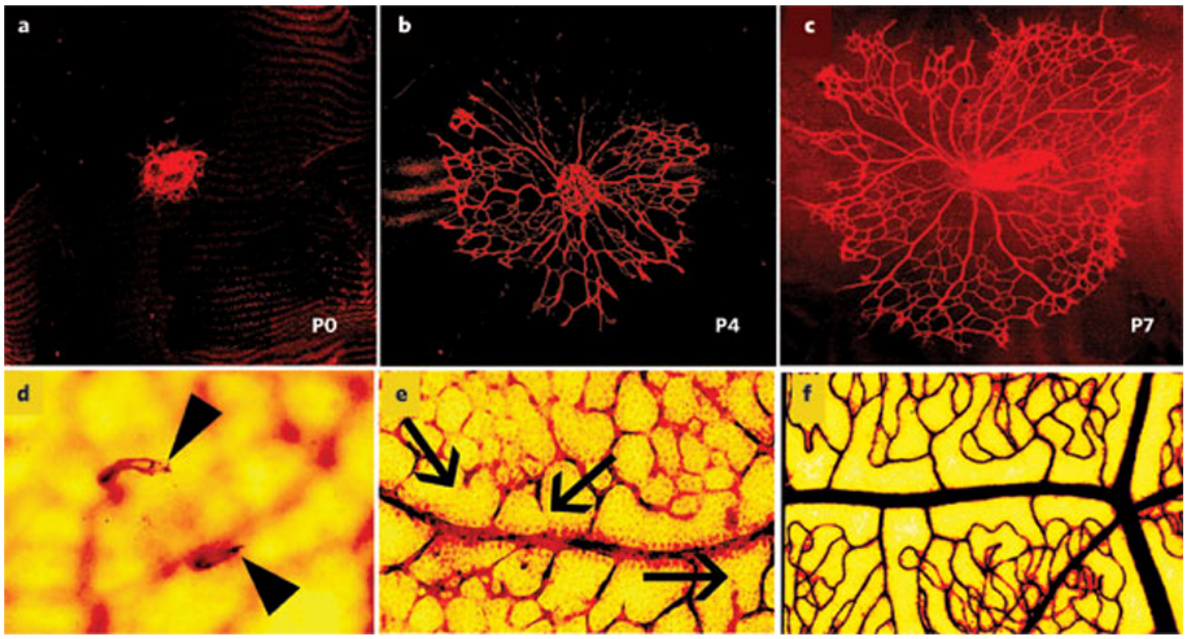

Figure 3- 4 : Mouse model of retinal angiogenesis

a–c In mice, retinal vessels (red) start growing next to the optic nerve around birth (P0), then extend radially in the superficial retina over 7–10 days to reach the periphery. **d**, In, The deeper capillary network forms by endothelial sprouting (arrowheads) from the previously formed superficial vascular network (blurred, in background). **e**, Shortly after retinal vessels have formed, capillary segments adjacent to nascent arteries (arrows) retract, to yield a periarterial capillary-free zone. Scheme is adapted from (Gariano and Gardner, 2005).

The vascularization of the murine retina has become one of the best established models to study postnatal angiogenesis. Most importantly, it is possible to activate and inactivate gene of interest in the retinal vasculature at specific cell type and different time points. Furthermore, it is possible to test the effects of pharmacological compound on retinal angiogenesis in vitro or after intraocular injection (Pitulescu et al., 2010; Sawamiphak et al.,2010).

3.1.5 Tumor angiogenesis

Pathological angiogenesis is a hallmark of solid tumors since tumors cannot grow beyond a critical size without formation of new blood vessels (Carmeliet, 2003; Ferrara and Kerbel, 2005). Tumor induced angiogenesis is regulated by tumor cells and the tumor microenvironment. In response to hypoxia or low pH, tumor cells and stromal cells release angiogenic factors that promote ECs survival, proliferation and migration. Also other factors such as mechanical stress or local inflammatory responses contribute to the angiogenic switch in ECs **(Figure 3-4) (**Bergers and Benjamin, 2003, Hanahan and Weinberg, 2000).

Tumor vessels develop by sprouting or intussusception from pre-existing vessels. The tumor vasculature is highly disorganized due to an imbalance of angiogenic signals. Tumor ECs show an increased expression of angiogenic genes, for example VEGFRs, FGFRs and Notch, leading to further enhancement of angiogenic signals. Therefore, tumor vessels show increased branching, uneven diameter and shunts (Jain, 2001). Tumor blood flow is chaotic and variable and leads to hypoxic and acidic regions. These conditions favor the survival of hypoxia-resistant tumor cells, which often also show higher malignancy and invasiveness (Jain, 2005). Tumor vessels are highly permeable, their vessel walls have numerous 'openings' and a discontinuous or absent basement membrane. In addition, the tumor ECs are abnormal in shape, growing on top of each other and projecting into the lumen. These defects make tumor vessels leaky and promote metastasis.

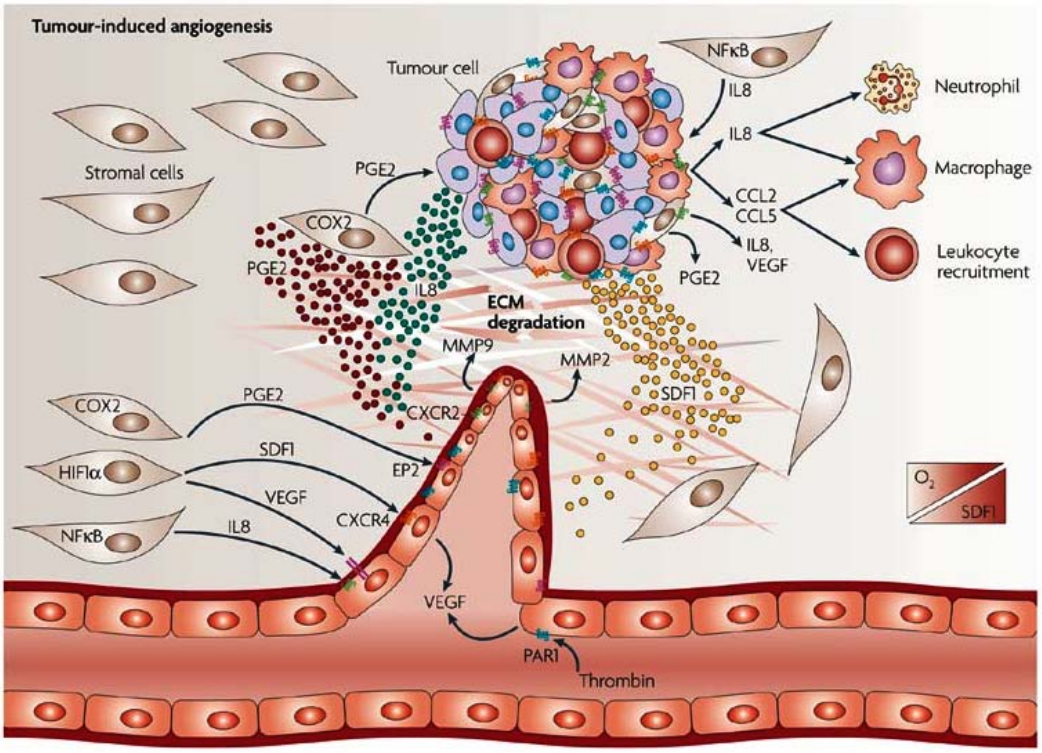

Figure 3-5: Mechanism of tumor angiogenesis

As tumors increase their need for oxygen and nutrients, they reprogramme the transcriptional profile of tumor and stromal cells to release factors that disrupt the endothelial monolayer and extracellular matrix (ECM), and promote survival, proliferation and migration of endothelial cells. From (Dorsam and Gutkind, 2007).

Vascular permeability and angiogenesis depend on the type of tumor and the host organ where the tumor is growing, because each organ has different stromal cells, which produce different pro- and anti-angiogenic molecules (Jain, 2005). Since solid tumor growth depends on angiogenesis, blocking angiogenesis has been proposed as a strategy to arrest tumor growth (Folkman, 1971). Most of the anti-angiogenic therapies currently available target VEGF and receptor tyrosine kinase (RTK) signaling pathways. While bevacizumab, a monoclonal antibody that specifically binds to VEGF, blocks the binding of VEGF to its receptor, Sorafenib and Sunitinib block several RTKs and their

signaling pathways (Ferrara and Kerbel, 2005). These therapies have shown limited and transient efficiency due to initial or acquired resistance (Bergers and Hanahan, 2008).

3.2 G-protein mediated signaling

Transmembrane signaling is a fundamental process that allows cells to communicate with each other or to respond to changes in the external milieu. All transmembrane signaling systems share two basic elements, a receptor that is able to receive signals from extracellular stimuli, and an effector that activates an intracellular signaling pathway (Oldham and Hamm, 2006).

3.2.1 G-protein coupled receptor (GPCR)

More than 800 GPCRs (approximately 2% of all genes) are encoded in the mammalian genome (Dorsam and Gutkind, 2007; Ritter and Hall, 2009). GPCRs represent the largest family of cell surface molecules involved in signal transmission (Bjarnadottir et al., 2006). While most of them code for sensory receptors like taste or olfactory receptors, approximately 400 of them recognize non-sensory ligands (Ritter and Hall, 2009; Wettschureck and Offermanns, 2005). GPCRs are activated by many agonists and control key physiological functions such as neurotransmission, hormone and enzyme release from endocrine and exocrine glands, immune responses, cardiac and smooth muscle contraction as well as blood pressure regulation. Their dysfunction

contributes to some of the most prevalent human diseases, as reflected by the fact that GPCRs represent the target, directly or indirectly, of 50–60% of all current therapeutic agents (Dorsam and Gutkind, 2007; Lappano and Maggiolini, 2011; Wettschureck and Offermanns, 2005).

For most GPCRs the physiological ligands are known; those for which no endogenous ligand has been found are termed ‘orphan’ receptors. GPCRs are regulated by many agonists, but all share a characteristic core composed of seven transmembrane α-helices that weave in and out of the membrane (Pierce et al., 2002). Upon activation by its endogenous ligand, the receptor exposes intracellular sites involved in the interaction with the G-protein heterotrimer, which consists of an α, a β and a γ subunit. This catalyzes the dissociation of GDP bound from the Gα subunit and its replacement with GTP, and leads to dissociation of Gα from Gβγ subunits. Both Gα-GTP subunits and Gβγ subunit complexes then stimulate several downstream effectors. Ultimately, the G-protein coupling specificity of each receptor determines the nature of its downstream signaling targets (Neves et al., 2002).

3.2.2 Principle of G-protein mediated signaling

The G-protein mediated signaling system allows convergence and divergence at the interfaces of receptor as well as G-proteins and effector. G-protein mediated transmembrane signaling is a relatively complex system that provides the basis for a huge variety of signaling pathways tailored to serve particular functions in distinct cell

types (Wettschureck and Offermanns, 2005). A schematic overview over the processes in G-protein activation and deactivation is shown in Figure 3-6.

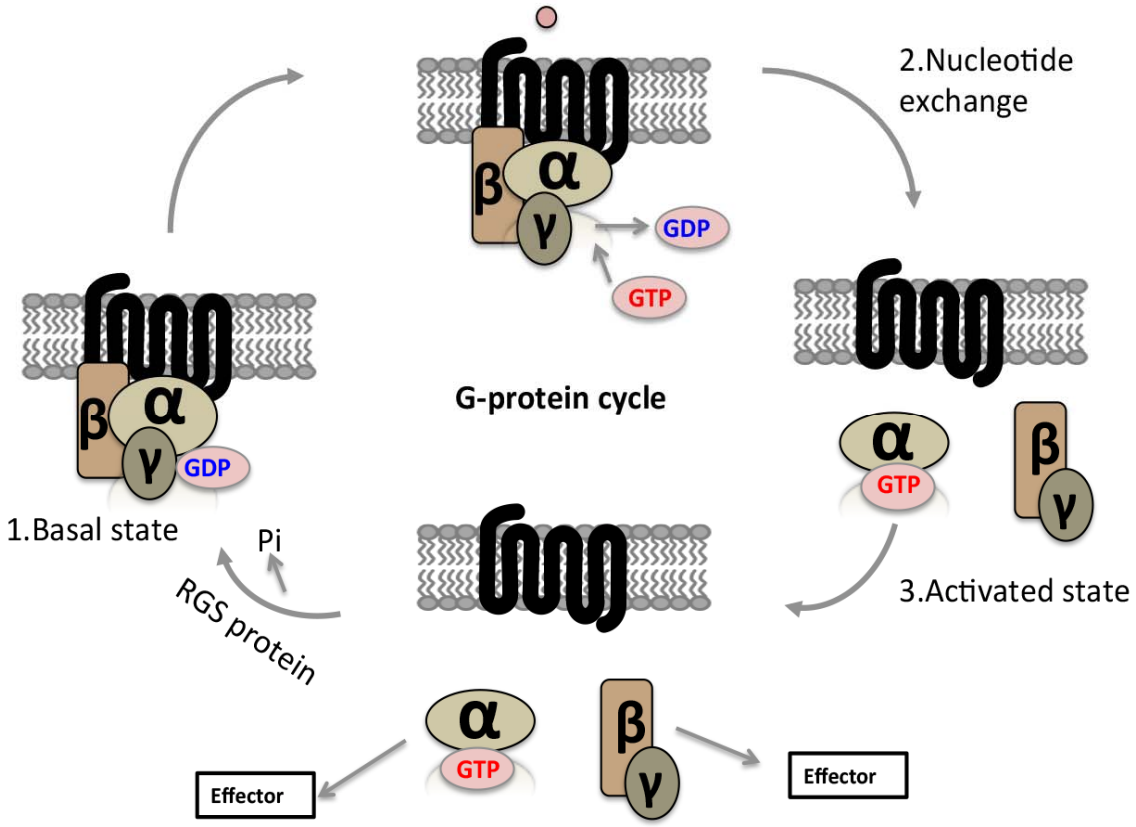

Figure 3-6: Principle of G-protein mediated signaling

Heterotrimeric G-proteins consist of an α subunit that binds and hydrolyses GTP and of a βγ subunit that forms an undissociable complex. Coupling of an activated receptor to the G-protein heterotrimer promotes the exchange of GDP for GTP on the G-protein α subunit, thereby leading to the dissociation of the GTP-bound α subunit and the βγ complex, which both are now able to modulate the activity of various effectors. This activation is terminated by the hydrolysis of GTP by the GTPase activity inherent to the G-protein α subunit. The resulting GDP-bound α subunit reassociates with the βγ complex and can enter a new activation cycle. The GTPase activity of the α subunit can be further increased by several effectors and by a group of proteins called regulators of G-protein signaling (RGS proteins) which, thereby promote the deactivation of G-protein mediated signaling. Schema is adapted from (Wettschureck and Offermanns, 2005; Worzfeld et al., 2008).

G-protein signaling is terminated by the hydrolysis of GTP by the GTPase activity inherent to the G-protein α-subunit. The resulting GDP-bound α subunit reassociates with the βγ-complex to enter a new cycle if activated receptors are present **(Figure 3-6).**

3.2.3 Families of heterotrimeric G-proteins

G-protein mediated signal transduction is a complex, very versatile transmembrane signaling system involving hundreds of different receptors and multiple G-proteins and effectors. Based on sequence homology of their α subunits, G-proteins can be grouped into four subfamilies: G_s, G_i, $G_{q/11}$ and $G_{12/13}$. Each G-protein family consists of various members that often show very specific expression patterns (Downes and Gautam, 1999) and often share some of their functional properties. A single GPCR can couple to either one or more families of G-proteins, and each G-protein can activate several downstream effectors (Simon et al., 1991). The βγ-complex of mammalian G-proteins is assembled from a repertoire of 5 G-protein β-subunits and 12 γ and can regulate various effectors. These βγ-mediated signaling events include the regulation of ion channels (Herlitze et al., 1996; Logothetis et al., 1987), of particular isoforms of adenylyl cyclase and phospholipase C, as well as of phosphoinositide-3-kinase isoforms **(Figure 3-6)** (Katz et al., 1992; Tang and Gilman, 1991).

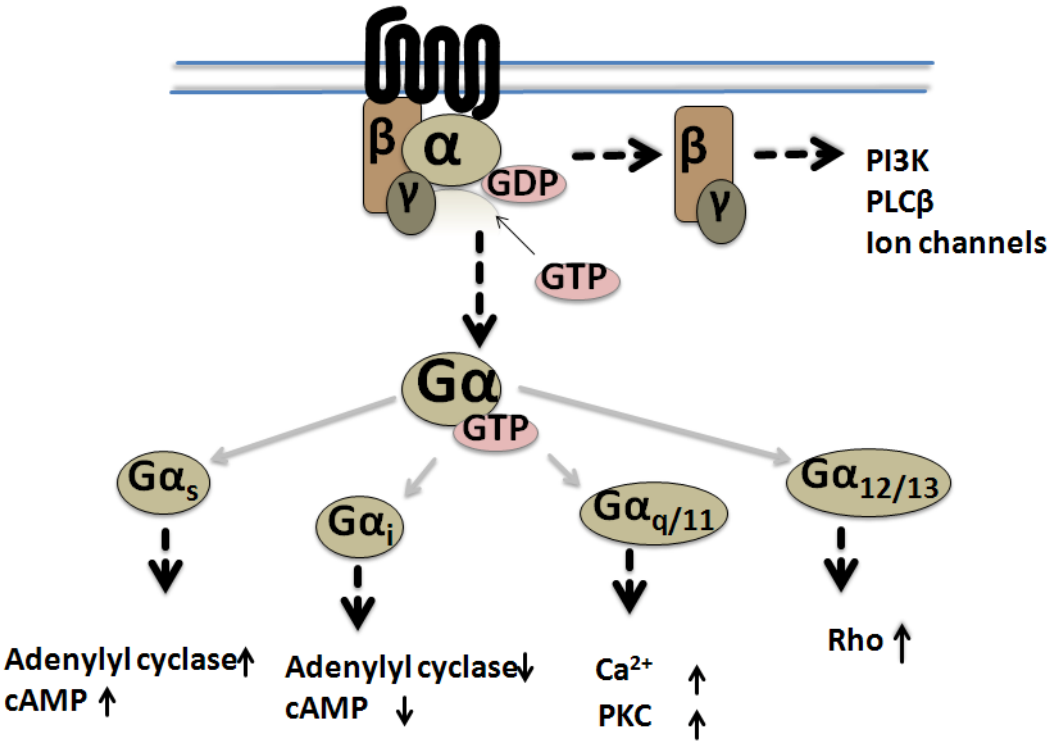

Figure 3-7: G-protein mediated GPCR signaling

Agonist binding triggers a conformational change in the receptor, resulting in activation of G-protein mediated signaling. The G-protein families G_s, G_i, $G_{q/11}$ and $G_{12/13}$ activate specific downstream effectors. Typically, $G\alpha_s$ stimulates adenylyl cyclase and increases levels of cyclic AMP (cAMP), whereas $G\alpha_i$ inhibits adenylyl cyclase and lowers cAMP levels. Members of the $G\alpha_{q/11}$ family bind to and activate phospholipase C (PLC) β isoforms, which cleave phosphatidylinositol bisphosphate (PIP_2) into diacylglycerol and inositol triphosphate (IP_3). G-proteins $G\alpha_{12}$ and $G\alpha_{13}$ control activation of the small GTPase RhoA. The Gβ subunits and Gγ subunits function as a dimer to activate many signalling molecules, including phospholipases, ion channels and lipid kinases. Schema is modified from (Dorsam and Gutkind, 2007; Neves et al., 2002; Wettschureck and Offermanns, 2005; Worzfeld et al., 2008)

G-proteins of the G_i family are broadly expressed. The α-subunits of the family member G_{i1}, G_{i2}, and G_{i3} mainly inhibit adenylyl cyclases (Sunahara et al., 1996), but since the expression levels of G_i and G_o are relatively high, also considerable βγ-mediated signaling ensues (Clapham and Neer, 1997). G_o signaling is specifically important for the nervous system, its effects appear to be primarily mediated through the βγ-subunit.

Also α-subunits like gustducin and transducin belong to the $G_{i/o}$ class, they control specific sensory functions through regulation of phosphodiesterase activty (Arshavsky et al., 2002).

The G_s family of G-proteins is ubiquitously expressed; it mediates receptor dependent adenylyl cyclase activation, resulting in increases in the intracellular cAMP concentration (Bastepe et al., 2002). The $G\alpha_s$ protein is encoded by the GNAS locus, which has a highly complex imprinted expression pattern and gives rise to several gene products due to various promoter activities and splice variants like $G\alpha_s$ and $G\alpha_{sXL}$ (Klemke et al., 2000; Pasolli et al., 2000).

The G-protein family $G_{q/11}$ has four members, G_q, G_{11}, G_{14} and $G_{15/16}$ (G_{15} being the murine, G_{16} the human ortholog). While G_q and G_{11} are widely expressed, G_{14} and G_{15} show a rather restricted expression pattern. The α subunits of the $G_{q/11}$ family, $G\alpha_q$, $G\alpha_{11}$, $G\alpha_{14}$ and $G\alpha_{15}$ regulate β-isoforms of phospholipase C (PLCβ) (Rhee, 2001). $G\alpha_q$-deficient mice show reduced platelet activation and prolonged bleeding time, a phenotype occasionally leading to perinatal death in newborns (Offermanns et al., 1997b) and reduced survival rate at postnatal day 30 (P30) (Gu et al., 2002). In addition, $G\alpha_q$-deficient mice suffer from cerebellar ataxia (Offermanns et al., 1997c). While the importance of $G\alpha_q$ and $G\alpha_{11}$ in various biological processes has been well established, the roles of $G\alpha_{14}$ and $G\alpha_{15/16}$ are not clear. Mice carrying inactivating mutations of the $G\alpha_{14}$ and $G\alpha_{15}$ genes have no or very minor phenotypical changes (Wettschureck and Offermanns, 2005).

The G-protein G_{12}/G_{13} family has two members, G_{12} and G_{13}; their α-subunits ($G\alpha_{12}$ and $G\alpha_{13}$) are expressed ubiquitously. The important cellular function of G_{12}/G_{13} is their ability to regulate the formation of actomyosin-based structures and to modulate their contractility by increasing the activity of the small GTPase RhoA. G_{12}/G_{13} mediated signaling leads to cytoskeletal rearrangement, extracellular matrix adhesion and stress fiber formation (Worzfeld et al., 2008). Activation of RhoA by $G\alpha_{12}$ and $G\alpha_{13}$ is mediated by a subgroup of guanine nucleotide exchange factors (GEFs) that include p115-RhoGEF/Lsc, PDZRhoGEF, and Leukemia-associated RhoGEF (LARG). While the GEF activity of PDZRhoGEF and LARG appears to be activated by both $G\alpha_{12}$ and $G\alpha_{13}$, p115-RhoGEF/Lsc activity is stimulated only by $G\alpha_{13}$ (Gohla et al., 1999; Gohla et al., 2000; Klages et al., 1999; Worzfeld et al., 2008). $G\alpha_{12}$ deficient mice are viable and fertile, and do not show apparent abnormalities (Gu et al., 2002). In contrast, mice lacking $G\alpha_{13}$ die at embryonic day 9.5 (E9.5) because they fail to develop a vascular system (Offermanns et al., 1997a). Cellular studies showed that in addition to RhoGEF-dependent RhoA activation, $G_{12/13}$ induces a variety of signaling pathways leading to the activation of various downstream effectors including phospholipase A2, Na+/H+ exchanger, or c-jun NH2-terminal kinase (Fromm et al., 1997). $G_{12/13}$ was also suggested to regulate cadherin-mediated signaling, since both $G\alpha_{12}$ and $G\alpha_{13}$ interact with the cytoplasmic domain of type I and type II class cadherins, causing the release of β-catenin from cadherins (Kelly et al., 2006; Krakstad et al., 2004; Meigs et al., 2002; Meigs et al., 2001; Solnica-Krezel, 2006). A recent study showed that $G_{12/13}$ mediated

RhoA activation is required for serum-induced nuclear translocation of MRTF-A in smooth muscle cells (Althoff et al., 2012) and cardiomyocytes (Takefuji et al., 2012).

3.2.4 G-protein mediated signaling in endothelial cells

Heterotrimeric G-proteins have been shown to play a major role in blood vessel formation (Richard et al., 2001). Disruption of the gene encoding the G-protein α subunit 13 ($G\alpha_{13}$) die at embryonic day 9.5 (E9.5) because they fail to develop an organized vascular system (Offermanns et al., 1997a). In addition, loss of $G\alpha_{13}$ in embryonic fibroblasts resulted in greatly impaired migratory responses to thrombin and LPA (Offermanns et al., 1997a) as well as to PDGF (Shan et al., 2006). These results demonstrate that $G\alpha_{13}$ participates in the regulation of cell movement in response to specific ligands, as well as in developmental vessel formation (Offermanns et al., 1997a). $G\alpha_{13}$ is highly expressed in endothelial cells at midgestation. Endothelial cell specific $G\alpha_{13}$ deficient embryos died at embryonic days E9.5–11.5 and resembled the constitutive $G\alpha_{13}$ knockout, and restoration of $G\alpha_{13}$ expression in endothelial cells rescued embryonic lethality and vascular phenotype in EC-$G\alpha_{13}$ knockouts (Ruppel et al., 2005). These results suggest a critical role of $G\alpha_{13}$ in endothelial cells during vascular development.

$G_{12/13}$ signaling is mediated by multiple RhoGEFs. PDZ-RhoGEF, LARG, p115-RhoGEF and lymphoid blast crisis (Lbc) are widely expressed in mammals (Fukuhara et al., 2001). In line with a role of $G\alpha_{13}$ signaling in angiogenesis it was recently shown that mice lacking the $G\alpha_{12/13}$ effectors PDZRhoGEF and LARG die at midgestation due to

multiple and complex vascular alterations including branching defects in cranial vessels and angiogenic defects in the entire embryo (Mikelis et al., 2013). These studies suggest that $G_{12/13}$ and RhoGEF mediated signaling is important for vessel formation.

4. AIM OF THE THESIS

Aim of the study is to understand the role of the endothelial G-proteins $G\alpha_{12}$ and $G\alpha_{13}$ in angiogenesis.

Angiogenesis, the formation of new blood vessels from existing ones, is a fundamental biological process required for embryonic development, tissue repair, chronic inflammation, and tumor growth. The role of G-protein signaling in physiological and pathological forms of angiogenesis is not well understood. Earlier studies in $G\alpha_{13}$ deficient mice showed an impaired ability to develop an organized vascular system, resulting in embryonic lethality (E9.5) (Offermanns et al., 1997a). The same phenotype was observed after endothelial cell specific deletion of $G\alpha_{13}$ (Ruppel et al., 2005), and in vitro studies suggested that impaired endothelial cell migration in response to GPCR-dependent stimuli underlies these findings (Offermanns et al., Science 1997a; Ruppel 2005). In addition, it was suggested that $G\alpha_{13}$ is essential for GPCR-independent, growth factor induced migration of endothelial cells (Shan et al., 2006). Based on these findings we would like to

1.) Investigate whether endothelial $G\alpha_{13}$ is also required for postnatal angiogenesis, for example in retinal and tumor angiogenesis.
2.) Dissect the molecular mechanisms underlying impaired angiogenesis in mice with endothelial cell-specific $G\alpha_{13}$-deficiency.

5. RESULTS

5.1 Endothelial $G\alpha_{13}$ in postnatal angiogenesis

To circumvent the embryonic lethality of global $G\alpha_{13}$ (Offermanns et al., 1997a) and $G\alpha_{12/13}$ (Gu et al., 2002) deficient mice we studied the role of endothelial $G\alpha_{12/13}$ in mice with tamoxifen-inducible, EC-specific inactivation of $G\alpha_{13}$ or $G\alpha_{12/13}$. To generate these animals, mice carrying a loxP flanked $G\alpha_{13}$ gene ($Gna13^{flox/flox}$) (Moers et al., 2003) alone or in a $G\alpha_{12}$ ($Gna12^{-/-}$) deficient background were crossed to the EC-specific, tamoxifen-inducible Tie2-CreERT2 mouse line (Korhonen et al., 2009)

5.1.1 Recombination in retinal endothelial cells

The Tie2-CreERT2 mouse line is a bacterial artificial chromosome (BAC) transgenic mouse line that expresses a fusion protein of the Cre recombinase with the modified estrogen receptor binding domain ($CreER^{T2}$) under the control of Tie2 (TEK-angiopoietin receptor) promoter (Korhonen et al., 2009). To check the efficiency of recombination in ECs after tamoxifen treatment, Tie2-$CreER^{T2}$ transgenic mice were crossed with the GFPGt (ROSA)26Sortm4(ACTB-tdTomato,-EGFP)Luo/J fluorescent reporter mice (Muzumdar et al., 2007). EC-specific Cre mediated recombination was induced in newborn mice by three consecutive intraperitoneal injections of tamoxifen on postnatal days 1-3 (P1-3) (**Figure 5-1A**). A high efficiency of Cre-mediated recombination of ECs (as shown by GFP expression) was observed in the whole mount retina and cornea in 6-day-old mice (**Figure 5-1B**). High magnifications showed efficiency of recombination in stalk and tip cells of retina (**Figure 5-1B**).

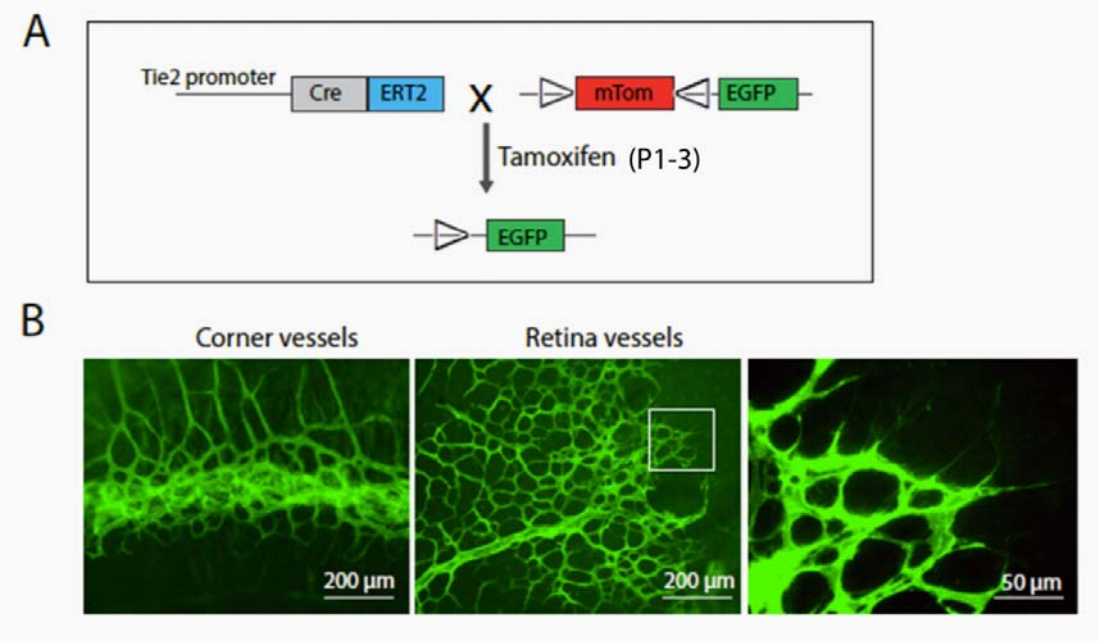

Figure 5-1: Tamoxifen induced recombination in the retina.

A, Schematic diagram of the reporter construct before and after tamoxifen inducible Cre mediated recombination in ECs. **B**, Efficiency of tamoxifen-induced, Cre-mediated recombination in the cornea and retina of 6-day-old mice was determined in GFPGt(ROSA)26Sor/Tie2CreERT2 double positive mice after injection of tamoxifen on postnatal days 1-3, (EGFP fluorescence indicates recombined cells).

5.1.2 $G\alpha_{13}$ is required for postnatal retinal angiogenesis

The retina is avascular at birth and a single superficial layer of blood vessels grows progressively from the center toward the periphery from postnatal day (P) 1 until P7 (Gariano and Gardner, 2005). The postnatal vascularization of the murine retina is an excellent model system for angiogenesis because sequentially occurring processes like sprouting, migration and proliferation can be visualized and quantified in retina whole mount preparations.

We studied the role of endothelial $G\alpha_{12}/G\alpha_{13}$-mediated signaling in the retinal vasculature at postnatal day 6 (P6) in mice that had received tamoxifen injections on P1-3. Retinae of endothelial cell-specific $G\alpha_{13}$- and $G\alpha_{12/13}$-deficient mice (EC-$G\alpha_{13}$-

KOs and EC-G$\alpha_{12/13}$-DKOs, respectively) displayed a delayed extension of the retinal vasculature towards the periphery. Further analyses of the retinal vasculature showed that vessel density and branching was reduced in the angiogenic front and vascular plexus compared to control littermates. No abnomalities were observed in constitutively Gα_{12}-deficient mice (Gα_{12}-KO) (**Figure 5-2A-C**).

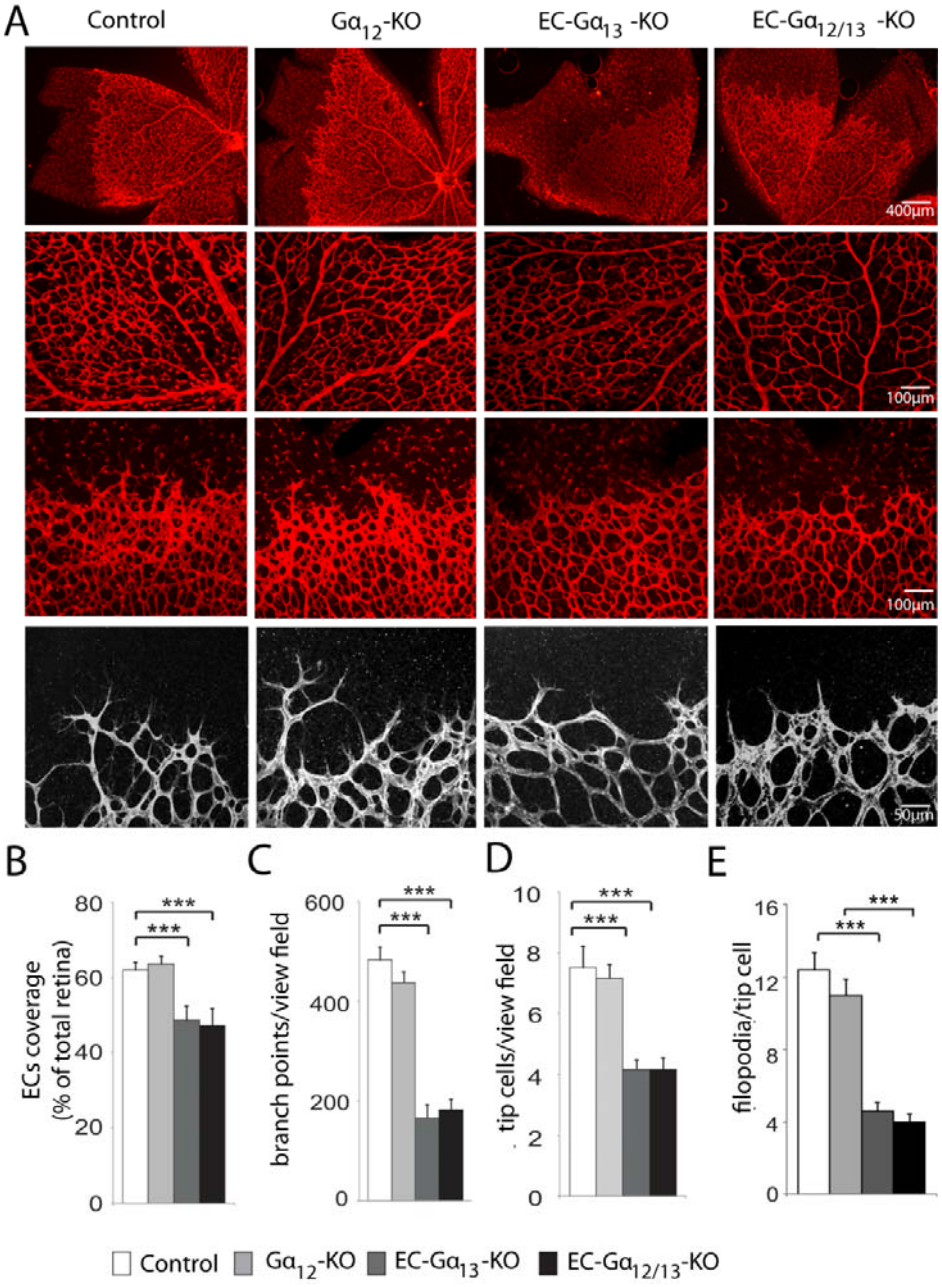

Figure 5-2: Endothelial $G\alpha_{13}$ is required for postnatal retinal angiogenesis.

A, Isolectin B4 (IB4)-staining of whole-mount retinae from 6-day-old mice after tamoxifen treatment on postnatal days 1-3. **B-E**, Quantification of vascular parameters in the EC-$G\alpha_{13}$-KO and EC-$G\alpha_{12/13}$-KO retina shows decreased EC coverage (B), branching (C), tip cells (D) and number of filopodia per tip cell (E) compared to control retina. No significant difference was observed in constitutive $G\alpha_{12}$ KO. (n=6-12).

Retinae of EC-$G\alpha_{12/13}$-KOs and EC-$G\alpha_{13}$-KOs showed a significantly decreased number of filopodia and tip cells, but again no difference was observed in $G\alpha_{12}$-deficient mice ($G\alpha_{12}$-KO) (**Figure 5-2 D&E**). These results suggest that ECs-specific $G\alpha_{13}$ signaling is important for the postnatal development of the retinal vasculature, whereas $G\alpha_{12}$ signaling is dispensable.

5.2 EC-$G\alpha_{13}$ signaling controls VEGFR-2 expression

Next, we investigated whether impaired retinal angiogenesis in EC-$G\alpha_{13}$-KOs was associated with an altered expression of angiogenesis-related genes. Many molecules have been implicated as positive and negative regulators of angiogenesis, for example angiopoietin receptors (Tie1,Tie2/Tek), vascular endothelial growth factors (Vegfa, Vegfb, Vegfc) and their receptors (Vegfr1/Flt1, Vegfr2/Kdr, Vegfr3/Flt4), Neuropilin receptors (Nrp1, Nrp2), platelet-derived growth factor (Pdgfb) receptors (Pdgfra, Pdgfrb), fibroblast growth factors (Fgf1, Fgf2) and their receptors (Fgfr1, Fgfr2, Fgfr3), ephrins (Efnb2) and ephrin receptors (Ephb4), matrix metalloproteinase (MMP2, MMP9) and their inhibitor (Timp2), endothelial cell adhesion molecules (Cdh5, Pecam1), Notch ligands (Jag1, Dll4) and their receptors (Notch1), Notch target genes (Hey1, Hes1), or hypoxia-inducible factor (Hif1a) (Adams and Alitalo, 2007; Carmeliet, 2005; Potente et al., 2011; Siekmann and

Lawson, 2007; Tammela and Alitalo, 2010). We isolated endothelial cells from lungs of 6-day-old mice and performed quantitative reverse transcriptase polymerase chain reactions (qRT-PCR). The efficiency of $G\alpha_{13}$ deletion in lung endothelial cell showed that the $G\alpha_{13}$ mRNA level was significantly decreased, but expression of other G-protein α-subunits such as $G\alpha_{12}$, $G\alpha_{11}$, $G\alpha_{q}$, $G\alpha_{i1}$, $G\alpha_{i2}$ and $G\alpha_{i3}$ were unaltered in tamoxifen induced Tie2-$G\alpha_{13}^{flox/flox}$ mice **(Figure 5-3A)**.

Interestingly, VEGFR-2 expression was selectively reduced in the absence of EC-$G\alpha_{13}$, whereas expression of other angiogenesis-related genes was normal **(Figure 5-3B)**. VEGFR-2 (also known as Flk1 and Kdr) is the primary receptor transmitting VEGF signals in ECs to promote angiogenesis. Decreased expression of VEGFR-2 was confirmed on the mRNA level in retinae of EC-$G\alpha_{13}$ deficient mice, but we did not observe significant changes in other VEGF family members **(Figure 5-3C)**. Further, VEGFR-2 immunostaining of the retinal vasculature at postnatal day 6 (P6) showed significantly less immunosignals in EC-$G\alpha_{13}$ deficient retinae **(Figure 5-3D)**. These results suggest that ECs-$G\alpha_{13}$ signaling controls VEGFR-2 expression in retina vasculatures.

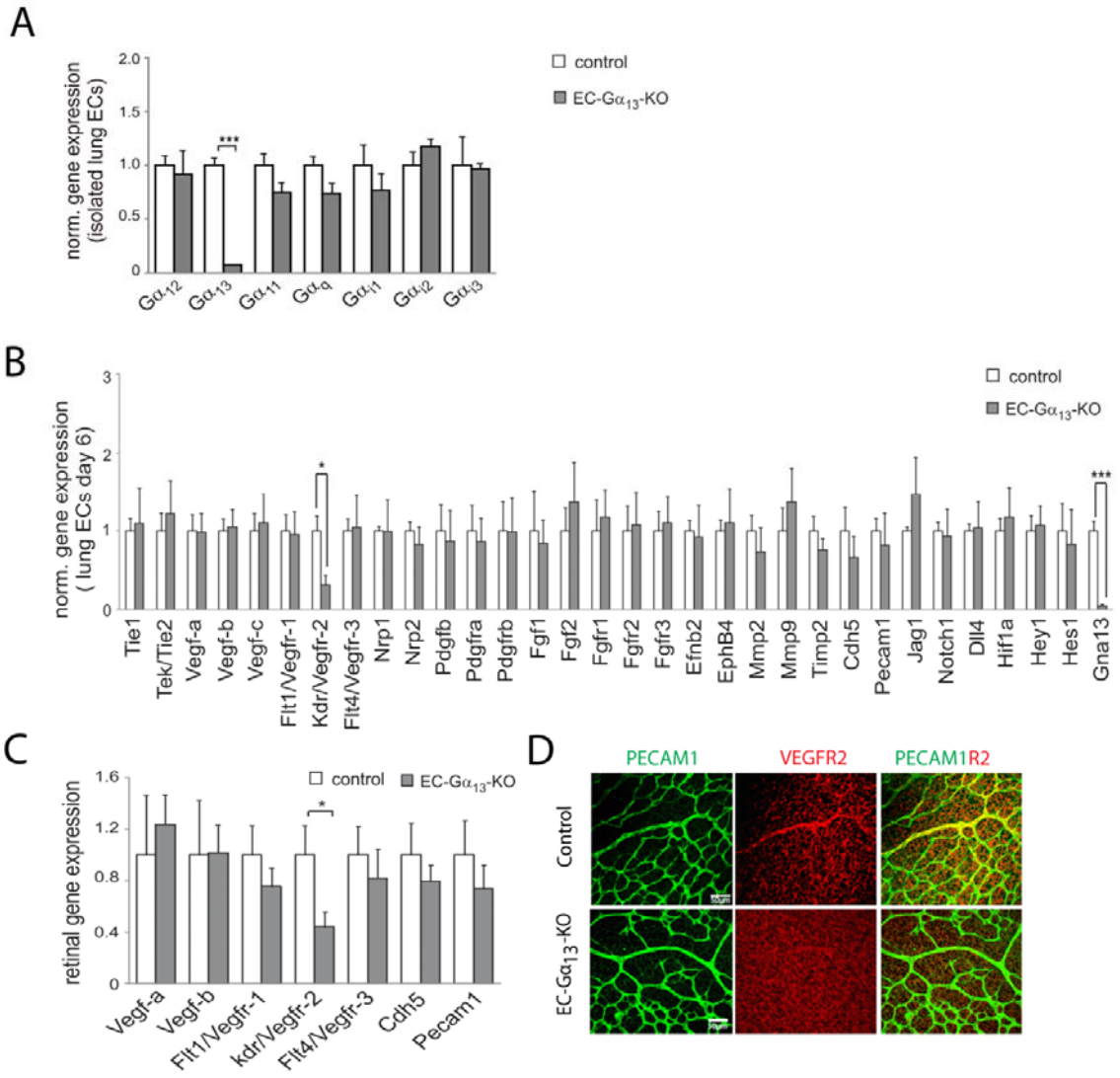

Figure 5-3: EC-Gα$_{13}$ signaling controls VEGFR-2 expression.

A, Expression of G-protein α-subunits was determined by quantitative RT-PCR in isolated lung endothelial cells from P6 control mice and EC-Gα$_{13}$-KOs (n = 3, all data normalized to GAPDH, control set to 1). **B & C,** Expression of angiogenesis-related genes was determined by quantitative real-time PCR in lung endothelial cells (B) and whole retinae (C) from 6-day-old control mice and EC-Gα$_{13}$-KOs (n = 6, all data normalized to GAPDH, control set to 1). **D,** Immunostainings of VEGFR-2 and PECAM1 in retinae from 6-day-old control mice and EC-Gα$_{13}$-KOs.

5.3 VEGF induced angiogenesis is impaired in EC-Gα_{13}-deficient mice

To investigate whether reduced VEGFR-2 expression in Gα_{13}-deficient endothelial cells was functionally relevant, we studied vessel ingrowth into subcutaneously implanted matrigel plugs in adult mice. To induce deletion of Gα_{13} in endothelial cells in adult mice, tamoxifen was injected intraperitoneally on five consecutive days and experiments were performed 1-2 weeks after the end of induction.

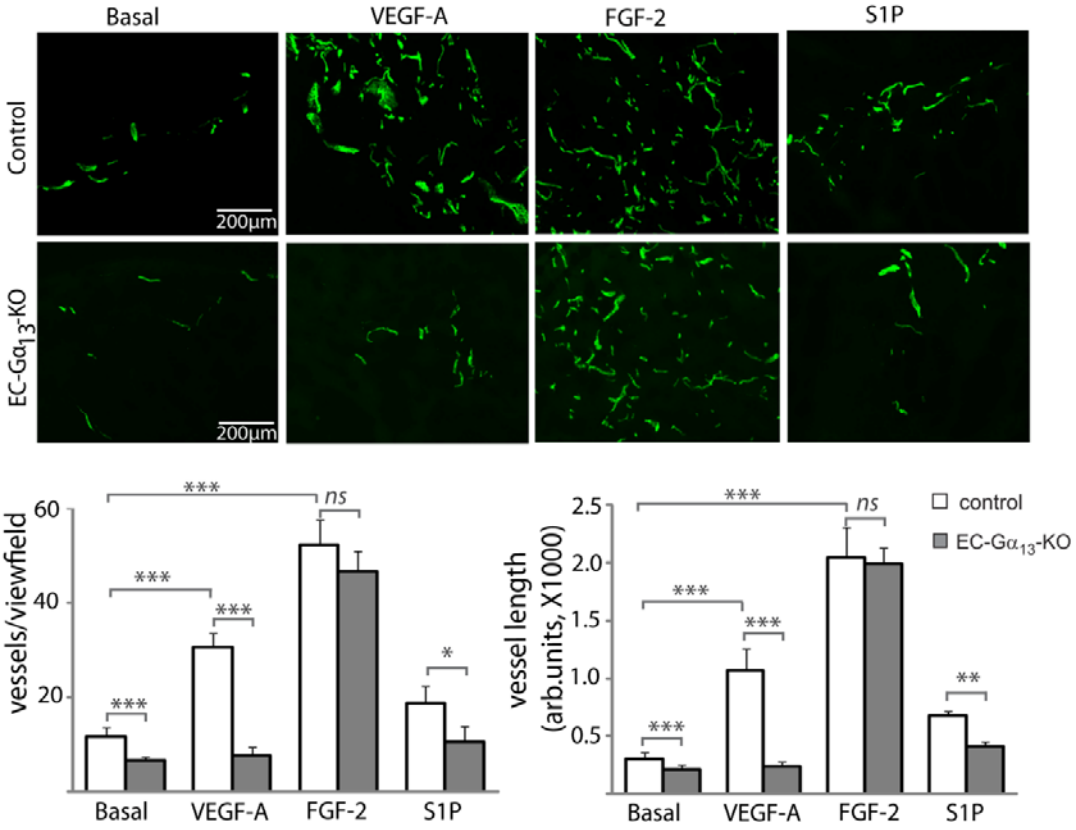

Figure 5-4: VEGF induced angiogenesis reduced in EC-Gα_{13} deficient mice

A, Vessel ingrowth into subcutaneous matrigel plugs containing VEGF-A (200 ng/ml) or FGF2 (200 ng/ml) or S1P (10 µM) implanted into a mouse. Plugs were harvested after 14 days, sectioned and immunostained with endothelial cell marker PECAM1.
B & C, Quantification of the number of vessels and the vessel length in EC-Gα_{13}-KOs and control mice. (n = 3).

Growth factor-reduced matrigel solutions were prepared with or without recombinant VEGF-A (200 ng/ml), bFGF/FGF2 (200 ng/ml) and S1P (10μM). The gel solutions (500 μl each) were injected subcutaneously into the right and left flank of anesthetized mice. After 14 days, matrigel plugs were harvested and analyzed by a PECAM1 (CD31) staining to detect blood vessels. We found that $G\alpha_{13}$-deficient endothelial cells were completely unresponsive to VEGF-A added to the matrigel, whereas responses to FGF2, another potent inducer of angiogenesis, were not significantly altered (**Figure 5-4**). Also the effects of sphingosine-1-phosphate (S1P), a GPCR agonist that has been implicated in angiogenesis, were largely preserved (**Figure 5-4**). These findings indicate that reduced VEGFR-2 expression in $G\alpha_{13}$-deficient endothelial cells results in a selective impairment of VEGF-A-mediated effects, whereas the effects of other angiogenic growth factors such as bFGF or S1P are not altered.

5.4 $G\alpha_{13}$ signaling controls VEGFR-2 expression in HUVEC

To learn more about the potential role of $G\alpha_{13}$ in the regulation of VEGFR-2 expression, we performed short-interfering RNA (siRNA)-mediated knockdown of $G\alpha_{13}$ ($G\alpha_{13}$-kd) in human umbilical vein endothelial cells (HUVEC). The efficiency of $G\alpha_{13}$ knockdown is showed that the $G\alpha_{13}$ mRNA level was significantly decreased, but other G-protein α-subunits were unaltered in mRNA levels (**Figure 5-5A**) As in murine cells, loss of $G\alpha_{13}$ resulted in reduced expression of VEGFR-2 on the mRNA level (**Figure 5-5B**), and this was also true on the protein level (**Figures 5-5C&D**). Conversely, adenoviral overexpression of $G\alpha_{13}$ increased VEGFR-2 expression (**Figures 5-5E&F**).

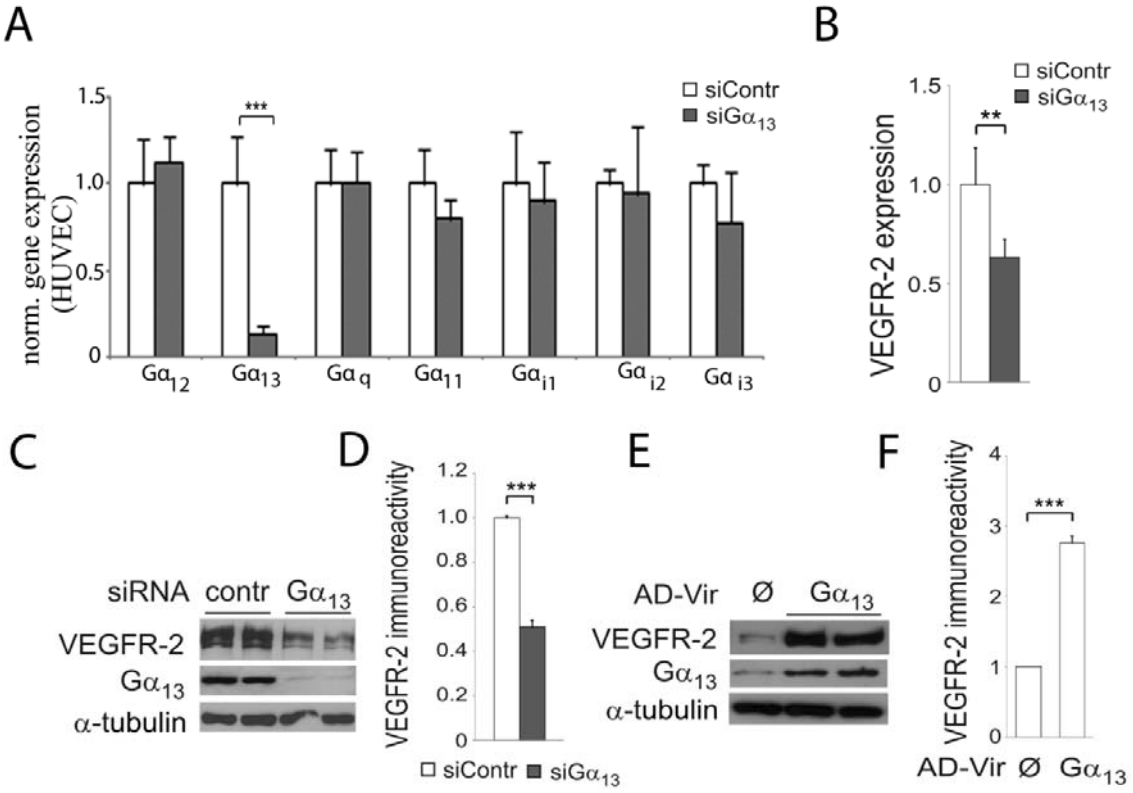

Figure 5-5: $G\alpha_{13}$ controls VEGFR-2 expression in HUVEC

A, Expression of G-protein alpha subunits $G\alpha_{12}$, $G\alpha_{13,}$ $G\alpha_{q}$, $G\alpha_{11,}$ and $G\alpha_{i1-3}$ determined by quantitative real-time PCR. **B**, Effect of siRNA-mediated knockdown of $G\alpha_{13}$ on VEGFR-2 expression. **C–F**, Effect of siRNA-mediated knockdown (C and D) or adenoviral overexpression (E and F) of $G\alpha_{13}$ on VEGFR-2 protein levels (B and D, immunoblots with α-tubulin as loading control; D-F, statistical evaluation after normalization to α-tubulin). (n=3).

5.5 VEGF-induced signaling is impaired in $G\alpha_{13}$ knockdown HUVEC

VEGF triggers the homodimerization of the endothelial VEGFR-2 receptor, resulting in the activation of downstream signal transduction cascades that control sprouting and proliferation of ECs (Olsson et al., 2006). We found that VEGF-A-induced phosphorylation of VEGFR-2 effectors such as extracellular-signal-regulated kinases 1/2 (ERK) or tyrosine kinase c-Src was significantly reduced in $G\alpha_{13}$-knockdown HUVEC **(Figure 5-6A).**

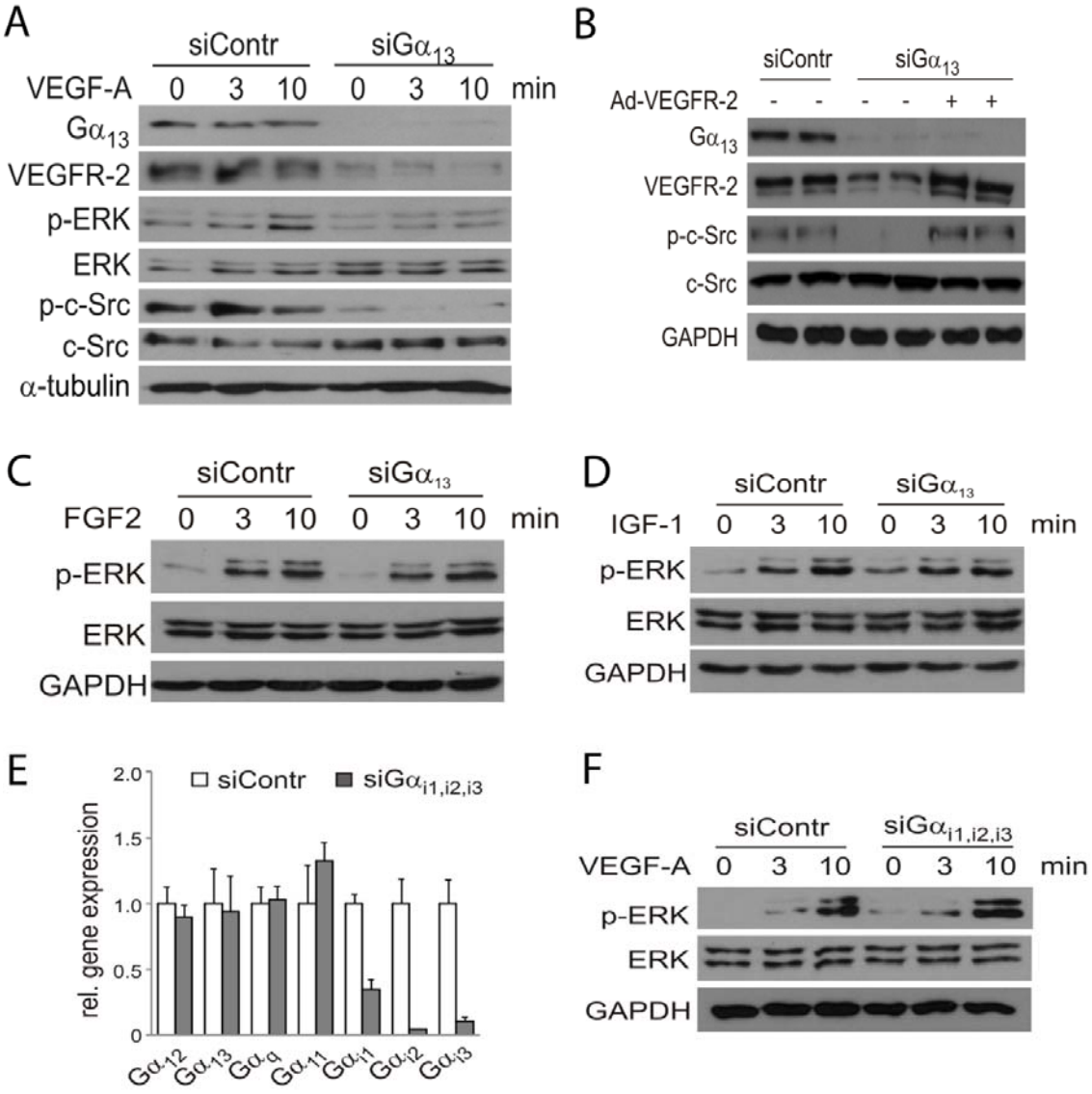

Figure 5-6: VEGF induced signaling impaired in $G\alpha_{13}$ knockdown HUVECA, The effect of $G\alpha_{13}$ knockdown on VEGF-A (50 ng/ml)-induced phosphorylation of ERK or c-Src (α-tubulin as loading control). **B,** Effect of adenoviral re-expression of VEGFR-2 on basal c-Src phosphorylation after siRNA-mediated knockdown of $G\alpha_{13}$ (GAPDH as loading control) (n = 2). **C&D,** Effect of siRNA-mediated $G\alpha_{13}$-knockdown on FGF2- or IGF-1- induced ERK-phosphorylation in HUVEC was determined by Western blotting (GAPDH as loading control) (n = 2). **E,** Efficiency of siRNA-mediated knockdown of Gαi isoforms $G\alpha_{i1}G\alpha_{i2}$, $G\alpha_{i3}$ ($siG\alpha_{i1,i2,i3}$) in HUVEC was determined by quantitative RT-PCR (n = 2). **F,** Effect of $G\alpha_{i1,i2,i3}$-knockdown on VEGF-A-induced ERK-phosphorylation (GAPDH as loading control) (n = 2).

Interestingly, knockdown of $G\alpha_{13}$ also lowered basal c-Src phosphorylation, which led us to investigate whether these basal defects were also due to reduced VEGFR-2 expression. When we normalized VEGFR-2 expression in $G\alpha_{13}$ knockdown HUVEC by adenoviral overexpression of $G\alpha_{13}$, basal c-Src phosphorylation was rescued **(Figure 5-6B)**. In contrast, ERK1/2 phosphorylation induced by FGF2 or insulin-like growth factor (IGF1) was not altered in $G\alpha_{13}$-kd HUVEC **(Figure 5-6C&D)**. Knockdown of other G-protein α-subunits, such as $G\alpha_{i1}$, $G\alpha_{i2}$, and $G\alpha_{i3}$, did not affect VEGF-A-induced ERK1/2 phosphorylation (**Figure 5-6E&F**). These results suggest that $G\alpha_{13}$-mediated signaling is required for VEGFR-2 expression and, consecutively, VEGF-dependent protein phosphorylation.

5.6 Tube formation is impaired in $G\alpha_{13}$ knockdown HUVEC

To test whether the observed reduction in VEGF-induced protein phosphorylation resulted in altered angiogeneic behavior of HUVEC, we anlysed growth factor-induced tubulogenesis (tube formation) in vitro. Control and $G\alpha_{13}$-kd HUVEC were plated onto growth factor reduced matrigel with and without VEGF or bFGF. We observed that both basal and VEGF-induced tube formation (total network and tube length) was significantly reduced in $G\alpha_{13}$-kd HUVECs. However, tube formation induced by other angiogenic factors, for example bFGF, was not affected **(Figure 5-7A-C).**

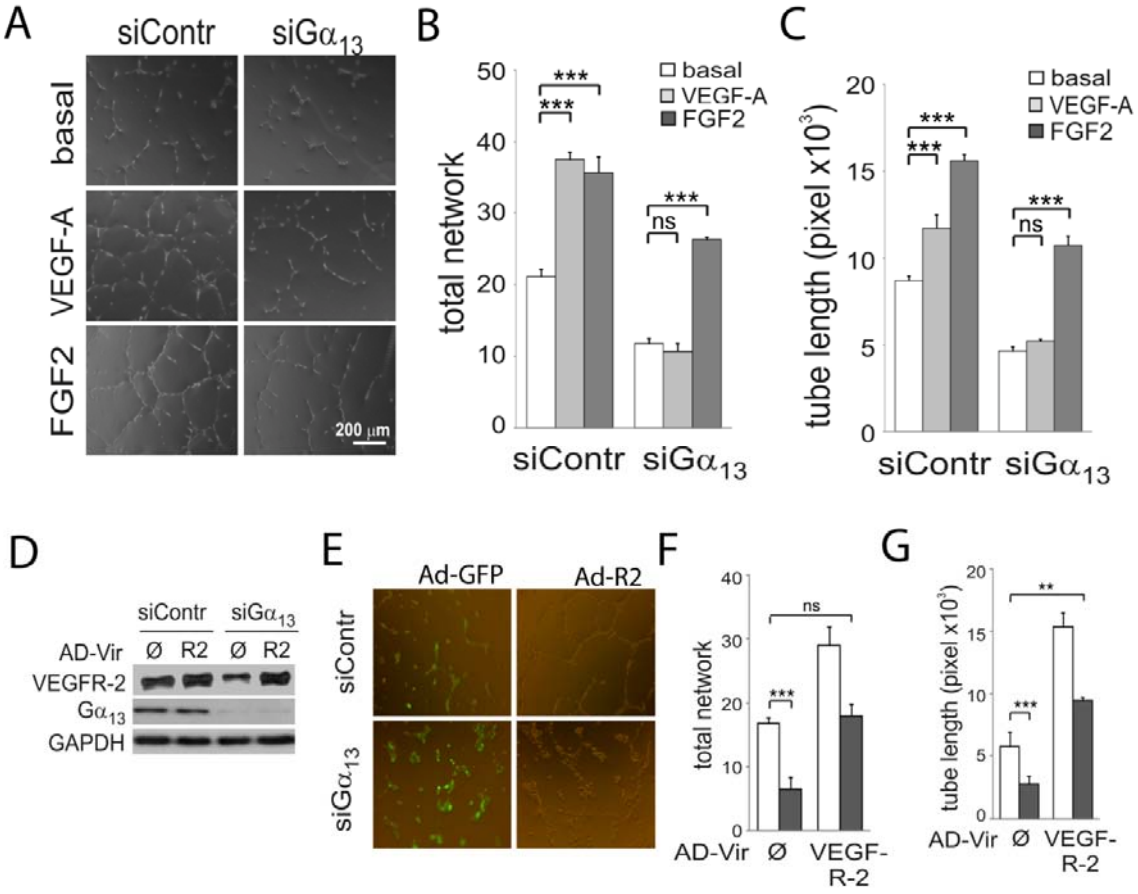

Figure 5-7: VEGF effect in tube formation is impaired in $G\alpha_{13}$-depleted HUVEC

A-C, Tube formation in response to Basal, VEGF-A (50 ng/ml), and FGF2 (50 ng/ml) induced effects in HUVEC, after knockdown of $G\alpha_{13}$. (B&C, Quantification of tube formation). **D–G**, Immunoblotting analysis of VEGFR-2 expression after adenoviral VEGFR-2 gene transfer to $G\alpha_{13}$ kd HUVEC (D). Effect of adenoviral overexpression of VEGFR-2 (R2) on basal tube formation after $G\alpha_{13}$-knockdown (E). (F&G, quantification of tube formation). Ad-Vir, adenovirus; siContr, scrambled control siRNA; $siG\alpha_{13}$, siRNA directed against $G\alpha_{13}$. (n=4).

Next, we tested whether basal and VEGF-induced effects were due to reduced VEGFR-2 expression. Adenoviral gene transfer of VEGFR-2 into $G\alpha_{13}$-kd HUVEC normalized the VEGFR-2 levels (Fig 5-7D) and restored tube formation **(Figure 5-7F-G),** suggesting that downregulation of VEGFR-2 underlies the observed defect in tube formation.

5.7 Gα$_{13}$ controls VEGFR-2 expression independently of the Notch pathway

The ability of Notch to regulate endothelial sprouting is connected to the VEGF pathway: VEGF signaling induces expression of Notch ligand Delta-like ligand 4 (Dll4) in angiogenic vessels, most prominently in the tip cells and endothelial cell sprouts. Dll4 leads to Notch activation in adjacent ECs, thereby suppressing VEGFR receptor expression (VEGFR-2 and VEGFR3-) and restraining endothelial sprouting and proliferation (Roca and Adams, 2007).

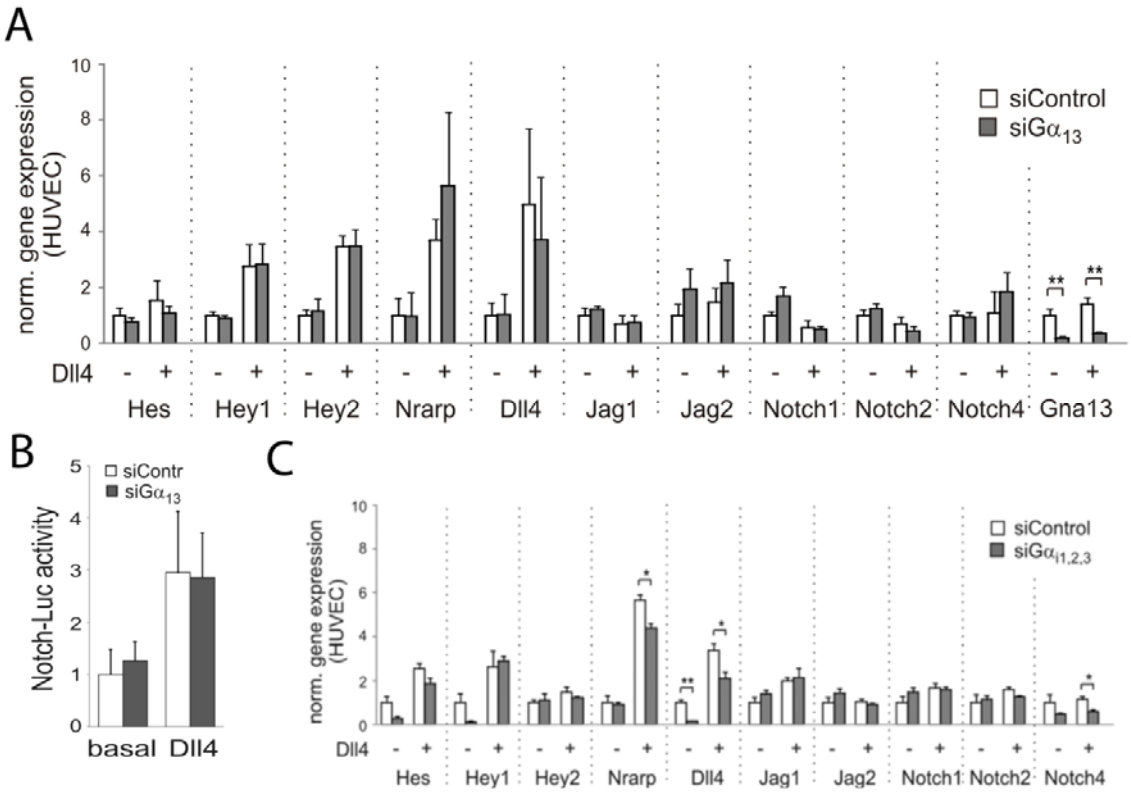

Figure 5-8: Gα$_{13}$ controls VEGFR-2 expression independently of the Notch pathway

A, Effect of Gα$_{13}$-knockdown on the expression of Notch-related genes in HUVEC under basal conditions (Dll4-) and in response to Dll4 stimulation (Dll4+). Data are shown after normalization to GAPDH, basal values of the control group were set to 1 (n = 6). **B,** Effect of Gα$_{13}$-kd on basal and Delta-like ligand 4 (Dll4, 10 µg/ml)-induced activity of a Notch-dependent luciferase reporter construct. siContr, scrambled control siRNA; siGα$_{13}$, siRNA directed against Gα$_{13}$. **C,** Effect of Gα$_{13}$-knockdown on

the expression of Notch-related genes in HUVEC. Notch ligands (hairy and enhancer of split-1 (Hes1), Hairy/enhancer-of-split related with YRPW motif protein 1 &2 (Hey1,2), Notch-regulated ankyrin repeat protein (Nrarp)), Notch ligand (Dll4, Jagged1,2), or Notch receptors (Notch 1,2,4)

Next, we tested basal and Dll4-induced Notch target gene expression, Notch ligand and Notch receptor expression in $G\alpha_{13}$–Kd HUVEC. We did not find significant differences in the expression of Notch target genes between control cells and $G\alpha_{13}$–kd HUVEC **(Figure 5-8A)**. For further conformation we tested Dll4-induced Notch activity using a luciferase reporter constrcut in HUVEC and found that Notch activity was not affected by loss of $G\alpha_{13}$ **(Figure 5-8B)**. These results suggest that loss of $G\alpha_{13}$ is not associated with altered Notch signaling in HUVECs.

5.8 VEGFR-2 transcriptional regulation

Most commonly, mammalian gene-promoters contain a TATA box, which recruits the transcription factor TFIID to start the transcription, but the VEGFR-2 promoter contains an initiator element (Inr), which overlaps the transcription start site instead of the TATA box. The VEGFR-2 promoter also contains four canonical E-box motifs, at least five Sp1 binding site, an NF-κB site, and an Ap1 binding sites (Patterson et al., 1995). To investigate whether $G\alpha_{13}$ regulates VEGFR-2 expression on the transcriptional level, we transfected HUVEC with a luciferase reporter construct driven by a VEGFR-2 promoter fragment containing base pairs -780 to +268 relative to the transcriptional start (VEGFR-2-Luc). We found that VEGFR-2-Luc activity was reduced in $G\alpha_{13}$-kd cells **(Figure 5-9A),** whereas overexpression of wild type or constitutively active $G\alpha_{13}$ increased it **(Figure 5-9B)**. Overexpression of $G\alpha_{12}$, in contrast, did not affect VEGFR-2-Luc activity **(Figure 5-9B)**.

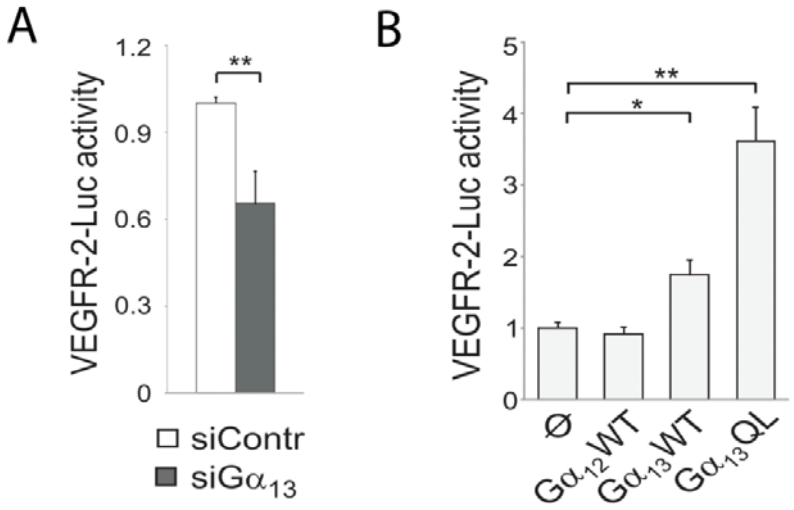

Figure 5-9: VEGFR-2 transcriptional regulation is controlled by $G\alpha_{13}$ signaling

A, Activity of a VEGFR-2 promoter (-780/+268)-driven luciferase reporter construct (VEGFR-2-Luc) after siRNA-mediated knockdown of $G\alpha_{13}$. **B**, Effect of overexpression of wild-type $G\alpha_{12}$ ($G\alpha_{12}$WT) or $G\alpha_{13}$ ($G\alpha_{13}$WT) as well as constitutively active $G\alpha_{13}$ ($G\alpha_{13}$QL) on VEGFR-2 promoter activity (n=4).

5.8.1 GPCR-mediated RhoA activation is required for $G\alpha_{13}$-dependent VEGFR-2 expression

We next tested whether GPCR agonists that are known to signal through $G\alpha_{13}$ (Worzfeld et al., 2008) were able to reproduce the effect of $G\alpha_{13}$-overexpression. We found that both the protease thrombin and the lysophospholipid S1P enhanced VEGFR-2 promoter activity, and this effect was completely abrogated after knockdown of $G\alpha_{13}$ (**Figure 5-10A**).

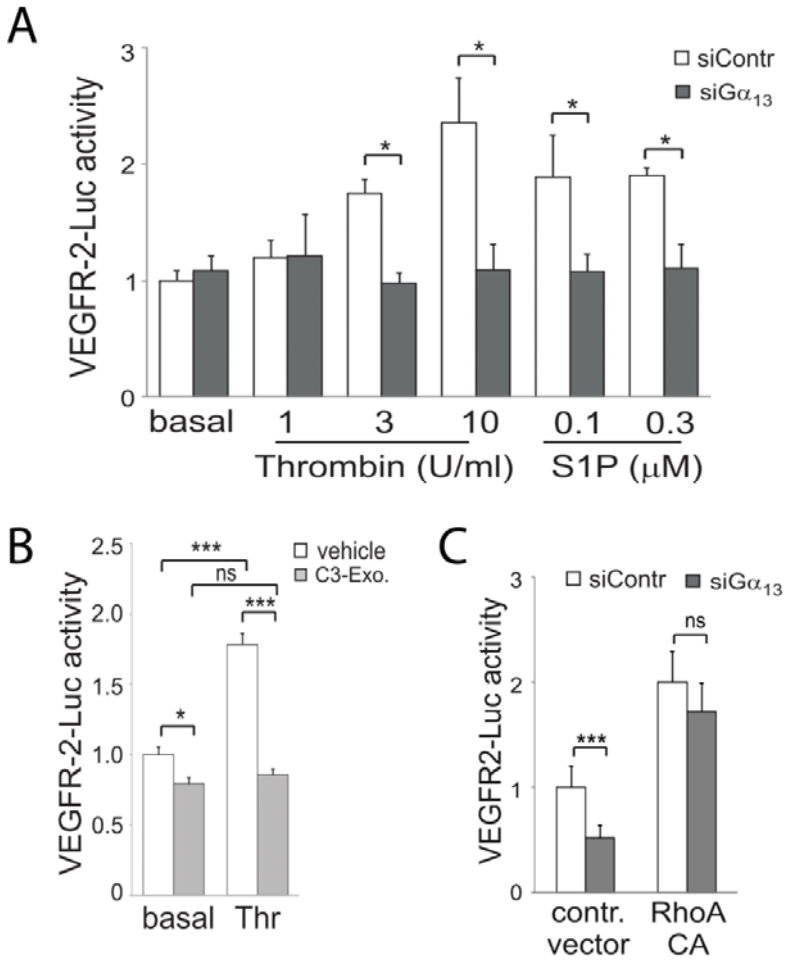

Figure 5-10: Activation of RhoA is required for $G\alpha_{13}$-dependent VEGFR-2 expression

A, Effect of $G\alpha_{13}$-knockdown on agonist-induced stimulation of VEGFR-2-Luc activity in serum-starved HUVEC. **B,** Effect of the RhoA-inhibitor C3 exoenzyme (C3, 0.5 mg/ml) on thrombin (10U/ml)-induced VEGFR-2-Luc activity. **C,** Effect of overexpression of constitutively active RhoA on VEGFR-2-Luc activity in control HUVEC or after knockdown of $G\alpha_{13}$ (n = 2).

To investigate whether the small GTPase RhoA, a well-known effector of the $G_{12/13}$ family (Brown et al., 2006; Worzfeld et al., 2008), mediates $G\alpha_{13}$-dependent VEGFR-2 promoter activity, we pretreated HUVEC with C3-exoenzyme, which ADP-ribosylates and thereby inactivates RhoA. Pretreatment with C3 exoenzyme completely abrogated thrombin-induced effects **(Figure 5-10B)**, indicating that RhoA

is required for $G\alpha_{13}$-dependent VEGFR-2 expression. In line with this notion, overexpression of constitutively active RhoA significantly increased VEGFR-2-Luc activity both in control HUVEC and after knockdown of $G\alpha_{13}$ **(Figure 5-10C)**.

5.8.2 G_{13} mediated signaling regulates the (-130 to -60)-promoter region of VEGFR-2

To further elucidate the molecular mechanism by which $G\alpha_{13}$/RhoA regulate VEGFR-2 expression, we employed deletion mutants of the original -780/+268 VEGFR-2 luciferase reporter construct that contained the promoter fragments -570/+268, -225/+268, -130/+268 and -60/+268 (**Figure 5-11A**).

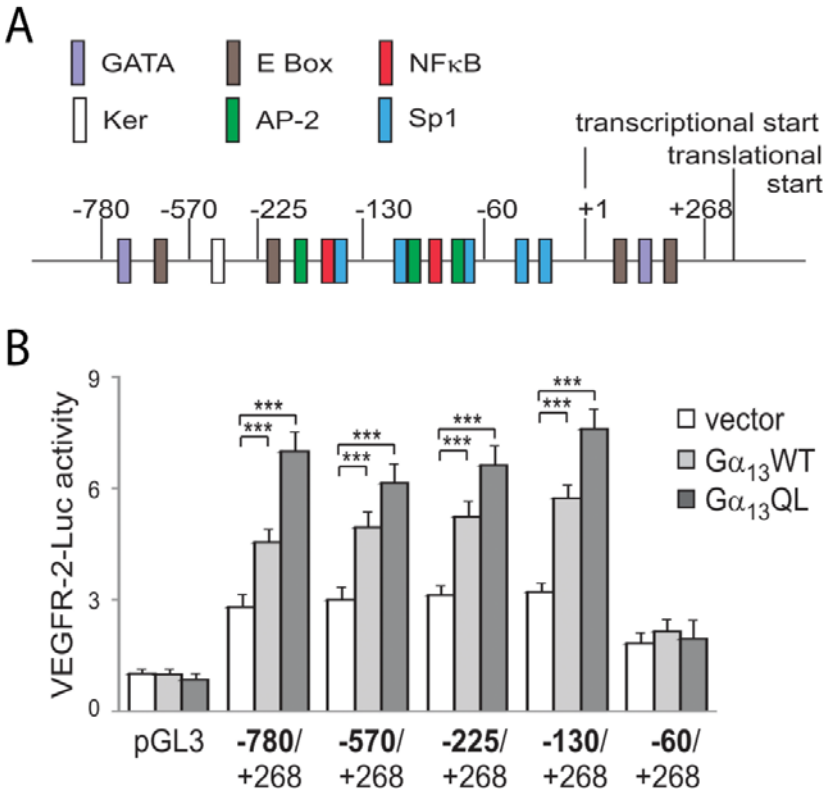

Figure 5-11: Promoter region -130/-60 of controlled by $G\alpha_{13}$ signaling

A, Schematic diagram depicting the organization of the VEGFR-2 promoter. **B,** Effect

of various deletion mutants of the original -780/+268 VEGFR-2-Luc construct on luciferase activity in the presence of control plasmid (vector) or plasmids expressing wild-type (WT) or constitutively active (QL) $G\alpha_{13}$. The size of the deletion mutants relative to the transcriptional start at position 1 is as indicated; pGL3 is the empty vector (n=3).

We found that $G\alpha_{13}$-dependent VEGFR-2 expression was preserved in all mutants except the -60/+268 fragment **(Figure 5-11B)**, suggesting that the critical elements are located between -60 and -130, a region that contains two Sp1 sites, 2 AP-2 sites, and an NF-κB site (Patterson et al., 1995).

5.8.3 $G\alpha_{13}$ regulates VEGFR-2 through RhoA and NF-κB signaling cascades

Since $G\alpha_{13}$/RhoA-mediated signaling has been implicated in NF-κB activation in various cell types (Brown et al., 2006; Martin et al., 2001; Profirovic et al., 2005), we studied the potential involvement of NF-κB in $G\alpha_{13}$-dependent VEGFR-2 expression. We found that knockdown of $G\alpha_{13}$ abrogated thrombin-induced degradation of the NF-κB inhibitor IκBα **(Figure 5-12A)**, and prevented thrombin-mediated luciferase expression from an NF-κB-responsive reporter construct **(Figure 5-12C)**. While thrombin-induced NF-κB activation was obviously $G\alpha_{13}$-dependent, the effects of GPCR-independent activators of NF-κB, such as tumor necrosis factor-α (TNFα), were not affected by knockdown of $G\alpha_{13}$ **(Figure 5-12B&C)**. We furthermore found that the NF-κB inhibitor Ro106-9920 reduced basal VEGFR-2 promoter activity and completely abrogated thrombin-induced effects **(Figure 5-12E)**, and that mutation of the NF-κB binding site at position -84 (Wt sequence – GGGAGAGCC; NF-κB mut – tttAGAGCC) of the VEGFR-2 promoter abrogated $G\alpha_{13}$-dependent transcription **(Figure 5-12F)**.

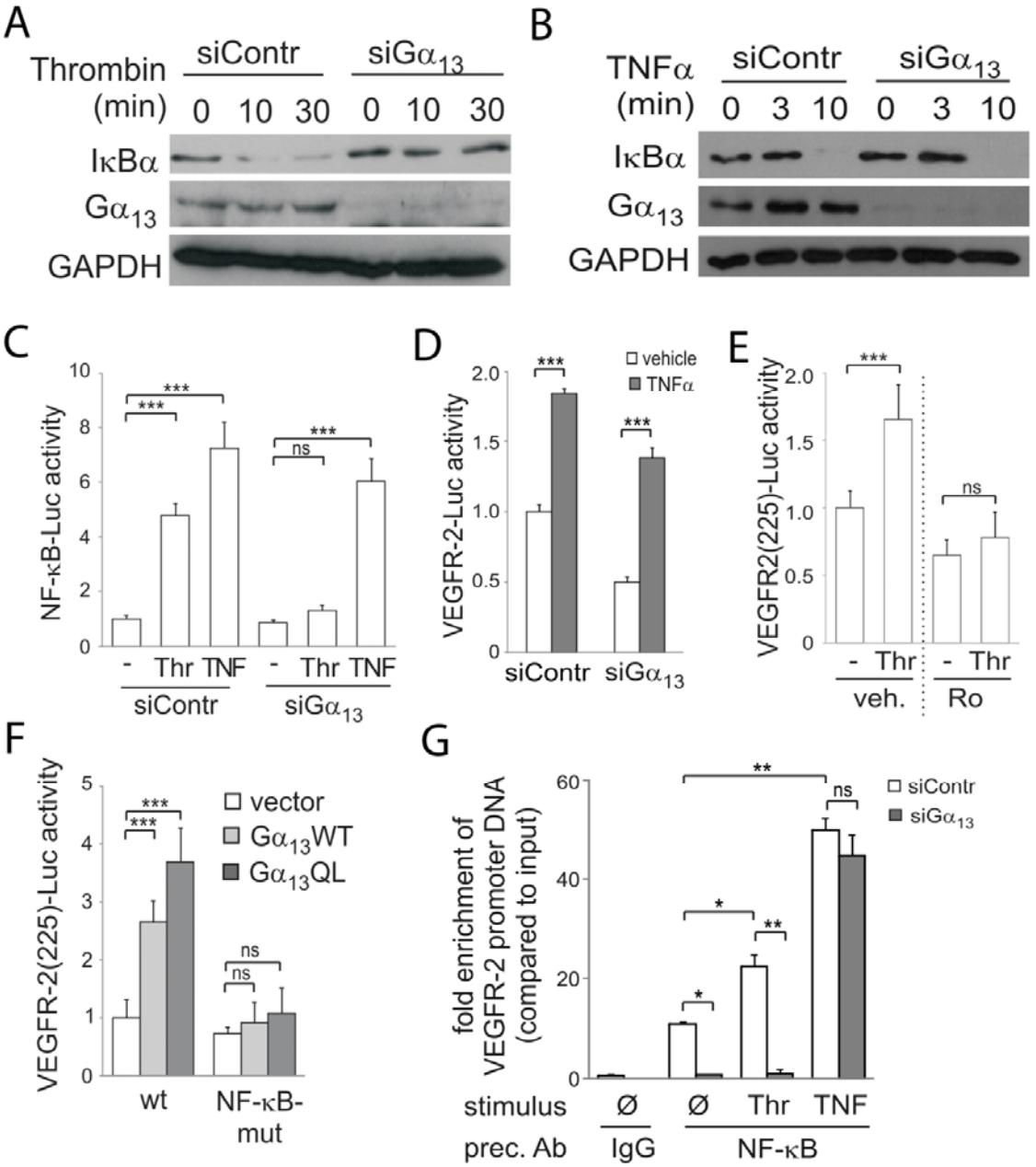

Figure 5-12: VEGFR-2 expression is regulated by $G\alpha_{13}$-mediated activation of NF-κB

A, Effect of $G\alpha_{13}$-knockdown on thrombin-induced IκBα degradation as determined by Western blotting (GAPDH as loading control). **B,** Effect of $G\alpha_{13}$-knockdown on TNFα-induced IκBα degradation was determined by Western blotting (GAPDH as loading control) (n = 3). **C,** Effect of $G\alpha_{13}$-knockdown of thrombin (Thr, 10 U/ml)- and TNFα (TNF, 10 ng/ml)-induced activation of an NF-κB-responsive luciferase reporter (NF-κB-Luc). **D,** Effect of $G\alpha_{13}$-knockdown on TNFα-induced VEGFR-2-Luc activity (n

= 2). **E,** Thrombin (10 U/ml)-induced activation of VEGFR-2-Luc in the absence and presence of NF-κB inhibitor Ro106-9220 (Ro) or vehicle (veh). **F,** Effect of empty vector, wild-type $G\alpha_{13}$ ($G\alpha_{13}$WT), or constitutively active $G\alpha_{13}$ ($G\alpha_{13}$QL) on luciferase reporter constructs containing the VEGFR-2 promoter fragment -225/+268 in its wild-type form (WT) GGGAGAGCC or after mutation of the NF-κB site at -84 (tttAGAGCC). **G**, Enrichment of VEGFR-2 promoter sequences after chromatin immunoprecipitation with unspecific IgG antibodies or specific NF-κB antibodies under basal conditions (Φ) or after stimulation with thrombin (Thr) or TNFα (TNF) in control HUVEC or after knockdown of $G\alpha_{13}$. Data are expressed as fold enrichment of amplified DNAs in immunoprecipitated DNAs compared to 1% of input DNA (n = 3).

Chromatin immunoprecipitation assays showed that VEGFR-2 promoter sequences located between –28 and –144 could be precipitated with NF-κB, in particular after stimulation with thrombin or TNFα. Knockdown of $G\alpha_{13}$ strongly reduced basal and thrombin-induced precipitation of VEGFR-2 promoter sequences with NF-κB, while responses to TNFα were preserved **(Figure 5-12G)**. We conclude that $G\alpha_{13}$ mediates thrombin-induced expression of VEGFR-2 through a signaling cascade involving RhoA-dependent NF-κB activation.

5.9 Endothelial $G_{12/13}$ signaling in tumor angiogenesis

Tumor angiogenesis is one of the hallmarks of cancer, once a tumor exceeds a few millimeters in diameter, hypoxia and nutrient deprivation triggers the 'angiogenic switch' in endothelial cells, resulting in tumor vascularization and, consecutively, tumor progression. By blocking tumor angiogenesis it is possible to reduce tumor growth and metastasis. Since VEGF and its receptor VEGFR-2 are key players both in developmental angiogenesis and tumor angiogenesis, blocking VEGF/VEGFR-2 signaling can help to slow tumor progression and metastasis by eradicating tumor vasculature (Carmeliet, 2005; Ferrara and Kerbel, 2005; Potente et al., 2011).

5.9.1 Endothelial $G\alpha_{12/13}$ signaling in tumorigenesis

We investigated whether $G\alpha_{13}$-dependent regulation of VEGFR-2 expression also contributed to tumor angiogenesis in adult mice. Mice were treated with tamoxifen on five consecutive days to induce Cre-mediated recombination; one or two weeks later, Lewis lung carcinoma (LLC1) or B16F10 melanoma (B16) cells were injected subcutaneously into the flank of control mice and EC-specific mutant mice and tumor growth was measured two times per week.

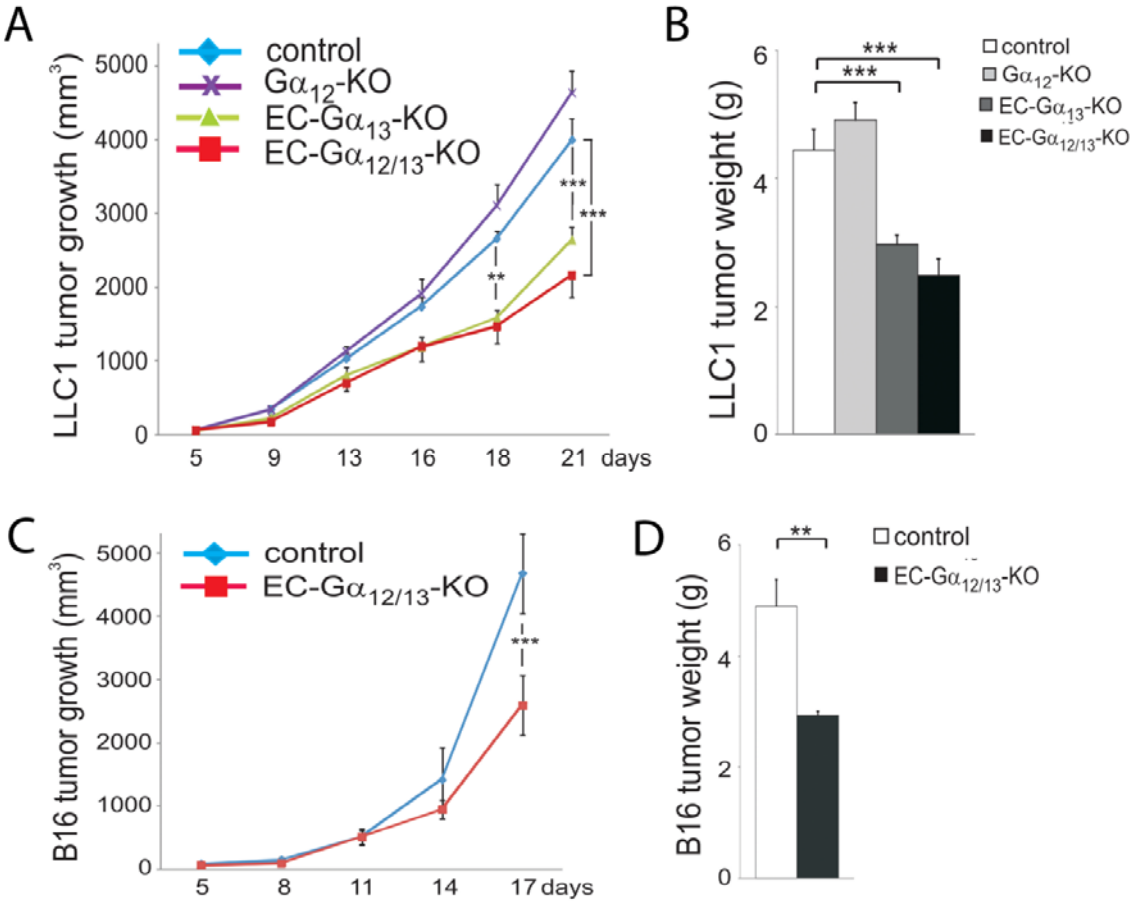

Figure 5-13: EC-$G\alpha_{13}$ KO mice reduced tumorigenesis

A&B, After subcutaneous inoculation of Lewis Lung carcinoma cells (LLC1): Tumor growth (A) and Tumor weight (B). **C&D,** B16 melanoma cells (B16): tumor growth (C) and final tumor weight (D) were determined in mice of the indicated genotypes (n = 8–12).

We found that EC-Gα_{13}-KOs and EC-G$\alpha_{12/13}$-KOs showed significantly decreased tumor growth and tumor weight compared with control mice (**Figure 5-13)**. However, tumor growth and weight were not altered in global Gα_{12} knockout mice.

5.9.2 Endothelial G$\alpha_{12/13}$ signaling in tumor angiogenesis

Next, we checked the tumor vascularization of LLC1 and B16 tumors. Staining for the EC marker PECAM1 in LLC1 tumors showed that vessel number and total vessel length were significantly reduced in EC-Gα_{13}-KOs and EC-G$\alpha_{12/13}$-KOs compared to control mice **(Figure 5-14A-C)**. These findings were confirmed in the B16 melanoma model (**Figure 5-14D-F**). Interestingly, immunostainings of LLC1 tumor vessels showed also in this model significantly reduced expression of VEGFR-2 in the absence of endothelial Gα_{13}.

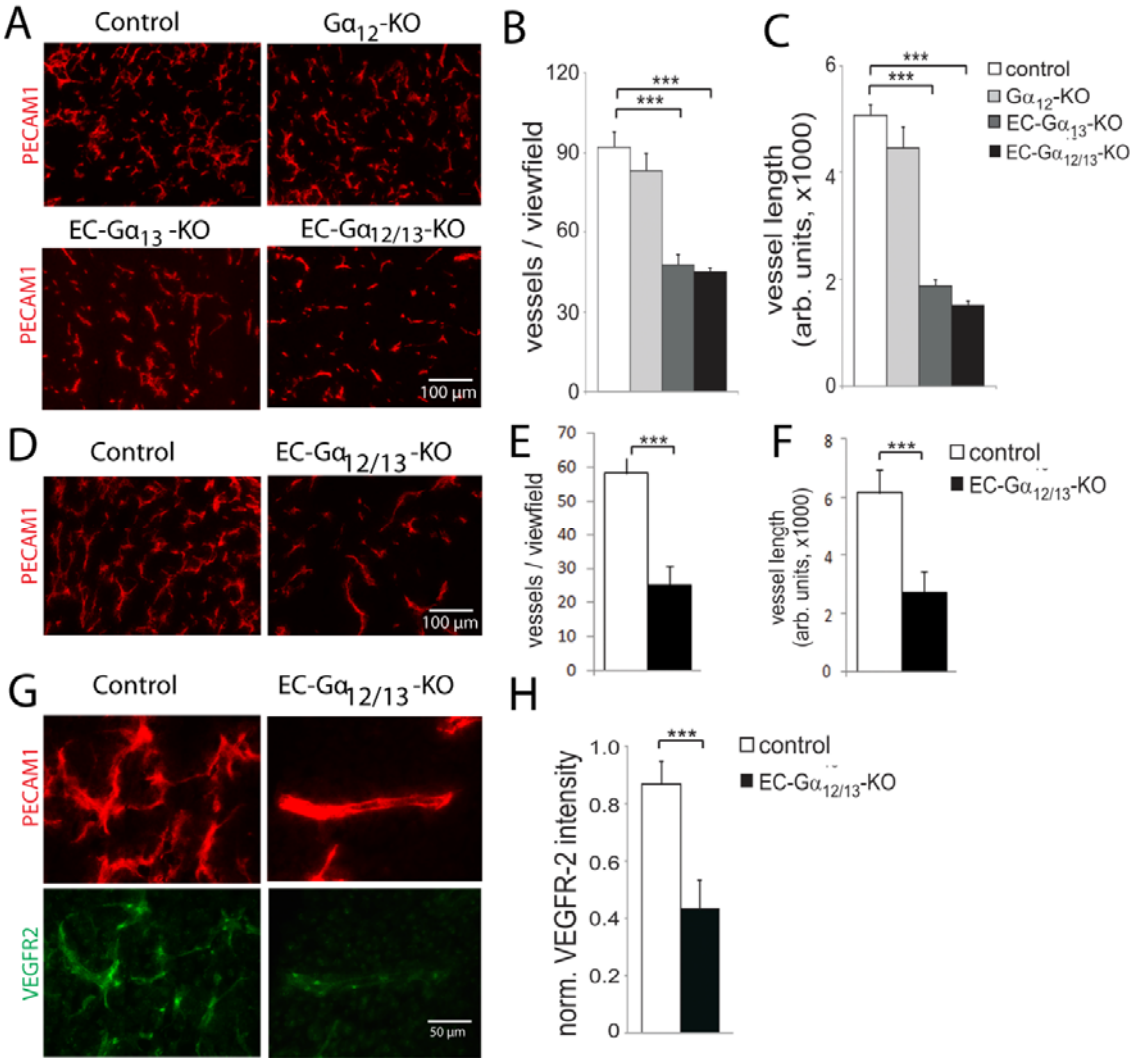

Figure 5-14: Relevance of $G\alpha_{13}$-mediated VEGFR-2 expression in tumor angiogenesis

A-C, Vascularization of LLC1 tumors was determined after PECAM1 staining (A, exemplary photomicrograph; B&C, statistical evaluation). **D-F**, B16 tumor vasculature (D, exemplary photomicrograph; E&F, statistical evaluation) (n=7–12). **G-H,** Immunostaining for VEGFR-2 in sections of LLC1 tumors grown in control mice and EC-$G\alpha_{12/13}$-KOs. The intensity of VEGFR-2 staining was normalized to the intensity of PECAM1 staining to correct for the general rarefaction of vessels (n = 4).

5.9.3 Endothelial $G\alpha_{12/13}$ signaling in vessel normalization

Tumor vessels are structurally and functionally abnormal. In contrast to normal vessels, tumor vasculature is highly disorganized; vessels are tortuous and dilated, with uneven diameter, excessive branching and shunts. This may be due to an imbalance of angiogenic regulators, such as VEGF and angiopoietins. Tumor vessels have numerous openings, widened interendothelial junctions, and a discontinuous or absent basement membrane. Tumor endothelial cells are abnormal in shape, growing on top of each other and projecting into the lumen. Theses defects make tumor vessels leaky and hyper-permeable. Consequently, tumor blood flow is chaotic and variable and leads to hypoxic and acidic regions in tumors. These conditions lower therapeutic effectiveness, modulate the production of angiogenic stimulators and inhibitors, and select for cancer cells that are more malignant and metastatic. Interestingly, tumor vessels grown in EC-$G\alpha_{13}$-KOs and EC-$G\alpha_{12/13}$-KOs showed signs of normalization as judged by morphology (**Figure 5-15A&B**). Since these parameters do not necessarily correlate with vessel function, we studied perfusion by delivery of isolectin B4. LLC1 tumor vessels grown in EC-$G\alpha_{13}$-KOs showed an increased percentage of perfused vessels compared to control tumor vessels (**Figure 5-15C&D**).

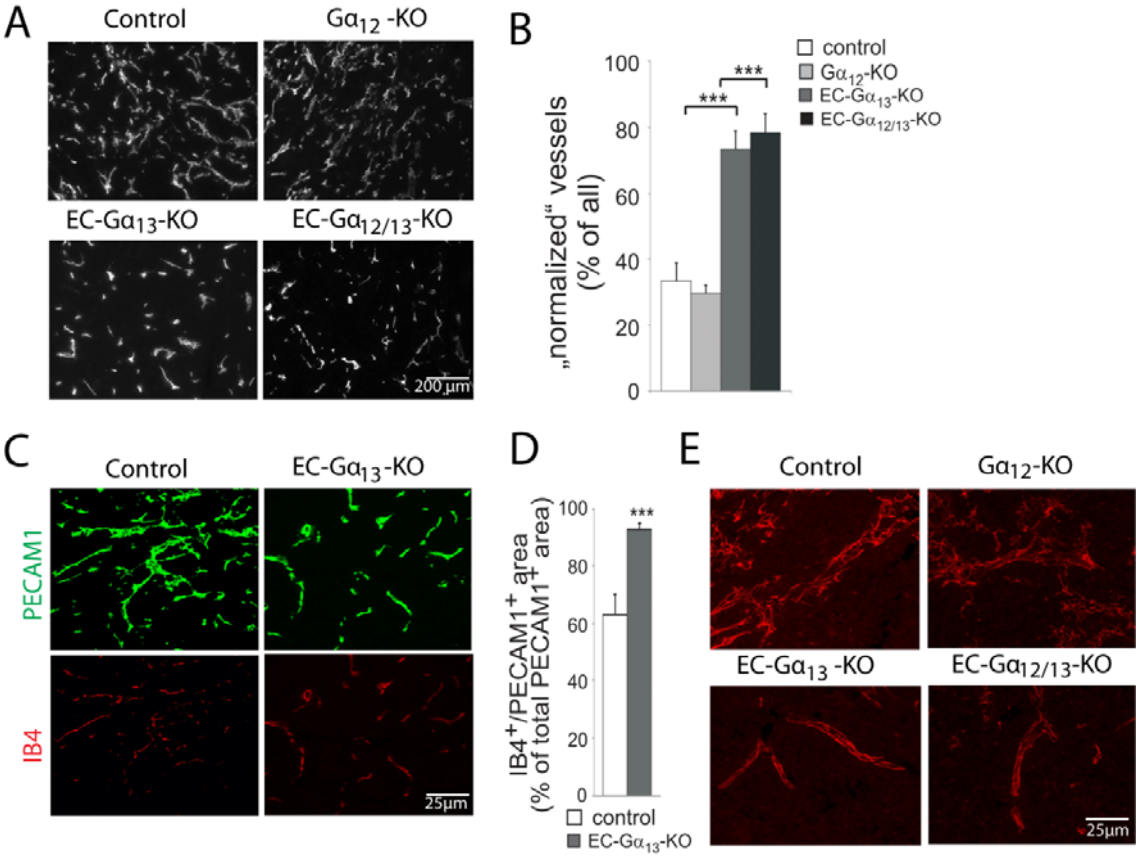

Figure 5-15: Tumor vessel normalization in EC-Gα$_{12/13}$-KOs.

A&B, Analysis of vessel morphology in PECAM1-stained sections of subcutaneous LLC1 tumors grown for 21 days in the indicated mouse lines. **C&D,** Tumor vessel perfusion was determined after retroorbital injection of isolectin B4 and PECAM1 immunostaining. The proportion of perfused vessels was determined as the percentage of IB4/PECAM1-double positive structures relative to the total number of PECAM1-positive structures. **E,** Staining of VE-cadherin in tumor vessels (n = 3-4 per group).

Tumor vessel staining for VE-Cadherin was more continous in EC- Gα$_{13}$-KOs than in control mice (**Figure 5-15E**). Since pericyte coverage is a hallmark of vessel maturation, we peformed co-stainings for PECAM1 and NG2 or α-smooth muscle actin (α-SMA), two pericyte markers. We observed increased pericyte coverage of tumor vessel in EC-Gα$_{13}$-KOs and EC-Gα$_{12/13}$-KOs (**Figure 5-16A&B**).

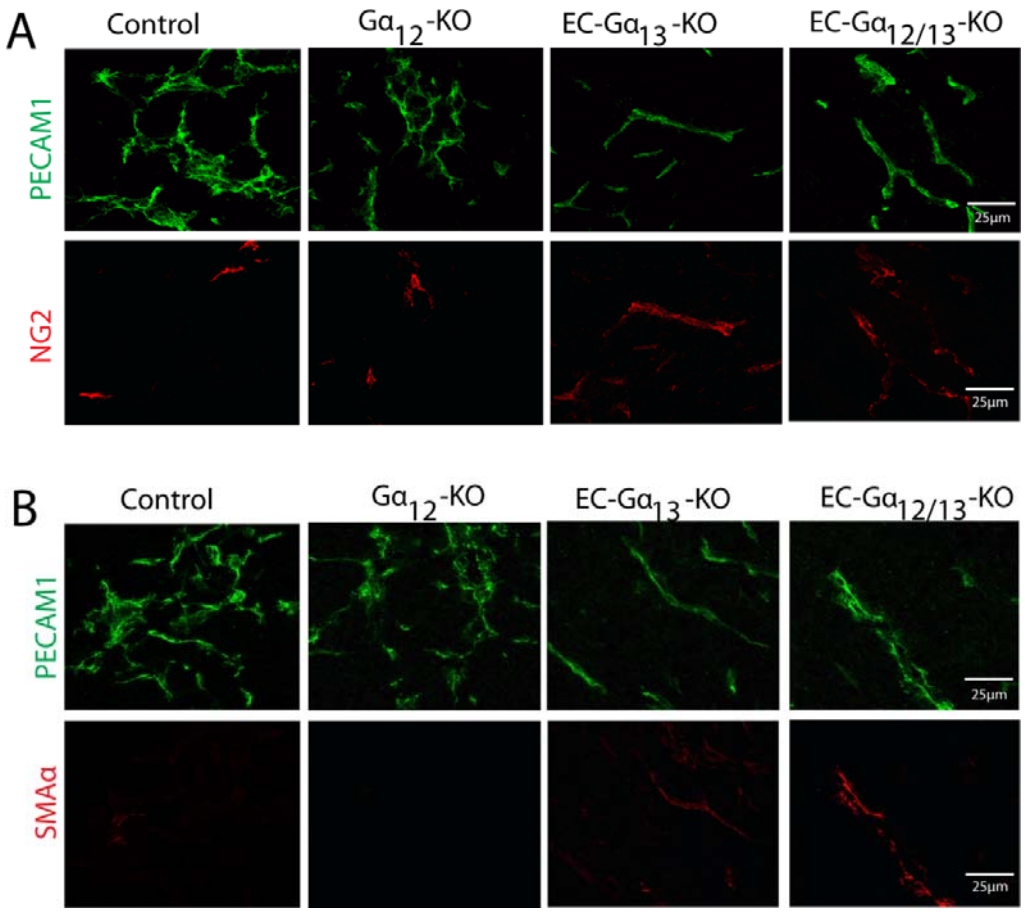

Figure 5-16: EC-G$\alpha_{12/13}$-KOs increased mural cell coverage in tumor vessel

A&B, Mural cell coverage in control, Gα_{12}-KO, EC-Gα_{13}-KO and EC-G$\alpha_{12/13}$-KO tumor vessels as determined by immunostaining using specific NG2 and SMAα markers. Pericyte coverage was determined as the proportion of PECAM1-positive areas that costained with pericyte markers NG2 (NG2/PECAM1) (A) or αSMA (αSMA/PECAM1) (B) relative to the total PECAM1-positive vessel area (n = 3-4 per group).

These findings show that endothelial Gα_{13} and G$\alpha_{12/13}$ signaling is not only important for developmental angiogenesis, but also plays a major role in tumor angiogenesis and tumor vessel normalization. Importantly, inactivation of endothelial Gα_{13} or G$\alpha_{12/13}$ in adult mice did not affect other endothelial functions such as control of permeability or vascular tone (data not shown) . Blocking endothelial Gα_{13} signaling therefore offers a new therapeutic target for the treatment of solid tumors.

5.10 GPCR dependent G-protein G_{13} signaling

Growth factor-induced G_{13}-mediated pro-migratory effects have been suggested to be partly due to GPCR independent activation of $G\alpha_{13}$. The C-terminus of Gα subunits of heteroterimeric G-proteins is essential for coupling to GPCRs, and deletion of the last five amino acids (QLMLQ) from the C-terminal end of $G\alpha_{13}$ has been shown to block GPCR/G-protein interactions (**Figure 5-17A**) (Shan et al., 2006).

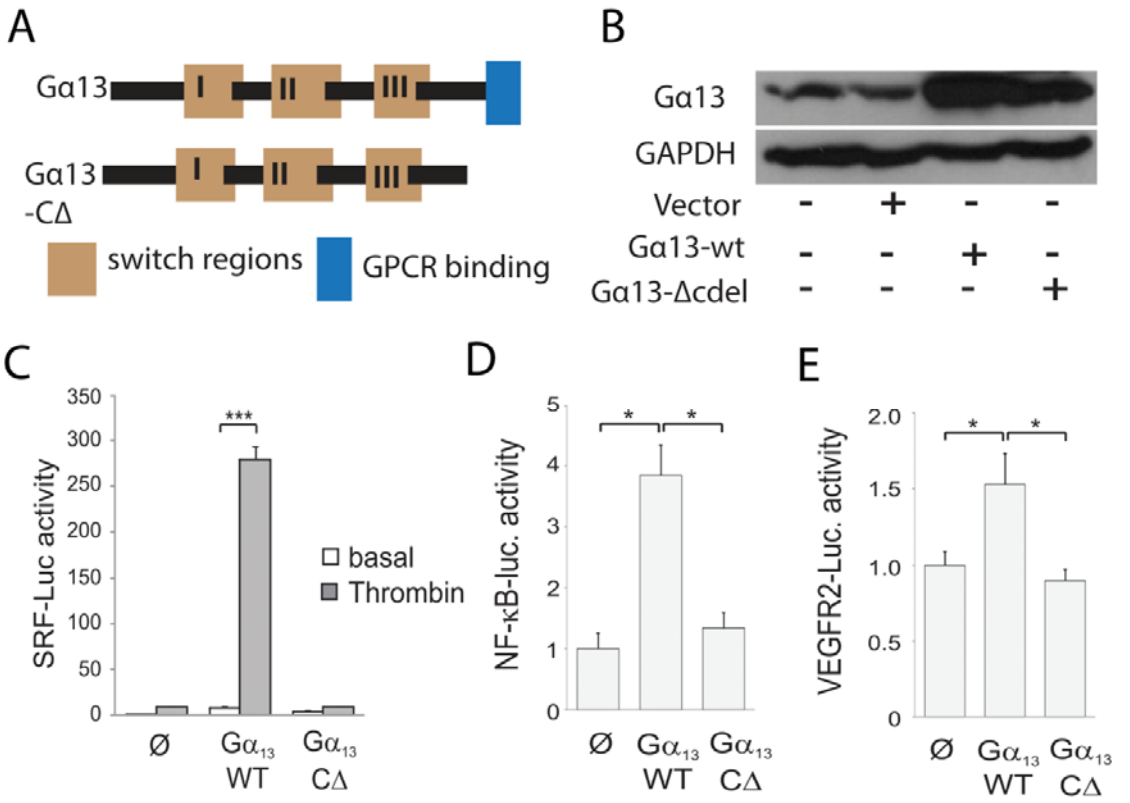

Figure 5-17: GPCR dependent $G\alpha_{13}$ mediated signaling

A, Schematic diagram of $G\alpha_{13}$-WT and $G\alpha_{13}$-CΔ mutant. **B,** Overexpression of control vector, $G\alpha_{13}$-WT and $G\alpha_{13}$-CΔ in HEK293 cells, **C,** Overexpression of $G\alpha_{13}$-WT, but not of $G\alpha_{13}$-CΔ, potentiates the effects of thrombin (10 U/ml) on serum response factor-dependent luciferase (SRF-Luc) expression in HEK293 cells (n = 2). **D,** An NF-κB-responsive luciferase reporter construct in HUVEC cells, (n = 2). **E**, Effect of overexpression of empty vector (Φ), $G\alpha_{13}$-WT and $G\alpha_{13}$-CΔ on the activity of a VEGFR-2 promoter-driven luciferase reporter construct; all data are presented as mean ± SEM.

To investigate whether GPCR-independent effects play a role in the pro-angiogenic effects of endothelial $G\alpha_{13}$, we generated wild-type $G\alpha_{13}$ ($G\alpha_{13}$-WT) and a C-terminally deleted $G\alpha_{13}$ mutant ($G\alpha_{13}$-CΔ), and transfected them into HEK293 cells. The protein expression levels of $G\alpha_{13}$-wt and $G\alpha_{13}$-CΔ were similar (**Figure 5-17B**). To confirm that the C-terminal deletion mutant could not couple to GPCRs, we examined agonist-induced serum response factor luciferase activity (SRF-Luc). Thrombin-induced SRF activity was increased in $G\alpha_{13}$-wt-transfected cells, but $G\alpha_{13}$-CΔ mutant abrogated the thrombin effect (**Figure 5-17B**). Next, we investigated the effect of the $G\alpha_{13}$-CΔ mutant on NF-κB and VEGFR-2 promoter activity in vitro. In contrast to wildtype $G\alpha_{13}$, the $G\alpha_{13}$-CΔ mutant impaired the ability to activate the VEGFR-2-Luc or NF-κB-Luc reporter constructs (**Figure 5-17C&D**). These in vitro results show that $G\alpha_{13}$-mediated signaling controls VEGFR-2 promoter activity and NF-kB activity in a GPCR-dependent manner.

Because $G\alpha_{13}$-mediated proangiogenic effects have been suggested to be due to GPCR-independent activation of $G\alpha_{13}$ (Shan et al., 2006), we tested whether the $G\alpha_{13}$-Cdel mutant was able to rescue defective tumor angiogenesis in EC-$G\alpha_{13}$-KOs. To do so, we reintroduced either wildtype $G\alpha_{13}$ or the C-terminal deletion mutant $G\alpha_{13}$-CΔ into EC-$G\alpha_{13}$-KOs (**Figure 5-18A**) and analysed tumor angiogenesis. We found that tumor growth and tumor angiogenesis was rescued in EC-$G\alpha_{13}$ KO overexpressing wild-type $G\alpha_{13}$ ($G\alpha_{13}$-WT), but not in EC-$G\alpha_{13}$-KOs overexpressing $G\alpha_{13}$CΔ **(Figure 5-19A-E)**.

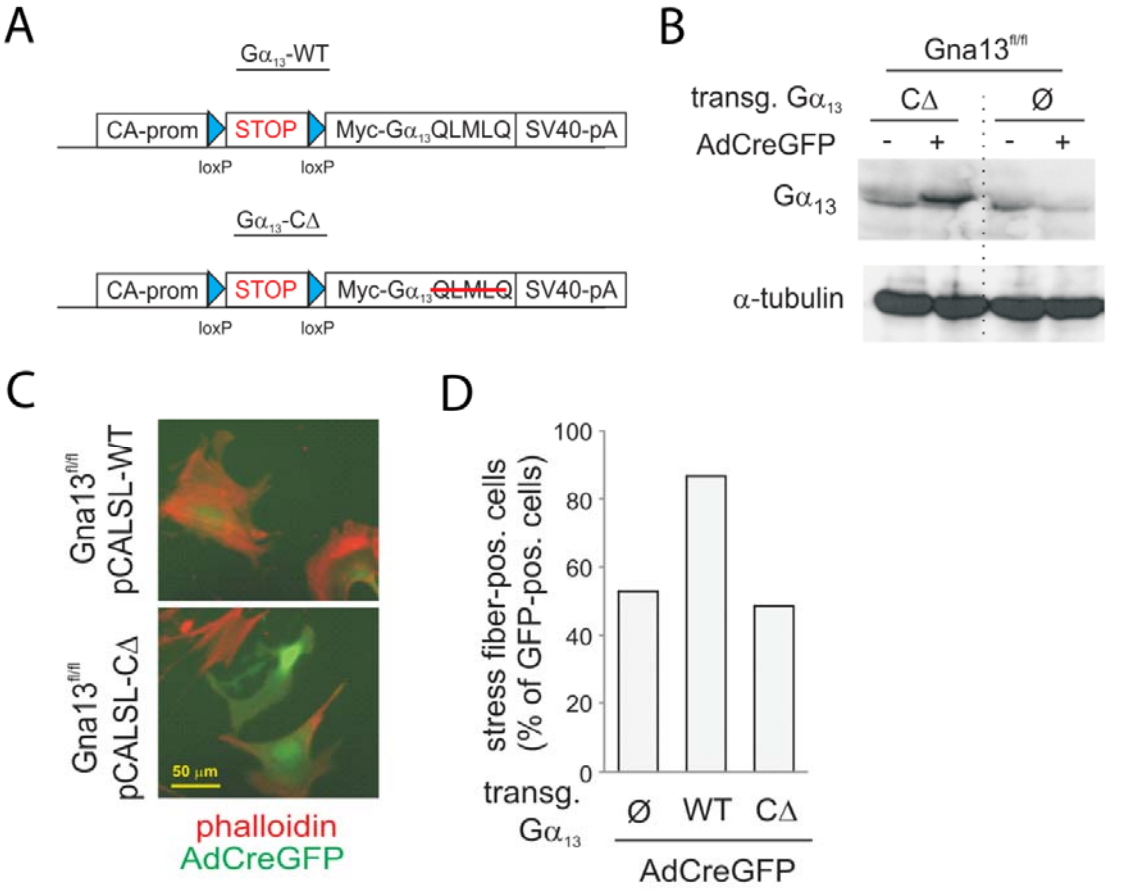

Figure 5-18: Generation of Gα$_{13}$-WT or Gα13-CΔ transgene mouse

A, Design of the plasmid-based rescue strategy, CA-prom, chicken actin promoter; SV40-pA, simian virus 40 poladenylation signal; loxP, loxP site mediating Cre-dependent recombination; myc, myc tag; stop, transcriptional and translational stop cassette. The 15 base pairs coding for the C-terminal amino acids QLMLQ mediating interaction with GPCRs were deleted in Gα13-CΔ. **B,** Lung endothelial cells from Gna13$^{fl/fl}$ mice carrying either no transgene (Φ) or the Gα13-CΔ transgene (CΔ) were infected with a Cre- expressing adenovirus (AdCreGFP) and Gα$_{13}$ immunoreactivity was determined after 72 hrs by Western blotting (α-tubulin as loading control) (n = 2). **C,** Lung endothelial cells obtained from Gna13$^{fl/fl}$ mice carrying either the Gα$_{13}$-WT transgene or the Gα13-CΔ transgene were infected with a Cre-expressing adenovirus (AdCreGFP) and LPA (1µM)-induced stress fiber formation was determined by phalloidin staining after 16 hrs of serum starvation (left: exemplary photomicrograph, magnification 400x; right: statistical evaluation) (n = 2).

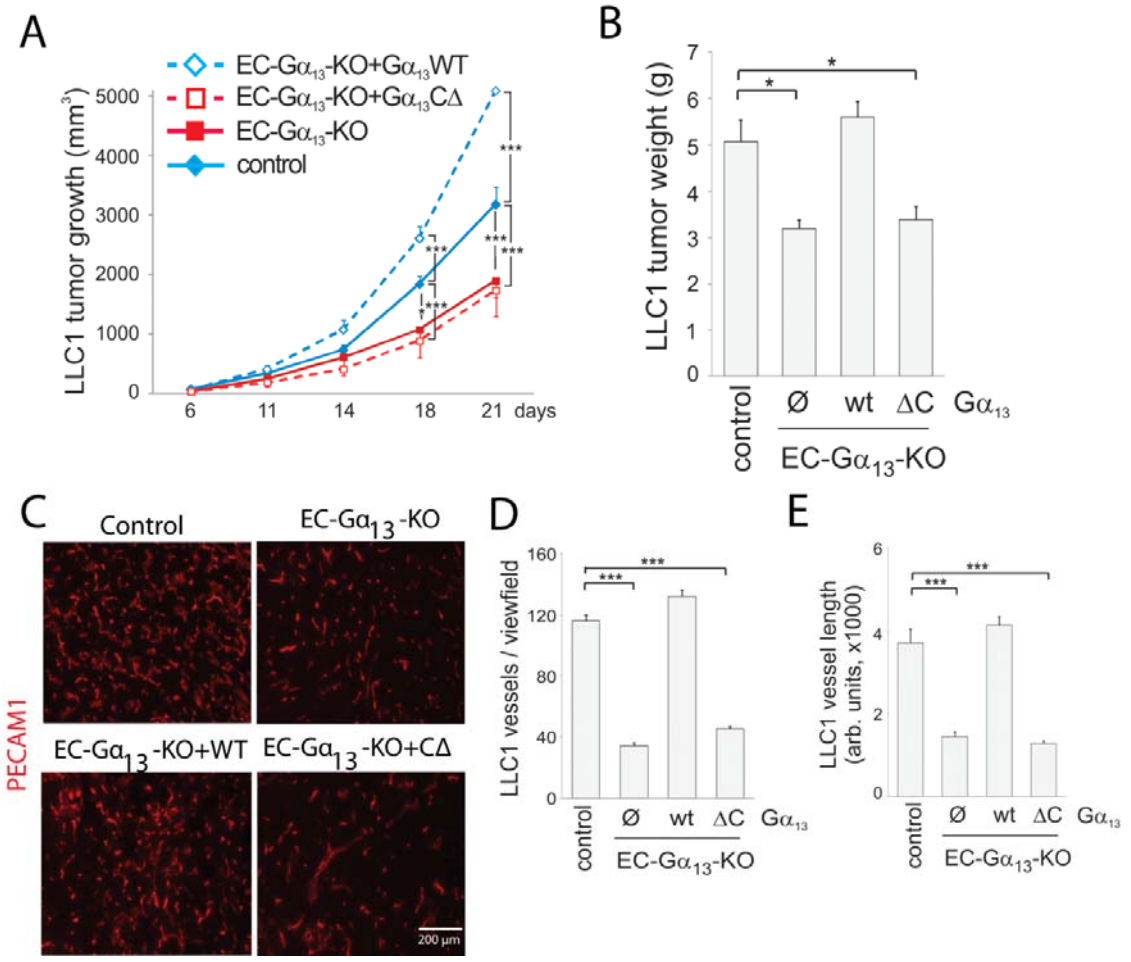

Figure 5-19: GPCR mediated $G\alpha_{13}$ tumor growth and tumor angiogenesis.

A&B, LLC1 tumor growth curve and final tumor weight. **C,** tumor vascularization of control, EC-$G\alpha_{13}$-KOs, and EC-$G\alpha_{13}$-KOs overexpressing wild-type $G\alpha_{13}$ ($G\alpha_{13}$WT) or a C-terminal deletion mutant of $G\alpha_{13}$ ($G\alpha_{13}$CΔ) tumor section stained by endothelial cell marker PECAM1. **D&E**, quantification of tumor vessels. (n = 6–10).

Taken together, these results show that GPCR-dependent G-protein $G\alpha_{13}$ signaling is important for regulation of VEGFR-2 expression through the small GTPase RhoA and transcription factor NF-κB and that loss of endothelial G_{13} signaling results in reduced physiological (retinal) and pathological (tumor) angiogenesis.

6. DISCUSSION

Angiogenesis plays an important role in embryonic development and during postnatal organ development, it is also crucial for various physiological and pathological remodeling processes of the adult organism. In this study we show that G-protein $G\alpha_{13}$ signaling controls retinal and tumor angiogenesis through regulation of VEGFR-2 expression. Moreover, we demonstrate that VEGFR-2 expression is controlled by GPCR agonists like thrombin and S1P and that $G\alpha_{13}$-mediated RhoA and NF-κB activation is required for VEGFR-2 expression in endothelial cells.

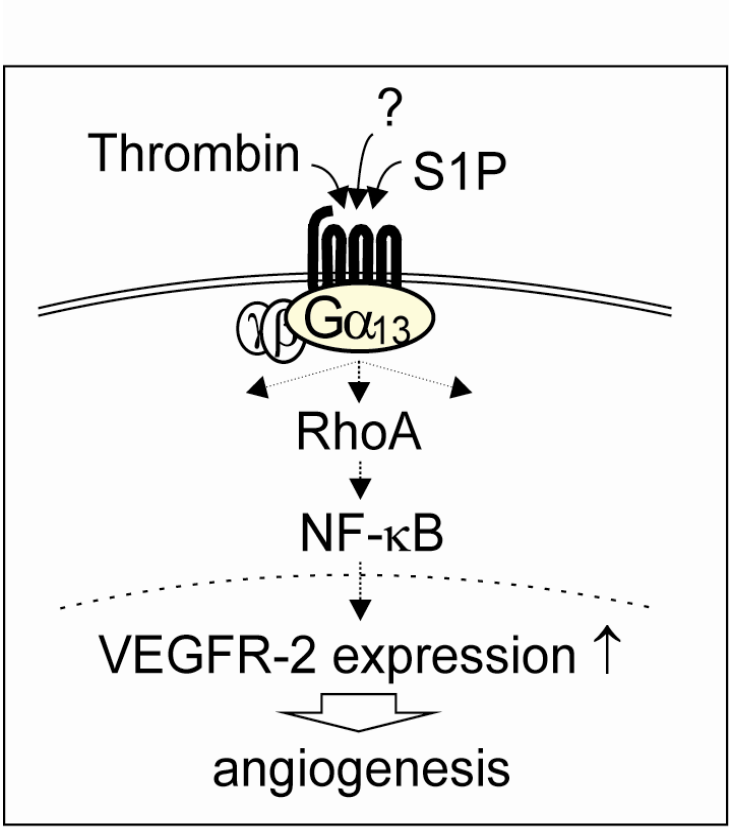

Figure 6-1: Schematic summary of G_{13} controls angiogenesis through regulation of VEGFR-2 expression. From (Sivaraj et al., 2013).

6.1 G_{13} signaling in angiogenesis

Heterotrimeric G-proteins of the $G_{12/13}$ family play multiple roles in biological functions. It has been reported that the constitutive $G\alpha_{13}$ knockout showed impaired ability of endothelial cells to develop into an organized vascular system, resulting in embryonic lethality at day E9.5 (Offermanns et al., 1997). EC-specific $G\alpha_{13}$-KOs showed similar phenotypes, suggesting that endothelial dysfunctions underlie the observed developmental defects (Ruppel et al., 2005). Our results show that inducible EC-$G\alpha_{13}$-KOs display reduced retinal vessel growth and sprouting. In contrast, mice lacking the closely related $G\alpha_{12}$ did not show any obvious defects in retinal vessel growth, and combined inactivation of $G\alpha_{12}$ and $G\alpha_{13}$ did not further aggravate the phenotype. These findings indicate that $G\alpha_{13}$ can compensate loss of $G\alpha_{12}$, while $G\alpha_{12}$ cannot make up for loss of $G\alpha_{13}$. These results suggest that $G\alpha_{13}$-mediated signaling pathways play an important role in postnatal angiogenesis.

6.2 G_{13} controls VEGFR-2 expression

In angiogenesis, endothelial sprouting involves the specialization of tip cells, a highly motile and invasive cell population that extends filopodia to detect tissue-derived cues such as VEGFs (Gerhardt et al., 2003). Activation of VEGFR-2 in tip cells leads to increased filopodia extension and stimulates the proliferation of stalk cells (Nakayama et al., 2013), and inducible ECs-specific inactivation of VEGFR-2 results in reduced retinal angiogenesis (Benedito et al., 2012).

Our analysis of angiogenic gene expression in EC-$G\alpha_{13}$-KO retinae showed a selective reduction of VEGFR-2 expression to approximately 50%, and our in vitro

studies suggest that this reduction suffices to impair VEGF-induced protein phosphorylation and tube formation. However, heterozygous VEGFR-2-deficient mice are without a clear angiogeneic phenotype, it might therefore be argued that a 50% reduction in VEGFR-2 levels is not sufficient to explain the observed in vivo defects. To directly address this issue we studied in collaboration with R. Adams / Münster retinal vessel development in mice with tamoxifen-inducible, endothelial cell-specific heterozygous inactivation of Vegfr-2. To generate these mice, the tamoxifen-inducible, endothelial cell-specific Pdgfb-iCre line (Claxton et al., 2008) was bred into a $Vegfr2^{lox/wt}$ (Haigh et al., 2003) background and Cre activity was induced in newborn mice by intraperitoneal injections of 50µg tamoxifen on postnatal days 1-3. Pdgfb-iCre;$Vegfr2^{lox/wt}$ mice showed a retinal phenotype resembling that of EC-$G\alpha_{13}$-KOs, with significantly reduced endothelial cell (EC) coverage and branch point number (**Figure 6-2**).

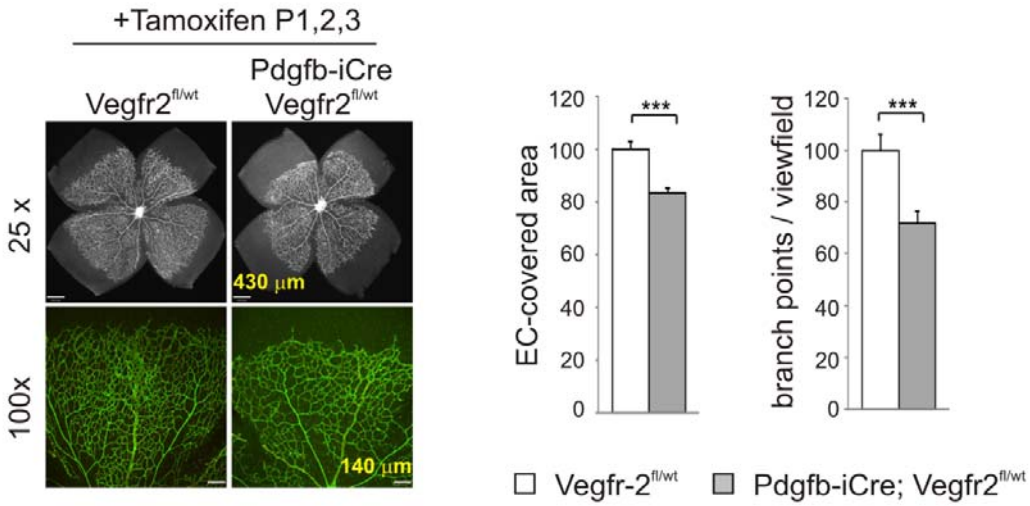

Figure 6-2: ECs-specific heterozygous of VEGFR-2 showed reduced retinal angiogenesis.

Retinal angiogenesis in mice with tamoxifen-inducible heterozygous endothelial-cell specific inactivation of Vegfr2 (Pdgfb-iCre;$Vegfr2^{fl/wt}$). EC-covered area and of branch point numbers in isolectin B4-stained retinae from 6-day-old mice after tamoxifen

treatment on postnatal days 1-3 (n = 4; values of control mice set to 100%). Endothelial nuclei are stained with anti-Erg antibodies (red). From (Sivaraj et al., 2013).

Though these data indicate that an acute reduction of VEGFR-2 expression to 50% may well underlie the observed angiogenic defect in EC-Gα_{13}-KOs, we can at this point not fully rule out that other defects of Gα_{13}-deficient ECs contribute to the phenotype, for example alterations in adhesion or migration. It is currently not clear to what degree reduced VEGFR-2 expression also underlies the embryonic lethality of constitutively Gα_{13}- and G$\alpha_{12/13}$-double deficient mice. It is in this context noteworthy that both VEGFR-2-deficient mice and G$\alpha_{12/13}$-deficient mice die at embryonic day E8.5 with similar abnormalities in vascular development (Gu et al., 2002; Shalaby et al., 1995)

VEGFR-2 expression is tightly controlled by Notch signaling in angiogenesis. VEGF signaling activates Notch in sprouting endothelial cell (tip cells), leading to down-regulation of VEGFR-2 expression in stalk cells. The activation of Dll4-Notch by VEGFR-2 and repression of VEGFR-2 expression downstream of Notch activation are seen as a two crucial process regulating endothelial sprouting and angiogenesis (Adams and Alitalo, 2007; Herbert and Stainier, 2011; Roca and Adams, 2007). Our in vitro studies revealed that Notch signaling is not altered by loss of Gα_{13} in endothelial cells.

6.3 $G\alpha_{13}$-coupled GPCRs regulate VEGFR-2 expression on the transcriptional level

Though it is clear that VEGFR-2 expression is upregulated at sites of angiogenesis (Gerhardt et al., 2003) the mechanisms regulating VEGFR-2 expression are incompletely understood. It has been shown that mechanosensitive signaling can control VEGFR-2 promoter activity in human microvascular endothelial cells by modulating the balance of activities between two antagonistic transcription factors, TFII-I and GATA2 (Mammoto et al., 2009). What is more, flow-induced shear stress was suggested to regulate VEGFR-2 expression through an Sp1 site (Urbich et al., 2003). In addition, angiogenic growth factor such as FGF are known to induce activation of ERK signaling, leading to the binding of transcription factor Ets to the E-box motif of the VEGFR-2 promoter (Murakami et al., 2011).

We show here for the first time that GPCRs agonists such as thrombin or S1P can induce VEGFR-2 promoter activity in an G_{13}-dependent manner. GPCRs have previously been suggested to regulate angiogenesis by modulating endothelial cell migration, permeability, or VEGF production (Dorsam and Gutkind, 2007; Richard et al., 2001), but their role in the regulation of VEGF receptor expression is not well understood (Tsopanoglou and Maragoudakis, 1999).

The serine protease thrombin has various biological functions including fribrin formation and platelet activation, its cellular effects are mediated by the family of Protease Activated G-protein coupled Receptors (PARs). Thrombin acts as pro-angiogenic stimulus through various mechanisms, including the increased

expression of VEGF in cancer cells and VEGF receptors in endothelial cells; it also promotes endothelial cell migration and survival. In addition, thrombin cleaves fibrinogen to form fibrin rich extracellular matrix, therefore creating an environment, favorable for endothelial cell adhesion and tubulogenesis (Dorsam and Gutkind, 2007; Nierodzik and Karpatkin, 2006; Richard et al., 2001). In line with an important role of thrombin receptors in angiogenesis, genetic inactivation of the thrombin receptor subtype PAR1 leads to a fatal bleeding defect in a fraction of early mouse embryos and partly recapitulates the phenotypes of $G\alpha_{13}$-deficient mice (Connolly et al., 1996). Interestingly, re-expression of PAR-1 in endothelial cells rescues the fatal vessel fragility and bleeding in PAR-1 deficient mice (Griffin et al., 2001), a finding that further supports the important role of endothelial PAR1 in vessel formation.

Sphingosine 1-phosphate (S1P) is a blood-borne lipid mediator that has been implicated in the regulation of vascular and immune functions. S1P binds to and activates a family of five G-protein coupled receptors, S1PR1-5, which initially were described as “endothelial cell differentiation gene” (EDG)-receptors (Spiegel and Milstien, 2003). S1PR1,-2 and -3 are expressed in endothelial cells. Complete abrogation of S1P production in sphingosine kinase 1/2 deficient mice results in embryonic death between E11.5 and E13.5 due to neurological and vascular defects (Kono et al., 2004). In addition, embryonic lethality due to defective vascular maturation is observed in mice deficient for S1PR1 (Liu et al., 2000).

6.4 $G\alpha_{13}$-dependent control of VEGFR-2 promoter activity involves the small GTPase RhOA

Our in vitro studies illustrate that G_{13} controls VEGFR-2 expression through regulation of RhoGTPase RhoA, a well known effector of $G\alpha_{12/13}$. In general, RhoGTPases control the organization of the actin cytoskeleton; they are crucial for cellular functions such as adhesion, migration, and polarization. For example, RhoA signaling was shown to be required for VEGF induced ECs migration and sprouting (van Nieuw Amerongen et al., 2003). $G\alpha_{12/13}$ –mediated RhoA activation depends on three RhoGEF proteins, PDZRhoGEF, LARG and Lsc/p115RhOGEF (Worzfeld et al., 2008). Absence of these three RhoGEF blocks thrombin induced RhoA activation, and PDZRhoGEF/LARG double deficienct mice die at embryonic day (9.5) due to multiple vascular defects (Mikelis et al., 2013).

6.5. $G\alpha_{13}$ and RhoA regulate the VEGFR-2-promoter activity through NF-kB

Most mammalian promoters contain a TATA box, which recruits the transcription factor TFIID to start the transcription, but the VEGFR-2 promoter contains an initiator element (Inr), which overlaps the transcription start site instead of the TATA box. The VEGFR-2 promoter also contains four canonical E-box motifs, at least five Sp1 binding sites, an NF-κB site, and a TFII-I binding to the initiator (Inr) region of the promoter (Patterson et al., 1995).

Our studies show that $G\alpha_{13}$/RhoA-dependent VEGFR-2 expression involves the transcription factor NF-κB. NF-κB-mediated regulation of gene expression plays a crucial role in the cellular responses to cytokines, free radicals, bacterial or viral antigens. In the inactivate state, NF-κB is kept in the cytosol by complex formation with the inhibitory protein IκBα. Upon activation of pro-inflammatory transmembrane receptors (for example receptors for TNFα, IL-1β, or Toll-like receptors), the enzyme IκBα-kinase (IKK) is activated, which in turn results in the phosphorylation and degradation of the inhibitory IκBα protein. The freed NF-κB dimers translocate to the nucleus, where they bind to specific sequences in the promoter or enhancer regions of target genes. Activated NF-κB can then be downregulated by newly synthesized IκBα protein (Perkins, 2007). RhoA has been shown to efficiently induce transcriptional activity of NF-κB-dependent genes by a mechanism that involves phosphorylation and degradation of IκBα, leading to translocation of p50/p65 dimers to the nucleus (Perona et al., 1997). In line with our own findings it was furthermore suggested that GPCR agonists such as thrombin are able to induce activation of NF-κB in endothelial cells (Rahman et al., 2001; Xue et al., 2009). Our study, however, is the first to directly link GPCR-induced activation of $G\alpha_{13}$, RhoA and NF-κB to the regulation of VEGFR-2 promoter activity. Interestingly, also other activators of NF-κB signaling, for example TNFα, have been shown to upregulate VEGFR-2 expression (Illi et al., 2000; Sainson et al., 2008), but this effect was not affected by knockdown of $G\alpha_{13}$. Given the fact that NF-κB signaling regulates a great number of genes, it is slightly surprising that loss of endothelial $G\alpha_{13}$ results in a selective reduction of VEGFR-2 expression. Our analysis of angiogenesis-related genes indicated that loss of $G\alpha_{13}$ in endothelial cells selectively affects VEGFR-2 expression, while other putative NF-κB target genes such as Mmp9, Vegf-c, Pdgfb or Hif1 are not altered.

Why exactly $G\alpha_{13}$-dependent NF-κB activation is important for VEGFR-2 expression, but not for expression of other NF-κB target genes, is currently unclear. To mention just one possibility, it has been suggested that parallel signaling pathways activated by a given receptor may result in signaling crosstalk that shapes the NF-κB response in ways that are unique to the individual receptor (Hayden and Ghosh, 2008). $G\alpha_{13}$-coupled receptors for example can modulate gene expression through myocardin-related transcription factors (Althoff et al., 2012) or MEF2c (Liu et al., 2009). Whereas the VEGFR-2 promoter does not contain binding sites for these transcription factors, other NF-κB target genes might do so, resulting in a gene-specific net effect of $G\alpha_{13}$ activation/inhibition on promoter activity. However, since our expression analysis contained only four out of more than 500 putative NF-κB-regulated genes, we can of course not exclude that effects on other NF-κB-regulated genes exist.

6.6 G_{13} mediated signaling in pathological angiogenesis

Our in vivo studies show that endothelial $G\alpha_{13}$ is not only required for physiological angiogenesis in the retina, but also for tumor angiogenesis. Many solid tumors rely on GPCRs to elicit an angiogenic response. Thrombin for example acts as a pro-angiogenic stimulus by increasing expression of VEGF in cancer cells and by promoting endothelial cell migration and survival. In addition, thrombin cleaves fibrinogen to form fibrin rich extracellular matrix, therefore creating an environment favorable for endothelial cell adhesion and tubulogenesis (Dorsam and Gutkind, 2007; Nierodzik and Karpatkin, 2006; Richard et al., 2001). Our data clearly show that endothelial $G\alpha_{13}$ signaling plays a crucial role in tumor angiogenesis. As

observed in retinal angiogenesis and in our in vitro studies, inactivation of endothelial $G\alpha_{13}$ was associated with reduced VEGFR-2 expression in tumor vessels, suggesting that also in pathological angiogenesis $G\alpha_{13}$ is an important regulator of VEGFR-2 expression.

Tumor vessels from EC-$G\alpha_{12/13}$ KOs not only showed reduced sprouting, but also signs of morphological normalization and increased pericyte coverage. Tumor vessels are structurally and functionally abnormal, with defective endothelium, basement membrane, and pericyte coverage (Jain et al., 2003). These abnormalities impair the delivery of oxygen and therapeutics to tumor cells (Jain et al., 2005). A number of studies showed that VEGFR-2 blockade using monoclonal antibodies can temporarily normalize tumor vessel structure (pericyte and basement membrane coverage), leading to improved vascular function (tumor oxygenation) and enhanced response to radiation therapy (Tong et al., 2004).

6.7 GPCR dependent G_{13} signaling

While ligand-bound GPCRs are certainly the major activators of $G\alpha_{13}$, a few GPCR-independent mechanisms of $G\alpha_{13}$ activation have been suggested. For example, Gong et al. showed that outside-in integrin (β1 and β3) signaling induces platelet spreading through $G\alpha_{13}$-mediated signaling (Gong et al., 2010). In addition, Shan et al. showed that $G\alpha_{13}$-mediated signaling controls PDGF induced cell migration. Our in vitro studies clearly indicate that $G\alpha_{13}$-mediated regulation of VEGFR-2 expression is strictly GPCR-dependent, since the $G\alpha_{13}C\Delta$ mutant was unable to induce VEGFR-2 expression and NF-κB activation. Furthermore, our in vivo findings show that G_{13}-

dependent pro-angiogenic effects are GPCR-dependent: In contrast to $G\alpha_{13}$-WT, re-expression of $G\alpha_{13}C\Delta$ did not normalize impaired LLC1 tumor vascularization in EC-$G\alpha_{13}$-KOs. We therefore conclude that at least in the context of postnatal angiogenesis, $G\alpha_{13}$-dependent endothelial effects are GPCR dependent.

6.8 G_{13} inhibitor is a possible anti-angiogenic therapy

Our findings suggest that blocking endothelial $G\alpha_{13}$ signaling might be used as an anti-angiogenic therapy, since endothelial $G\alpha_{13}$ deficiency resulted in reduced tumor growth by reducing the number of blood vessels. What is more, endothelial $G\alpha_{13}$ deficiency resulted in normalization of the tumor vasculature, which might improve the delivery of anti-neoplastic drugs and prevent the selection of highly malignant tumor cells (Jain, 2005). It is in this context important to mention that acute inactivation of endothelial $G\alpha_{13}$ in the adult mouse did not have major effects on other basal endothelial functions such as endothelial permeability or baseline blood pressure regulation (Korhonen et al., 2009). Unfortunately, currently no small-molecule inhibtors are available for $G\alpha_{13}$, and we are also lacking effective strategies to selectively target endothelial cells in order to prevent unwanted effects in other organ systems (Herroeder et al., 2009)(Althoff et al., 2012).

7. METHODS

7.1 Bacterial culture and competent cell preparations

Single colonies of DH5α or DH10β were picked from a LB agar plate. Bacteria colony was inoculated into 5 ml of LB medium. The bacteria culture was grown at 37°C with shaking 200 rpm an overnight (o/n). 1 ml of bacterial culture was inoculated into 300 to 500 ml of LB medium was grown at 37°C with shaking 200 rpm until the optical density measured with 600 nm wavelength reached 0.5-0.8. The culture was chilled on ice for 30 min followed by centrifuged at 4000xg at 4°C. The pellet was resuspended in 200ml of cold 10% glycerol and repeated two to three times. The bacteria suspension was then centrifuged as above and resuspended in 3 ml of 10% glycerol. Aliquots of 50 µl were frozen in liquid nitrogen and stored at -80°C.

7.2 Plasmid transformations and isolation

Electroporation of DNA: Competent bacteria were thawed on ice and 1- 2 µl of plasmid DNA (0.1-1.0 µg) was added. The mixture was transferred into a sterile, pre-chilled 0.2 cm cuvette without making bubbles. The gene pulser apparatus was set to 25 µF and 2.5 kV, the pulse controller to 200 Ω. The dried cuvette was placed into the chamber slide and pulsed once. Immediately, 950 µl of SOC or LB medium without antibiotic was added to the cells, which were then transferred to a 1.5 ml tube and shaken 60 min at 37ºC. Subsequently, the bacteria were spread on LB plates containing selective antibiotic and grown o/n at 37°C.

Heat Shock methods: Thaw a tube of DH10β competent E.Coli cells on ice. Mix gently and carefully pipette 50 µl of cell into the transformation tubes on ice. Add 5-10 µl of ligation products to the cell mixture. Place the mixture on ice for 5 min. Heat shock at exactly 42^{o}C for 90 seconds. Place the tube on ice for 5 min. Pipette 950 µl of SOC medium and shaken for 60 min at 37ºC. Spread 50-100 µl of bacteria spread to a selection plate and incubate overnight at 37^{o}C.

Plasmid DNA isolation: Plasmid DNA was purified from small-scale (5 ml, mini preparation) or from large-scale (250 ml, maxi preparation) bacterial cultures. Single colonies of transformed bacteria or from a bacterial glycerol stock were picked each into LB medium containing 100 µg/ml selective antibiotic and grown for 14-18 h at 37°C with shaking at 200 rpm. Mini- and maxi preparation of plasmid DNA were carried out according to the QIAGEN protocol using lysis of the cells and binding of the plasmid DNA to a special resin. After washing, elution and precipitation the plasmid DNA was dissolved in a suitable volume of pure PCR grade water. QIAGEN EndoFree Plasmid Maxi kit was used for nucleofection to the HUVEC. DNA concentration was measured by using Nano trop.

7.3 Enzymatic digestions and ligation

Plasmid digestions: Approximate 1-2 µg of DNA was digest in with 1-2 µl of restriction enzymes in 20 to 50 µl of the reaction with appropriate buffer. The incubation temperatures were as indicated for optimal activity of each enzyme.

Ligating vector and target DNA fragments: A 10 µl reaction containing purified linearized vector and DNA fragments in 1:5 molar ratio, 1 µl of 10x ligation buffer, and 1 µl of T4 DNA ligase was incubated o/n at 16^{o}C or at RT for 2 h, followed by 30 min at 37^{o}C for sticky end ligations. Approximately 2-5 µl of the reaction was used to transformation.

7. 4 Polymerase chain reaction (PCR)

Cloning PCR: Interested double stranded DNAs were amplified by PCR reactions using specific primers. Amplified products digested and cloned into target vector.

Mutation PCR: Site specific mutation was introduced by two complimentary oligonucleotide (Primers) containing the desired mutation, flanked by unmodified nucleotide sequence. For mutation PCR circular double stranded DNA (Vector) with an insert of interest and two oligonucleotide primers containing the desired mutation. The primers, each complementary to opposite strands of the vector, are extended during PCR by Pfu DNA polymerases and incorporate the mutagenic primers resulting in nicked circular strands. Digest the methylated, nonmutated parental DNA template with DpnI. Transformed into the competent cells and right mutating were screened by sequencing.

Genotyping PCR: Tail tips (1-3 mm) were taken from mice, tail samples were incubated overnight at 56°C on a thermomixer (900 rpm) in 300 µl of Tail-buffer. Next day, samples are vortex and centrifuged 13000 rpm for 5 min at RT. 200 µl of the supernatant were transferred to fresh tube containing 700 µl of DNA precipitation

buffer. Centrifuge for 10 min -13000 rpm at 4^{o}C, supernatant were discarded and DNA washed with 1 ml of 70% ethanol. DNA pellet were dissolved 200 µl of PCR grade water, and concentration was measured by using Nano trop. For PCR, 1-2 µl of tail DNA was used as template in the PCR reaction containing 200 µM dNTPs, 10 pmol of each primers to amplify a sequence of genomic DNA specific for a given allele, 1x PCR buffer and 0.5 µl of Taq polymerase. The PCR was carried out in a total volume of 50 µl. Agarose gel electrophoresis was used to separate PCR products.

7.5 Agarose gel electrophoresis and DNA purification

Agarose gel electrophoresis: According to the DNA sizes, 0.8-2% agarose gel was prepared by microwave melting agarose in TAE buffer. After the agarose solution cooled down to ~45°C, ethidium bromide was added and the solution was poured into a gel chamber. When the gel solidified DNA solution mixed with loading buffer were loaded onto the gel and run for 30-35 min at 180-200 V. DNA was visualized and photographed under UV light using a gel documentation system.

DNA purification: The appropriated DNA band (according to its size) was excised from the agarose gel with a scalpel and purified by the QIAquick Gel Extraction Kit (QIAGEN) as recommended by the manufacturer. The DNA was eluted in 15 µl of deionized water or elution buffer.

7.6 Cell culture

Cells: Human umbilical vein endothelial cells (HUVEC:Lonza) was cultured in EGM 2 medium with supplement and passages < P4 were used for all experiments. Fibroblasts were cultured in Dulbecco modified Eagle medium (DMEM) supplemented with 10% of fetal bovine serum (FBS). Human embryonic kidney (HEK)–293, mouse Lewis lung carcinoma cells, and B16-F10 cells were cultured in Dulbecco modified Eagle medium supplemented with 10% FBS at 37^0 C in 5% Co_2.

Subculture: Confluent cells in 10 cm dishes were washed once with warm PBS, and incubated with 2 ml of Trypsin/EDTA for approximately 2 min to detach cells from the dish. Growth medium containing FBS was added to stop trypsin enzymatic activity. Cells were usually seeded in a 1:3 HUVEC or 1:6 ratio for other cell line experiments in the following day.

Cell freezing: Cell lines were frozen in 40% growth medium, 50% FBS, and 10% DMSO. Cells from a 10 cm confluent plate were aliquot into 3 cryotubes (2 ml) which were quickly transferred into an isopropanol container and stored at -80°C. Once the cells were frozen they were transferred to liquid nitrogen tank for long-term storage. To recover frozen cells, cells were thawed slowly on ice, resuspended in growth medium, pelleted to remove DMSO and seeded.

7.7 siRNA and DNA transfections

siRNA transfections for HUVEC: One day before cells is plated in 6 well plates. Cells are grown in 2 ml growth medium (EGM2). siRNA were diluted in 250 µl of

opti-MEM and mixed, 5 µl of RNAiMAX add into 250 µl of opti-MEM. Combine the diluted siRNA and RNAiMAX, mixed gently and incubated for 20 mints at room temperature (RT). The mixture was added to each well. Medium was changed after 6 hrs and after 48hrs assay was performed.

DNA transfections use lipofectamine 2000: One day before transfection, cells were plated onto 6 well plates with normal growth medium. On the day of transfection, cells (~70-80% confluence) were washed once with PBS and medium was changed to growth medium without antibiotics (exposure to antibiotics during transfection will cause cell death). 2-5 µg of plasmid DNA was mixed with 250 µl of opti-MEM medium. In a separate tube 3-5 µl of lipofectamine2000 was gently mixed with 250 µl of opti-MEM medium. After 5 min incubation at RT, DNA and lipofectamine diluents were mixed and gently and incubated at RT for 20 min. The mixture was then added to the cells drop-wise and mixed gently by rocking the plate back and forth. Cells were incubated at 37°C in 5% CO2 and transfection efficiency could be assessed after 16-24 h.

DNA Nucleofection using amaxa system: HUVEC cell were grown in 10 cm dish with culture EGM2+supplement medium. Cell were washed with PBS and harvested by trypsinization. Appropriate number of cell (10^5 to 10^6) was used nucleofection. Cells are reseupend in 100 µl of HUVEC Nucleofector solution, and added 2-5 µg of DNA. Transfer the nucleofection sample into an amaxa cuvette. Insert the cuvette into cuvette holder and start the program A-34. Cells are transfer to pre-warmed culture medium using plastic pipettes.

7.8 Generation of recombinant adenovirus

Homologous Recombination in E.coli: High competence of bacteria cells is desired to achieve efficient recombination. Typically, 5–10 µg of a shuttle vector plasmid was linearized with PmeI, purified by phenol chloroform extraction and ethanol precipitation, and mixed with 1-5 µg of supercoiled pAdEasy-1 in a total volume of 6.0 ml. 20 µl of electrocompetent E.coli BJ5183 cells were added, and electroporation was performed. The cells were immediately placed in 500 ml of LB medium and grown at 37^{o}C for 20 min. 100µl of the cell suspension then were inoculated onto LB-agar plate plus 50 mg/ml of kanamycin. After 16–20 hr growth at 37^{o}C, 10–25 colonies per dish generally were obtained. The smaller colonies (which usually represented the recombinants) were picked and grown in 2 ml of LB-medium containing kanamycin. Clones were tested by restriction digestion and positive clones were transformed into DH10B cells for large-scale amplification by electroporation.

Production of Adenoviruses in Mammalian Cells: Approximately 10^6 AD-293 HEK cells were plated in 10 cm dish 24 h before transfection, by which time they reached 50–70% confluency. Cells were washed with 1x PBS, then 5 ml of OptiMEM was added to each flask and the flasks returned to the CO2 incubator for 15–30 min before transfection. 4 µg of recombinant adenoviral vector DNA, digested with PacI and ethanolprecipitated, were used for transfection of each 10 cm dish. A transfection mix was prepared by adding 4 µg of linearized plasmid DNA and 10 µl of Lipofectamine 2000 to 500 µl of OptiMEM according to the manufacturer's instructions. After incubation at room temperature for 15–20 min, the transfection mix was added to the cells. After 4–6 hrs at 37^{o}C, the media containing the transfection

mix was removed, and 10 ml of growth medium was added. Transfected cells were monitored for GFP expression and collected 7–10 days after transfection by scraping cells off dish and pelleting them along with any floating cells in the culture. After three cycles of freezing in a dry ice bath and rapid thawing at 37^{o}C, 1 ml of viral lysate was used to infect 10^6 cells in a 10 cm dish. The efficiency of such infections could be conveniently followed with GFP. Three to four days later, viruses were harvested as described above. Viruses were used for gene transfer experiments in cultured cells.

7. 9 Isolation of mouse pulmonary endothelial cells

Mouse lung endothelial cells were isolated as described before (Korhonen et al., 2009). Lungs were minced and digested in dispase (5U/ml) for 1 h at 37° C with shaking (350 rpm). After filtration the cells were washed in PBS containing 0.5% BSA. Cells were incubated with anti-CD144 antibody-coated (BD Biosciences) magnetic beads (Invitrogen Dynal AS) for 1 h at room temperature, washed and isolated with a magnet (Invitrogen Dynal AS). Cells were grown in DMEM/F12 (Invitrogen) supplemented with 10% FBS, penicillin/streptomycin and endothelial cell growth supplement with heparin (PromoCell) on fibronectin-coated wells.

7.10 Endothelial cells (HUVEC)- tube formation assay

HUVEC cells were treated with Scrambled siRNA and $G\alpha_{12}$ and $G\alpha_{13}$ siRNA using standard procedures, the cells were serum-starved for 4 hrs before being to performed tube formation assay using growth factor reduced Matrigel matrix (BD

Biosciences). Briefly, 24-well plates were coated with 200 µl of GFR Matrigel and incubated at 37 °C for 30 min to promote polymerization. Quiescent HUVECs in serum-starved medium, without or without VEGF (50 ng/ml), were added to each well (5×10^5 cells/well). After 8 hrs of incubation, a wide field, representing an area was examined for each sample and photographed using contrast microscopy. Pictures were captured as 8-bit TIFF files and were processed using ImageJ software (NIH).

7.11 Luciferase assay

For luciferase reporter assay, different VEGFR-2-promoter or NF-κB-RE or SRF-RE or CSL reporter constructs and renila plasmid and siRNA were transfected to HUVEC cells using Nucleofector kit (amaxa biosystem) according to the manufacturer's protocols. After 48 h luciferase activity was measured by Dual-luciferase reporter assay kit (Promega). Firefly luciferase activity was normalized to cotransfected Renilla luciferase (phRL-TK, Promaga). Luciferase assay measured by luminometer (Fluoroskan Ascent FL, Thermo Scientific).

7.12 Immunoblotting

For Immunoblotting, Cells were lysed in RIPA lysis buffer. Protein were separated by 10% SDS-PAGE (sodium dodecyl sulfate-polyacrylamide) gel were transferred onto nitrocellulose membranes. Membrane was incubated with blocking solution (5% BSA or 5% non fat milk in PBST) for 1 hour at RT, and overnight incubation with primary antibody against goat anti-Gα13, mouse anti-phospho ERK1/2, Rabbit anti-c-Src

(Santa Cruz), Rabbit anti–VEGFR-2, Rabbit anti-IκBα, Rabbit anti- Phospho Src416, Rabbit anti-ERK, Rabbit anti-p38, Rabbit anti-phospho p38, Rabbit anti-GAPDH (cell signaling); 1 hour incubation with horseradish peroxidase-conjucated secondary antibodies. The blots were visualized by enhanced chemiluminescence reagent (Millpore) using Fuji medical X-Ray films. Protein band were analyzed by Adobe photoshop CS4 or imageJ software (NIH). If subsequent detection of another protein was necessary the membrance was incubated with stripping buffer (PBS containing 2% SDS and 0.02% β-mercaptoethanol for 30 min at 65^0C and re-blotted as described above.

7.13 Chromatin immunoprecipitation (ChIP)

ChIP assays were performed as described previously (Carey et al., 2009). In brief, 10^7 HUVEC were treated for 1 hr with vehicle, 5 U/ml thrombin or 10ng/ml TNFα, then cross-linked with 1% formaldehyde for 10 minutes at room temperature. Samples were then sonicated into 200-700 bp fragments using a SONOPULS Ultrasonic homogenizer (Bandelin, Berlin, Germany) and chromatin was immunoprecipitated with 2 µg of anti-rabbit IgG or anti-NF-κB p65 (both Cell Signaling), followed by reverse cross-linking. The recovered DNA was purified using the Qiagen blood DNA isolation kit and DNA was analyzed using qRT PCR. The VEGFR-2 promoter sequence was amplified using 5' GCTTGGGGAGCTGGAGAT 3' and 5' GAGCTGGTGCCGAAACTCTA 3' primer pair. The DNA recovered from chromatin that was not immunoprecipitated was used as input.

7.14 Quantitative real time –PCR

Total RNA was isolated from p6 retinas, lung endothelial cells or HUVEC using the RNeasy Micro or Mini Kit (Qiagen). Quality control of samples was carried out using Nanodrop ND-100 Spectrophotometer. RNA was reverse transcribed using the Transcriptor high fidelity cDNA synthesis kit (Roche) according to the manufacturer's instructions. Three qRT-PCR reactions were carried out using TaqMan Probe Master or SYBR Green I Master, (Roche). Gene expression was carried out using Light Cycler 480 II (Roche) according to a standardized protocol. Primers were designed by the online tool universal Probe library (Roche) or Primer-BLAST (NCBI).

7.15 Experimental animals

Littermate EC-Gα_{13}-KOs (Tie2CreERT2^{pos}; Gna13$^{fl/fl}$), EC-G$\alpha_{12/13}$-KOs (Tie2CreERT2^{pos}; Gna13$^{fl/fl}$; Gna12$^{-/-}$), Gα_{12}-KOs (Gna13$^{fl/fl}$; Gna12$^{-/-}$), and control mice (Gna13$^{fl/fl}$; Gna12$^{+/-}$) were generated by intercrossing Tie2CreERT2^{pos}; Gna13$^{fl/fl}$; Gna12$^{+/-}$ and Gna13$^{fl/fl}$; Gna12$^{+/-}$ mice (7th generation backcross to C57BL/6). Genotyping was performed as described previously (Korhonen et al., 2009) For induction of Cre-mediated recombination, 6-10 weeks old mice were injected intraperitoneally with 1 mg tamoxifen dissolved in 50 µl Miglyol oil on five consecutive days (all genotypes), experiments were performed 1-2 weeks after the end of induction.

7.16 Generation and Characterization of $G\alpha_{13}$-WT and $G\alpha_{13}$-CΔ rescue mutants

To generate mice with Cre-dependent transgenic expression of $G\alpha_{13}$-WT or $G\alpha_{13}$-CΔ, we modified the plasmid pCALSL, in which chicken β-actin promoter-dependent transgene expression is prevented by a stop cassette flanked with loxP sites (7). To generate pCALSL-$G\alpha_{13}$-WT or pCALSL-$G\alpha_{13}$-CΔ, the cDNAs of wildtype murine $G\alpha_{13}$ or a C-terminally deleted $G\alpha_{13}$ mutant (lacking the bases CAGCTCATGCTGCAG coding for the C-terminal amino acids QLMLQ) were amplified from expression plasmid pCis$G\alpha_{13}$ using primers carrying XbaI/NotI restriction sites and cloned into pCALSL. The cDNAs of both $G\alpha_{13}$-WT or $G\alpha_{13}$-CΔ are preceded by a MycTag. The plasmids were purified by Sepharose separation and injected into male pronuclei derived from fertilized FvB/N oocytes. Transgenic offspring was analyzed by PCR using primers P1 (5´-agaggccgttgtaccacc-3´) and P2 (5´-taagatacattgatgagtttg-3´). Cre-dependent expression of transgenic $G\alpha_{13}$ was confirmed by immunoblotting after infection of lung endothelial cells with the Cre-expressing adenovirus Ad-Cre-GFP or control vector pCMV-GFP (both VectorLabs). To investigate whether re-expression of $G\alpha_{13}$-WT or $G\alpha_{13}$-CΔ rescued defective stress fiber-formation in $G\alpha_{13}$-deficient cells (2), endothelial cells isolated from lungs of $Gna13^{fl/fl}$ mice carrying no transgene, transgenic $G\alpha_{13}$-WT, or transgenic $G\alpha_{13}$-CΔ were incubated with 10^7 PFU/ml AdCreGFP for 48 hours to induce Cre-mediated inactivation of endogenous $G\alpha_{13}$ and concomitant re-expression of transgenes. Cells were then serum starved for 16 hours, stimulated with 1 µM LPA for 15 minutes, fixed in 4% PFA for 10 minutes, washed twice in PBS, permeabilized with 0.1% TritonX/PBS for 15 minutes, washed twice in PBS, incubated in 1:200 Alexa Fluor BODIPY FL Phallacidin for 1 hr (Invitrogen, Karlsruhe, Germany). After washing twice in PBS, cells were mounted in

Mowiol and the percentage of stress fiber-positive cells among AdCreGFP-infected cells was determined by an investigator blinded to genotype and treatment using a Zeiss AxioObserver Z1.

7.17 Retinal angiogenesis model

For retinal angiogenesis, Tie2-iCreER^{T2}; Gα13flox/flox, Tie2-iCreER^{T2}; TomEGFR mice were used. Gene inactivation was induced in newborn mice by three consecutive intraperitoneal injections of 50 µl of tamoxifen (1mgml^{-1} in miglyol oil) on postnatal days P1, P2 and P3. The phenotypes of mutant and reporter mice were analysed at postnatal day P6 or P7. Littermate animals were used as control (Pitulescu et al., 2010). Cre activity in retinal EC was analyzed by using TomEGFP reporter mice.

7.18 Xenograft tumor models

Two subcutaneous tumor models were used. B16F10 melanoma and Lewis lung carcinoma (LLC1) adherent growing murine cells were harvested and single-cell suspensions of 10^6 cells (B16/F10 or LLC1) 100µl in PBS were injected subcutaneously into the right flank of mice, respectively. Tumor volumes were measured every two days with a caliper using the formula: $V = 0.52 \times [d^2 \times D]$, where d is the minor tumor axis and D is the major tumor axis. The mice were sacrificed at defined time intervals after cell inoculation or when tumors reached a maximum size of 4000 mm^3. Growth curves were statistically analyzed. Primary tumors were removed, weighed and analyzed histology and immunostaining.

7.19 In vivo matrigel angiogenesis assay

For in vivo Matrigel plug angiogenesis assays, growth-factor-reduced Matrigel solutions were prepared with or without recombinant VEGF-A (200 ng/ml), bFGF/FGF2 (200 ng/ml), and S1P (10 mM). The gel solutions (500 ml each) were injected subcutaneously into the right and left flanks of anesthetized mice. After 14 days, Matrigel plugs were harvested and frozen in O.C.T. compound (Tissue-Tek) for histologicalanalysis.

7.20 Immunostaining

Whole mount of immunostaining of retinas: Retinas were fixed in 4% PFA at room temperature for 2hr. After fixation retina were washed three times with PBS and incubated with 1% BSA and 0.3% Triton X for 60 min. Wash with ice cold PBS containing 1% Triton X-100. Incubate the retinas overnight at 4 °C in PBS with 1% Triton X-100 and 1:50 Alexa Fluor 594 conjugated Isolectin IB4.

Immunostaining of tumor tissue: Tumor sections fixed with 4% PFA for 1 hr at 4^{o}C. Sections were incubated with 30% sucrose solution for 1 day and processed for OCT compound embedding and montage. Staining was carried out on 15 to 20 µm thick sections, blocked with 4% normal serum and permeabilized with 0.5% Triton X-100. Sections were incubated at 4^{o}C for overnight using the following primary antibodies: rat anti-CD31, rat anti-Cd144, Cy3-conjugated mouse anti-SMA antibody, Rabbit polyclonal anti-NG2 Chondroitin sulfate proteoglycan, Rabbit polyclonal active Caspase 3 and Rabbit polyclonal ki67, rabbit anti VEGFR-2. Sections were washed in PBS and incubated with the appropriate fluorescent conjugated secondary

antibodies, Alexa 488 or 594 for 1 hr. Wash the sections with PBS, and stained in DAPI (Sigma) for 20 mints and mounted in Aquatex. Tissues were imaged using a confocal Leica SP5. Tumor angiogenesis were analyzed by CD31 positive area. Vessel coverage and maturation were analyzed for αSMA and NG2 positive vessels. Angiogenesis quantification was performed by taking pictures from three random fields per tumor, imaging three to four tumors for each genotype. CD31 stained vessels was quantified using ImageJ and photoshop based on previously described (Wild et al., 2000). Angiogenic properties were measured by vessel number and length.

7.21 Statistical analyses

Data are presented as means ± standard errors of the means (SEM). Normality of distribution was tested by Kolmogorov-Smirnov test with a = 0,05. Comparisons between two groups were performed with unpaired student's t-test, comparisons between more than two groups by ANOVA followed by Bonferroni post hoc test. Comparisons between more than two groups at different time points were done by repeated measures ANOVA/Bonferroni post hoc test. "n" refers to the number of independent experiments or mice per group. P-values are indicated as follows: *, $p<0.05$; **, $p<0.01$; ***, $p<0.001$; ns, not significant.

8. APPENDIX

Bacteria and Bacteria growth media

LB medium (Luria-Bertani medium) per liter

Bacto-Tryptone	10 g
Bacto-Yeast extracts	5 g
NaCl	5 g

To 950 ml of deionized water was add, shake until the solutes have dissolved, adjust the pH to 7.0 with 5 N NaOH. Adjust the volume of the solution to 1 liter with deionized H_2O. Sterilize by autoclaveing.

SOC medium per litter

Bacto-Tryptone	20 g
Bacto-Yeast extracts	5 g
NaCl	0.5 g

To 950 ml of deionized water was add, shake until the solutes have dissolved, adjust the pH to 7.0 with 250mM- KCl. Ater the medium autoclaved, allow it cool to 60^{o}C. Add 20 ml of a sterile 1 M glucose solution. Adjust the volume the medium 1-liter with deionized H_2O and sterilize by passing it through a 0.22µm filter.

NZY+ Broth per liter

NZ amine (casein hydrolysate)	10 g
Yeast extracts	5 g
NaCl	5 g

Add deionized H_2O to a final volume of 1 liter.Adjust to pH 7.5 using NaOH, Sterilize by autoclaveing. Add the following filer-sterilized supplements prior to use:

MgCl2 (1M)	12.5 ml
MgSO4 (1 M)	12.5 ml
Glucose (2M)	10 ml

LB-Agar plate per liter

Bacto-Tryptone	10 g
Bacto-Yeast extracts	5 g

NaCl	5 g
Bacto Agar	7 g

Sterilize by autoclaving. The medium is removed from autoclave; allow the medium to cool 50-60^{o}C and added antibiotics.

Antibiotics (1000x stocks)

Ampicillin	50 mg/ml in H_2O
Kanamycin monosulfate	10 mg/ml in H_2O
Chloramphenicol	30 mg/ml in ethanol
Streptomycin	10 mg/ml in H_2O
Tetracycline	5 mg/ml in ethanol

Antibiotics sterilized by passing it through a 0.22µm filter and stored at -20^{0}C.

Plasmid Isolation reagents and kits

AlKaline Lysis Solution I (P1)

Glucose	50 mM
Tris-Cl (pH 8.0)	25mM
EDTA (pH 8.0)	10mM

Autoclave and store at 4^{O}C.

AlKaline Lysis Solution II (P2)

NaOH	0.2 N
SDS	1% (W/V)

AlKaline Lysis Solution III (P3)

Potassium acetate (5 M)	60.0 ml
Glacial asetic acid	11.5 ml
H_2O	28.5 ml

Plasmid islation kit

Mini (Qiagen: 12125), Maxi – (Qiagen: 12165) and Endofree Maxi (Qiagen; 12362)

Plasmid

Table 1: **List of plasmid**

Plasmid	Plasmid details	Company	Applications
PGL3-Luc	Basic vector	Promaga	Luciferase assay
PGL3-VEGFR2-780/+268	Human VEGFR2 promoter different regions subcloned into pGL3 vectors	Add gene(Prof. Donald Ingber) Wyss Institute, Harvard University	
PGL3-VEGFR2-550/+268			
PGL3-VEGFR2-225/+268			
PGL3-VEGFR2-130/+268		Modified	
PGL3-VEGFR2-60/+268			
PGL3-VEGFR2-225/+268 ΔNFκB mutant	NFκB binding site mutanted at R2-90 (GGGAGA-TTTAGA)		Luciferase assay
PGL4.32-Luc2p/NFkB-RE/hygro) vector	NFκB responsive luciferase reporter.	Promaga	Luciferase assay
PGL4.34-Luc2p/SRF-RE/hygro) vecto	SRF-RE responsive luciferase reporter.	Promaga	
Pshuttle-IHRES-hrGFP-1	IHRES-GFP	Agilent tech	Over expression
Pshuttle-$G\alpha_{13}$wt	Mouse $G\alpha_{13}$ WT cloned into Pshuttle-IHRES-hrGFP-1 vector at the Sal I site.	Modified	Over expression
Pshuttle-Gα13Δcdel	$G\alpha_{13}$-C terminal qlmlq amino acids deleted (GPCR binding site) – $G\alpha_{13}\Delta$cdel	Modified	Over expression
pCSL-luc	luciferase reporter.		Luciferase assay
pCis G13QL	$G\alpha_{13}$ constitutively active	From –(Prof. Stefan Offermanns)	
pCis G13GA	$G\alpha_{13}$ dominant negative		

pCis G12WT	Mouse $G\alpha_{12}$ WT		
prhoA CA (V14)	RhoA constitutively active	Gift- Dr. Kozo Kaibuchi, Nagoya university, Japan	

Buffer and stock solutions

Phosphate- buffered saline (PBS) per liter

NACl (137 mM)	8 g
KCl (2.7 mM)	0.2 g
Na_2HPO_4 (10mM)	1.44 g
KH_2PO_4 (2nM)	0 .24 g

Dissolved in 800 ml of distilled H_2O. Adjest the pH to 7.4 with HCl. Add H_2O to 1 liter and sterilization in autoclaving.

Tris EDTA (TE) 10X

Tris-Cl (pH 7.6)	100 mM
EDTA (pH 8.0)	10 mM

TAE Buffer (1X)

Tris-acetate	40 mM
EDTA	1 mM

Tail digestion buffer:

EDTA (pH 8.0)	0.1M
SDS	0.5 %
Tris pH (8.0)	50mM
Proteinas K	0.5 mg/ml

Polymerase chain reaction (**PCR**)

PCR buffer 10X: 200mM Tris, 500mM KCl. Set pH 8.4 with HCl

dNTPS :dATP+ dGTP+dCTP+dTTP (25 µmol)

$MgCl_2$: 50 mM

Target DNA amplifications & mutation PCR -Invitrogen PCR kits (cat no. 11708-013).

PCR reactions (50µl): Buffer 10x: 5 µl, $MgCl_2$: 1.5 µl, dNTPs: 0.5 µl, Taq polymerases: 1 µl, primer (Forward & reverse): 2 µl, DNA: 1-2 µl and makeup with PCR grade water.

DNA purification - (Qiagen: 28106)

DNA precipitation buffer:

Ammonium acetate (7.5M)	100 µl
Ethanol (99-100%)	600 µl

Cell culture Medium

Medium for cell line:

DMEM+NAA +4.5 mg/l D-glucose (450 ml) 1X (Gibco:10938-025)

L-Glutamine(100X) (Gibco: 25030-081)	5 ml
Pyruvate (100X) (Gibco: 11360088)	5 ml
Penicillin-streptomycin(100X) (Gibco: 15140-122)	5 ml
Fetal bovine serum (10%) (Gibco: 16000044)	50 ml

PBS ($CaCl_2$-, $MgCl_2$ -) (Gibco: 14190-094)

Medium for HUVEC:

EGM2 medium (Lonza: CC-3156)

EGM2 supplements (Lonza: CC-4176)

Primary lung ECs medium (500 ml)

DMEM/F12 (Gibco cat: 21041-025)	400ml
FCS (20%)	100 ml
Penicillin-streptomycin (100X)	5 ml
ECGS-H (Promocell cat: C30120) 8µl/ml- 4ml	

Cells

Table 2: Cell lines and primary cells

Cell line	Name	Company name /cat no.	Applications
HEK293	Human Embryonic Kidney 293 cells	ATCC CRL-1573	Cell biology, luciferase
AD-293	HEK293 cells- improved cell adherence and plaque formation properties	Agilent tech: cat no. 240085	Virus productions
LLC1	Mouse Lewis lung carcinoma cells	ATCC CRL-1642	Tumor model
B16/F10	Murine melanoma cells	ATCC CRL-6475	Tumor model
Primary cells from human			
HUVEC	Human umbilical vein endothelial cells	Lonza : C2519A	Expression, Luciferase assay, angiogensis assay
Primary cells from mouse			
LECs	Lung endothelial cells	Self	Cell biology
LFBs	Lung fibroblasts	self	Cell biology

Transfections to mammalian cells

Opti-MEM - Reduced-Serum Medium (Gibco: 31985-062)

RNAiMAX (Invitrogen: 13778-100)

Lipofectamine 2000 (Invitrogen: 11668019)

HUVEC nucleofector kit (Lonaza: VPB-1002)

Amaxa system (Lonza)

Primary lung endothelial cell isolations

Hanks balanced salt solution (HBSS) without CA+/Mg (Gibco: 14175-129)

ECs buffer**:** PBS+0.5%BSA

Cell digestion: Dispase II – 5 U7ml in HBSS (Gibco: 17105-041)

Dynabeads M450, Sheep anti-rat IgG (Dyna: 110.07)

Table: 3 List of siRNA

Gene (Human)	Sequence	Company Qiagen: catalog no.
Control siRNA	Qiagen control siRNA	1027280
GNA12 (Gα12)	CCGGATCGGCCAGCTGAATTA	SIO0096558
GNA13 (Gα13)	TAGGCATATTTCAGGCTTTAA	SIO2637572
VEGFR2 (KDR)	AACGCTGACATGTACGGTCTA	SIO0605528
GNAi1 ($G\alpha_{i1}$)	CGGGCGGATGATGCACGCCAA	SI03087140
	TACGACCTGGTTCTAGCTGAA	SI03109414
GNAi2 ($G\alpha_{i2}$)	CAGCCCAAGTCCAAATGTTTA	SI02780505
	CCGGGCGGTTGTCTACAGCAA	SI02780981
GNAi3 ($G\alpha_{i3}$)	AAAGTGTGATTCGATCGTCAA	SI00088956
	CAGATGATGCCCGGCAATTAT	SI03064803

Table 4: Adeno virus

Virus	Catalong no.	Company	Applications
Ad-CMV-GFP	1060	Vector Biolabs	WB
Ad-Cre	1045		Cre recombination's
Ad-VEGFR2	1621		Overexpression

Ad-Pshuttle-IHRES-hrGFP-1	Self made	Self made	WB, overexpression
Ad- Gα13WT			
Ad- Gα13 cdel			

Luciferase assay:

Dual-luciferase reporter assay kit (Promega: E1910)

Fluoroskan Ascent FL (Thermo Scientific)

Western blot Buffers

Cell Lysis buffer (RIPA 4X)

NaCl (5M)	12ml
Tris pH 7.4 (2M)	10ml
EDTA pH 8 (0.5 M)	4ml
SDS (20%)	2 ml
Na-DOC (10%)	20ml
Triton X-100	4 ml

Distilled water was added to final volume 100 ml. Solution was stored at 4°C.

Prepared 1X RIPA buffer for 50 ml. Added freshly Protease inhibitor cocktail

AEBSF (100 mM)	50µl
Leupeptin (10 mg/ml)	50µl
Aprotinin (10 mg/ml)	50µl
Pepstatin A (10 mg/ml)	50µl

SDS PAGE separating gel 7.5% (10 ml)

H_2O	4.85 ml
Tris pH 8.8 (1.5M)	0.4%
SDS	2.6 ml
Acrylamind/bisacrylamid30% w/v	2.5 ml
APS (10%)	50 µl
TEMED	5 µl

SDS PAGE stacking gel 4% (5 ml)

H_2O	3.05 ml
Tris pH 6.8, 0.4%	1.5M
SDS	1.3 ml
30% w/v Acrylamind/bisacrylamid	65 ml
10% APS	50 µl
TEMED	5 µl

Sample buffer for reducing conditions (6x)

SDS (12%)	3.6 g
Tris-HCl, pH 6.8	300 mM
Tris(1.5M)	6 ml
DTT (600 mM)	2.77 g
BPB (0.6%)	0.18 g
Glycerol (60%)	18 ml

Distilled water was added to 30 ml. Buffer was stored in 0.5 ml aliquots at -20°C. Add 50 µl β-mercaptoethanol in 1 ml of 4x buffer.

Electrophoresis buffer (5x) Stock

Tris base	154.5 g
Glycine	721 g
SDS	50 g

Distilled water was added to 10 l. Buffer was stored at RT.

Protein transfer buffer (1x)

Tris base	25 mM
Glycine	192 mM
Methanol	20%

PBS-Tween (PBST)

1x PBS

0.1% Tween®20

Solution was kept at RT.

Blocking solution

Skim milk (5%)	5 g
PBST	100 ml

Solution was prepared freshly just before use.

Stripping buffer

Sodium Phosphate buffer (pH 7-7.4)	5 mM
SDS	2%

Freshly before use, 10 µl of β-Mercaptoethanol was added to 50 ml of the buffer.

Chromatin immunoprecipitation (ChIP) buffers

Formaldehyde (37%)	27µl/ ml
Glycin (2.5M)	55µl/ ml

SDS lysis buffer

(final concentration of 1% SDS, 5 mM EDTA, 50 mM Tris. HCl (pH 8.1)

SDS (10%)	5 ml
EDTA (0.5 M)	500 µl
Tris HCl (p.H 8.1) 1M	2.5 ml

Distilled water was added to final volume 50 ml. Added freshly Protease inhibitor cocktail

Triton X-100 lysis buffer

(Need final concentration of 0.25% Triton X-100, 10mM EDTA, 10mM Tris.HCl[pH8.1], 10mM NaCl, 1X protease inhibitor)

Triton X-100 (10%)	2.5 ml
EDTA (0.5 M)	2.0 ml
Tris HCl (p.H 8.1) 1M	1.0 ml
NaCl (1M)	1.0 ml

Distilled water was added to final volume 100 ml. Added freshly Protease inhibitor cocktail.

Dilution buffer

(Need final concentration of 1% Triton X-100, 2mM EDTA, 20mM Tris.HCl[pH8.1],

150mM NaCl, 1X protease inhibitor)

Triton X-100 (10%)	10ml
EDTA (0.5 M)	400 µl
Tris HCl (p.H 8.1) 1M	2.0 ml
NaCl (1M)	15 ml

To prepare 100ml of autoclaved H2O, added freshly Protease inhibitor cocktail.

TSE I buffer

(Need final concentration of 0.1% SDS, 1% Triton X-100, 2mM EDTA, 20mM Tris.HCl [pH8.1], and 150mM NaCl)

SDS (10%)	1 ml
Triton X-100 (10%)	10 ml
EDTA (0.5M)	400µl
Tris.HCl[pH8.1] 1M	2 ml
NaCl (1 M)	15 ml

To prepared in 100ml of autoclaved H_2O.

Buffer III

(Final concentration of 0.25M LiCl, 1% NP-40, 1% deoxycholate, 1mM EDTA,

10mM Tris.HCl [pH8.1])

LiCl (4M)	6.25ml
NP-40 (10 %)	10 ml
Deoxycholate (10 %)	10 ml

EDTA (0.5 M)	200 µl
Tris.HCl[pH8.1] 1M	1.0 ml

Distilled water was added to final volume 100 ml.

TE buffer for washing beads

(Need final concentration of 2mM EDTA, 10mM Tris.HCl [pH8.0])

EDTA (0.5 M)	400µl
Tris.HCl[pH8.0] 1M	1 ml

Distilled water was added to final volume 100 ml.

TE buffer for dissolving DNA

(Need final concentration of 1mM EDTA, 10mM Tris.HCl[pH8.0])

EDTA (0.5M)	200µl
Tris.HCl [pH8.0] 1M	1 ml

Distilled water was added to final volume 100 ml.

Elution buffer

(Final concentration of 1% SDS, 10mM EDTA, 50mM Tris.HCl[pH8.1])

To prepare 100ml, need

SDS (10%)	10 ml
EDTA0.5M	2.0 ml
Tris.HCl[pH8.1] 1M	5ml

Distilled water was added to final volume 100 ml.

Immunofluorescence staining

Fixation: 4% PFA

Wash buffer I: 50mM Glycine in PBS (RT)

Wash buffer II: PBST (1X)

Blocking Buffer: PBST (1X), 4% FBS or normal serum.

Antibodies

Table 8-5: List of antibody

Gene name	Source	Company/Catalog no.	Diluctions	Application
Primary antibody				
GNA13(Gα13)	Rabbit polyclonal	Santa Cruz/Sc-410	1:300	WB
	Goat polyclonal	Santa Cruz/Sc-26788	1:300	WB
VEGFR2	Rabbit mAb	Cell signalling/#2479	1:100/1:1000	IF/ WB
Phospho ERK1/2	Mouse mAb	Santa Cruz/Sc-7383	1:500	WB
ERK1/2	Rabbit mAb	Cell signalling/#4695	1:1000	WB
Phospho Src 416	Rabbit mAb	Cell signalling/#2113	1:1000	WB
c-Src	Rabbit polyclonal	Santa Cruz/Sc-18	1:1000	WB
Total p38	Rabbit	Cell signalling/#9212	1:500	WB
GAPDH	Rabbit	Cell signalling/#2118	1:2000	WB
IκBα	Rabbit mAb	Cell signalling/#4812	1:500	WB
NFκB	Rabbit mAb	Cell signalling/#4764	1:100/1:500	IF/WB
Alpha tubulin	mouse	Sigma/T 9020	1:3000	WB
CD31(PECAM 1)	Rat	BD Bioscience/550274	1:100	IF/ EC isolation
CD144(VE-cad)	Rat	BD Bioscience/555289	1:100	IF/ EC isolation
	Rabbit mAb	Cell signalling/#2500	1:100/1:1000	IF/WB

Alpha-SMC	Cy3 -Mouse mAb	Sigma/C6198	1:200	IF
	Rabbit polyclonal	Abcam/ab5694	1:100	IF
NG2	Rabbit polyclonal	Millipore	1:100	ÎF
Cleaved Caspase 3	Rabbit polyclonal	Cell signalling/#9661	1:100	IF
F-actin/Phalloidin	Alexa Fluor 488 or 594	Invitrogen/A12379	1:50	IF

Secondary antibody				
Name/ Against	label	Company- Molecular Probes	Dilutions	Application
Doncky anti- rat IgG	Alexa Fluor-488	A-21208	1:200	IF
Doncky anti- rat IgG	Alexa Fluor-594	A-21209	1:200	IF
anti- rabbit IgG	Alexa Fluor-488	A-11034	1:200	IF
anti- rabbit IgG	Alexa Fluor-594	A-11012	1:200	IF
Anti-mouse IgG	Alexa Fluor-488	A-11029	1:200	IF

Isolectin B4

FITC conjugated lectin from Bandeiraea simplicifolia (Isolectin B4, Invitrogen) was dissolved in Dulbecco's phosphate buffer saline (D-PBS, Sigma) to a final concentration of 1mg/ml, aliquoted and stored at 4ºC in the dark.

Oligonucleotides

Primers were designed by the online tool universal Probe library (Roche) or Primer-BLAST (NCBI). All oligonucleotides were synthesized by MWG (www.mwg-biotech.com) and sigma.

Table 6: Human primers (for TaqMan Probe Master)

Gene	Forward Primer	Reverse Primer	Prob
VEGFR-2	GCTCAAGACAGGAAGACCAAG	GGTGCCACACGCTCTAGG	#27
GAPDH	CCCCGGTTTCTATAAATTGAGC	CACCTTCCCCATGGTGTCT	#63
GNA12	GCGAGTTCGACCAGAAGG	CATCAACAAGAACCCTTGAGC	#67
GNA13	TCGGGAAAAGACCTATGTGAA	CAACCAGCACCCTCATACCT	#3
GNAq	GACTACTTCCCAGAATATGATGGAC	GGTTCAGGTCCACGAACATC	#27
GNA11	GCATCCAGGAATGCTACGAC	GGTCAACGTCGGTCAGGTAG	#53
GNAI1	AAGTACAATTGTGAAGCAGATGAAA	TGGTGTTACTGTAGACCACTGCTT	#35
GNAI2	CTCAACGACTCAGCTGCCTA	TGCTGTGTGGGGATGTAGTC	#1
GNAI3	TGGGACGGCTAAAGATTGAC	ATAATTGCCGGGCATCATC	#60
HES1	GAAGCACCTCCGGAACCT	GTCACCTCGTTCATGCACTC	#60
HEY1	CGAGCTGGACGAGACCAT	GGAACCTAGAGCCGAACTCA	#39
HEY2	CCCGCCCTTGTCAGTATC	TTGTTTGTTCCACTGCTGGT	#73
NRARP	GCTGCACCAGTCGGTCAT	GCCGAACTTGACCAGCAG	#1
Dll4	CCCTGGCAATGTACTTGTGAT	GTGGTGGGTGCAGTAGTTGA	#23
JAG1	GGCAACACCTTCAACCTCA	GCCTCCACAAGCAACGTATAG	#28
JAG2	TCATCCCCTTCCAGTTCG	ATGCGACACTCGCTCGAT	#17
NOTCH1	CGGGGCTAACAAAGATATGC	CACCTTGGCGGTCTCGTA	#52
NOTCH2	TGGTGGCAGAACTGATCAAC	CTGCCCAGTGAAGAGCAGAT	#86
NOTCH4	CCTCTCTGCAACCTTCCACT	GCCTCCATTGTGGCAAAG	#51

Table 7: Mouse Primers (for SYBR Green)

Gene	Forward Primer	Reverse Primer
Vegfa	CAGGCTGCTGTAACGATGAA	GCATTCACATCTGCTGTGCT
Vegfb	CAAGTCCGAATGCAGATCCT	TGTCTGGCTTCACAGCACTC
Vegfr1	GATGTGGAAGGAGACGAGGA	CGATGAATGCACTTTCTGGA
Vegfr-2	GCCTTATGATGCCAGCAAGT	AAGCGTCTGCCTCAATCACT
Npn1	GGAGCTACTGGGCTGTGAAG	CCTCCTGTGAGCTGGAAGTC
Ve-Caderin	CGAATAACCAAGCAGGGAAA	GGTTACCCCGAGAATCCAGT
Pecam1	AGTGACAGCGGGGAGTACAG	TACTGGGCTTCGAGAGCATT
Tie2	CGGACTGACTACGAGCTGTG	TTGGCAGGAGACTGAGACCT
Gapdh	GATCAACACGTACCAGTGCAA	CGCCTGTACACTCCACCAC

Table 8: Mouse primers (for TaqMan Probe Master)

Gene	Forward primer	Reevrse primer	Probe
Tie1	AAGCCCTCGGATTTGGTAG	TGTTGTGCACATAGAGAACTCG	2
Tek	AACATCCCTCACCTGCATTG	GGATCTTGGTGCTGGTTCAT	9
Vegf-a	GCCTCCGAAACCATGAACT	GGTGGAGGTACAGCAGTAAAGC	108
Vegf-b	ATGGAACTCATGGGCAATGT	AGCGCTGCACAGTCACAC	104
Vegf-c	TCCTGTACCCAGACTACTGGAAA	TCCCCTGTCCTGGTATTGAG	66
Flt1	GGCCCGGGATATTTATAAGAAC	CCATCCATTTTAGGGGAAGTC	55
Kdr	CCCCAAATTCCATTATGACAA	CGGCTCTTTCGCTTACTGTT	18
Flt4	CGAGGGTGACTACGTGTGTG	ACTTCTTGTGGCAGTGCTTG	71
Nrp1	TGTGGGTACACTGAGGGTCA	CCACCATCCAGACCAGTTG	6
Nrp2	TCATTGAGATTCGGGATGG	CGATGTTCCCACAGTGCTT	79
Pdgfb	TGAGGAACTGTATGAAATGCTGAG	AGCAGGCGCTGAAGATCA	58
Pdgfra	CAACAGTGGCCTCTTTGTCA	CAAGTGTACCATCCGGTGTG	11
Pdgfrb	GAAGCGGCCATGAATCAG	GTGTCTCCCCCAGTGACATT	47
Fgf1	CCAAATGAGGAATGTCTGTTCC	GCATGCTTCTTGGAGGTGTAA	11
Fgf2	CGGCTCTACTGCAAGAACG	CGTGTGGGTCGCTCTTCT	4
Fgfr1	ACCGAGGACTTTTCTCAGGTC	CAGCCCGAGTTCCATCAC	45
Fgfr2	ACCCTCTCTGACCCACCAT	CACCTGTCTGCCTTGAGTCC	76
Fgfr3	CCAGGGCCTGAACCTAGC	AGGAGGATGGCAGCTCAG	68
Efnb2	CCCAGTGACGTTATCATACCAC	CATAGTCCCCGCTGACCTT	29
Ephnb4	CAGAACATCTGACTCGGAAGC	CGCAGCGTCTTGATATTAACTTT	1
Mmp2	AGACACTGGTCGCAGTGATG	CCATACTTGCCATCCTTCTCA	6
Mmp9	TCGTGGCTCTAAGCCTGAC	GTCGGCTGTGGTTCAGTTG	19
Timp2	GTCCCATGATCCCTTGCTAC	GTGACCCAGTCCATCCAGAG	52
Cdh5	CACTGCTTTGGGAGCCTTC	AAGTTAGGGCCTGCCATTG	79
Pecam1	GGACCACGTGTTAGTGTTTCG	TGGGTTCTGACTCCTGCAAT	33
Jag1	TGGAGAGCTACAGAATGGGAAC	CTTTGAAGTACGTATCACACTCGTC	22
Notch1	CCTCACCTGGTGCAGACC	GTTCTGAGGCTGGAGCTGTAA	5
Dll4	CTGTGTCCCCCAGGCTACTA	CATTGAAGCAGGGTGAGTCC	100
Hey1	CTCGGCCTCCAAACTGTCT	GAAAAGGGGAAGGCTGAGAG	82
Hes1	TGCCTTTCTCATCCCCAAC	GGTGTAGACCGGGATGACC	100
Gapdh	GCTCATGACCTTCTTTGTGCT	TTTGATGTTAGTGGGGTCTCG	9
Gna12	GATAACTTGGACCGGATTGG	CTTGGTGGCCTTTCTAGCC	60
Gna13	CCACTGCTTAAGAGACGTCCA	TGGTACAACGGCCTCTGC	31
Gna11	CACTGGCATCATCGAGTACC	GATCCACTTCCTGCGCTCT	80
Gnaq	GACTACTTCCCAGAATATGATGGAC	TCAGGATGAATTCTCGAGCTG	105
Gnai1	AACGATTCGGCAGCGTACT	ATCCTGCTGAGTTGGGATGT	76
Gnai2	TCAATGACTCAGCCGCTTAC	GGGATGTAGTCACTCTGTGCAA	50
Gnai3	GGAGTCCATTAACAATCTGTTATCC	TCTTCAAACTGGCACTGAATGT	34

Quantitative RT-PCR

RNA isolation

For retian RNA isolation –RNAeasy Plus Micro kit (Qiagen, Cata no. 74034)

Lung ECs and HUVEC RNA isolation- RNAeasy Mini kit (Qiagen, Cata no. 47106)

cDNA Synthesis

cDNA synthesis kit (Roche)

qRT-PCR

TaqMan Probe Master or SYBR Green I Master (Roche, Mannheim, Germany)

Table 9: Growth factors and Agonist

Grwoth factors and Agonist	Company name/cata log number		Application
mVEGF/hVEGF	Santa Cruz Biotechnology	Sc-4571/Sc-4570	In vivo, in vitro, WB
S1P	Enzo life Science	SL-140-0001	Luciferase, in vivo
Thrombin	Sigma	T4648	Luciferase, WB
LPA	Enzo life Science	325465-93-8	luciferase
FGFb/ FGF2	PeproTech R&D Systems	450-33 233-FB-025	In vivo, in vitro, WB
hDLL4	R&D Systems	1506-D4	Luciferase,gene expression

Table 8-10: Pharmacological inhibitor

Inhibitor	Company name/catalog number		Application
C3	Cytoskeleton	CT03	luciferase
Y27632	Tocris Bioscience	1254	luciferase
Ro 106-9920	Tocris Bioscience	1778	luciferase

Tube formation assay and matrigel assay:

Basement Membrane Matrix-Growth factor reduced material gel (BD Bioscience, Cata no. 356231)

Chemicals, reagents and enzymes:

Chemicals were purchased from the companies Merck, Serva, Sigma, Fluka and Roth. Water used to prepare all solutions was filtered with the “Milli-Q-Water System” (Millipore). Restrictions enzymes were purchased from New England Biolabs (NEB).

9. Zusammenfassung

9.1 Einführung

Angiogenese, die Entstehung neuer Blutgefäße aus bereits vorhandenen Gefäßen, ist von grundlegender Bedeutung für die embryonale Entwicklung; sie spielt darüber hinaus eine wichtige Rolle bei der postnatalen Organentwicklung sowie verschiedenen physiologischen und pathologischen Umstrukturierungsprozessen im adulten Organismus. Der endotheliale Wachstumsfaktor *Vascular endothelial growth factor* (VEGF) und sein Hauptrezeptor, der VEGF-Rezeptor Subtyp 2 (VEGFR-2), spielen eine zentrale Rolle bei der Angiogenese. Die VEGFR-2-Expression ist in angiogenetisch aktiven Gefäßen stark erhöht, es ist jedoch wenig über die Regulation der VEGFR-2-Expression bekannt.

G-Protein-gekoppelte Rezeptoren (GPCR) wurden zwar immer wieder mit Angiogenese in Verbindung gebracht (Dorsam and Gutkind, 2007; Richard et al., 2001), die zugrunde liegenden molekularen Mechanismen blieben jedoch unklar. Es wurde vermutet, dass das heterotrimere G-Protein G_{13} eine Rolle spielen könnte, da die genetische Inaktivierung der α-Untereinheit von G_{13} ($G\alpha_{13}$) in Mäusen aufgrund einer gestörten Gefäßentwicklung zum Tod am Tag 9.5 der Embryonalentwicklung führt (Offermanns et al., 1997). Dieser Defekt in der Entwicklung embryonaler Gefäße schien von der Abwesenheit von $G\alpha_{13}$ in Endothelzellen herzurühren, da der gleiche Phänotyp bei Mäusen mit Endothelzell-spezifischer $G\alpha_{13}$-Defizienz beobachtet werden konnte und Endothelzell-spezifische Expression von $G\alpha_{13}$ den Phänotyp rettete (Ruppel et al., 2005). Obwohl $G\alpha_{13}$ an mehreren Endothelzell-Funktionen *in vitro* beteiligt ist (Chen et al., 2009; Ruppel et al., 2005), bleiben die

der in Abwesenheit von $G\alpha_{13}$ gestörten Gefäßbildung zugrunde liegenden Mechanismen weiterhin unbekannt. Ebensowenig ist geklärt, ob $G\alpha_{13}$ für die adulte Angiogenese relevant ist.

9.2 Ziele der Studie

1) Untersuchungen zur Fragestellung, ob endotheliales $G\alpha_{13}$ auch für die postnatale Angiogenese notwendig ist, zum Beispiel bei der retinalen und Tumor-Angiogenese.
2) Analyse des molekularen Mechanismus der gestörten Angiogenese bei Mäusen mit Endothelzell-spezifischer $G\alpha_{13}$-Defizienz.

9.3 Ergebnisse

Um herauszufinden, ob endotheliales $G\alpha_{13}$ und sein naher Verwandter $G\alpha_{12}$ eine Rolle bei der postnatalen Angiogenese spielen, untersuchten wir die retinale Angiogenese 6 Tage nach der Geburt in Mäusen mit Endothel-spezifischer Defizienz für $G\alpha_{13}$ (EC-$G\alpha_{13}$-KO) oder $G\alpha_{12}$ und $G\alpha_{13}$ (EC-$G\alpha_{12/13}$-KO). Da es sich um ein Tamoxifen-induzierbares Model handelt, wurden die neugeborenen Mäuse an den ersten drei Tagen nach der Geburt mit Tamoxifen behandelt (Pitulescu et al., 2010). Diese Methode ergab eine effiziente Rekombination von gefloxten Allelen in retinalen sowie kornealen Gefäßen. Netzhäute von EC-$G\alpha_{13}$-KOs und EC-$G\alpha_{12/13}$-KOs wiesen eine Reduktion der gefäßbedeckten Fläche, der Anzahl von

Gefäßverzweigungen sowie aussprossender *tip cells* auf. Auch die Anzahl der Filopodien pro *tip cell* war geringer im Vergleich zu denen bei Kontrolltieren. Hingegen konnten keine Abweichungen bei konstitutiv $G\alpha_{12}$-defizienten Mäusen ($G\alpha_{12}$-KO) beobachtet werden.

Um herauszufinden, ob eine gestörte retinale Angiogenese mit veränderter Expression Angiogenese-relevanter Gene einhergeht, untersuchten wir Endothelzellen aus Lungen von 6 Tage alten Mäusen mittels quantitativer RT-PCR. Die Analyse zeigte, dass die Expression von VEGFR-2 bei Abwesenheit von endothelialem $G\alpha_{13}$ selektiv reduziert war, wohingegen die Expression anderer an der Angiogenese beteiligter Gene oder G-Protein-α-Untereinheiten unverändert blieb. Eine verringerte Expression von VEGFR-2 konnte auch in den Netzhäuten EC-$G\alpha_{13}$-defizienter Mäuse auf mRNS-Ebene sowie auf Proteinebene nachgewiesen werden. Bei Untersuchungen, die zeigen sollten, ob die reduzierte VEGFR-2-Expression in $G\alpha_{13}$-defizienten Endothelzellen funktionell relevant ist, ergab sich, dass $G\alpha_{13}$-defiziente Endothelzellen in einem *in vivo Matrigel-Assay* nicht mehr auf VEGF-A reagierten. Diese Ergebnisse legen nahe, dass eine verminderte VEGFR-2-Expression in $G\alpha_{13}$-defizienten Endothelzellen zu einer selektiven Störung VEGF-A-vermittelter Effekte führt. Zur weiteren Untersuchung der potentiellen Rolle von $G\alpha_{13}$ bei der Regulation der VEGFR-2-Expression führten wir einen „*small interfering RNA*“ (siRNA)-vermittelten *knockdown* von $G\alpha_{13}$ ($G\alpha_{13}$-kd) in Endothelzellen der menschlichen Umbilikalvene (*human umbilical vein endothelial cells*, HUVECs) durch. Wie auch in murinen Zellen führte der Verlust von $G\alpha_{13}$ zu einer verringerten VEGFR-2-Expression auf mRNS-Ebene und auf Proteinebene. Im Gegensatz dazu

erhöhte eine adenovirale Überexpression von $G\alpha_{13}$ die Expression von VEGFR-2. Verminderte VEGFR-2-Expression führte zur Störung der von VEGF-A induzierten Phosphorylierung von VEGFR-2-Effektoren und *in vitro* Tubenbildung.

Um zu überprüfen, ob $G\alpha_{13}$ die VEGFR-2-Expression auf transkriptioneller Ebene reguliert, transfizierten wir HUVECs mit einem Luciferase-Reporterkonstrukt, das über ein VEGFR-2-Promoterfragment gesteuert wurde, welches die Basenpaare -780 bis +268 relativ zum Transkriptionsstart enthielt (Mammoto et al., 2009) (VEGFR-2-Luc). Wir beobachteten, dass sich durch $G\alpha_{13}$-*knockdown* die VEGFR-2-Luc-Expression verringerte, wohingegen sie bei Überexpression von wildtypischem oder konstitutiv-aktivem $G\alpha_{13}$ erhöht war. Überexpression von $G\alpha_{12}$ jedoch hatte keinen Effekt auf die Aktivität von VEGFR-2-Luc. Als nächstes testeten wir, ob GPCR-Agonisten, die dafür bekannt sind, über $G\alpha_{13}$ zu signalisieren (Worzfeld et al., 2008), dazu fähig waren, den Effekt der $G\alpha_{13}$-Überexpression zu reproduzieren. Wir beobachteten, dass sowohl die Protease Thrombin als auch das Lysophospholipid Sphingosin 1-Phosphat die VEGFR-2-Promoter-Aktivität verstärkten, und dass dieser Effekt nach *knockdown* von $G\alpha_{13}$ vollständig aufgehoben war. Um herauszufinden, ob die kleine GTPase RhoA, ein bekannter Effektor der $G_{12/13}$-Familie (Brown et al., 2006; Worzfeld et al., 2008), $G\alpha_{13}$-abhängige VEGFR-2-Promoter-Aktivität vermittelt, behandelten wir HUVECs mit C3-Exoenzym, einem Toxin, das eine ADP-Ribosylierung und damit Inaktivierung von RhoA bewirkt. Die Vorbehandlung mit C3-Exoenzym hob die durch Thrombin ausgelösten Effekte vollständig auf, ein Hinweis darauf, dass RhoA für die $G\alpha_{13}$-abhängige VEGFR-2-Expression benötigt wird. Bei weiteren Untersuchungen zur Aufklärung der

molekularen Mechanismen der Regulation der VEGFR-2-Expression durch $G\alpha_{13}$/RhoA beobachteten wir, dass *knockdown* von $G\alpha_{13}$ die Thrombin-induzierte Degradierung des NF-κB-Inhibitors IκBα außer Kraft setzte und die Thrombin-vermittelte Aktivierung eines NF-κB-responsiven Reporterkonstrukts verhinderte. Während eine über Thrombin ausgelöste Aktivierung von NF-κB offensichtlich $G\alpha_{13}$-abhängig war, waren die Effekte GPCR-unabhängiger NF-κB-Aktivatoren, beispielsweise Tumornekrosefaktor-α (TNFα), nicht vom $G\alpha_{13}$-*knockdown* betroffen. Wir schlossen hieraus, dass $G\alpha_{13}$ die Thrombin-induzierte Expression von VEGFR-2 über RhoA-abhängige NF-κB-Aktivierung vermittelt.

Schlussendlich untersuchten wir, ob die $G\alpha_{13}$-abhängige Regulierung der VEGFR-2-Expression auch zur Tumorangiogenese beiträgt. *Lewis lung carcinoma* (LLC1)- oder B16F10-Melanom-(B16)-Zellen wurden subkutan in die Flanke von Kontrolltieren und EC-spezifischen Mausmutanten injiziert. Dann wurden Tumorgröße und Vaskularisierung gemessen. Wir beobachteten, dass EC-$G\alpha_{13}$-KOs und EC-$G\alpha_{12/13}$-KOs ein deutlich geringeres Tumorwachstum sowie eine verringerte Tumorvaskularisation aufwiesen. Auch wiesen die in EC-$G\alpha_{13}$-KOs und EC-$G\alpha_{12/13}$-KOs herangewachsenen Tumorgefäße deutliche Zeichen der morphologischen Normalisierung auf.

9.4 Schlussfolgerung

Unsere Untersuchungen haben ergeben, dass die G-Protein-α-Untereinheit $G\alpha_{13}$ eine wichtige Rolle bei der Regulation der VEGFR-2-Expression spielt. *In vitro*

beobachteten wir, dass Knockdown von $G\alpha_{13}$ die VEGFR-2-Expression in Endothelzellen der menschlichen Umbilikalvene verringert und die Responsivität gegenüber VEGF-A stört. Dieser Phänotyp wurde durch adenovirale Normalisierung der VEGFR-2-Expression gerettet. Die $G\alpha_{13}$-abhängige Regulation der VEGFR-2-Expression erfordert die Aktivierung der kleinen GTPase RhoA und des Tranksriptionsfaktors NF-κB; sie wurde aufgehoben durch die Deletion der NF-κB-Bindungsstelle an Position -84 des VEGFR-2-Promoters. *In vivo* führte die Endothelzell-spezifische Inaktivierung von $G\alpha_{13}$ zu einer verringerten VEGFR-2-Expression, einer gestörten Responsivität gegenüber VEGF-A in *Matrigel-Assays* und einer verminderten retinalen Angiogenese. Ein weiterer wichtiger Befund war die in Abwesenheit von endothelialem $G\alpha_{13}$ herabgesetzte Tumorvaskularisation, was wiederum ein geringeres Tumorwachstum zur Folge hatte. Kurz gefasst gelang uns die Identifizierung der $G\alpha_{13}$-abhängigen Aktivierung von NF-κB als neuen der transkriptionellen Regulierung von VEGFR-2 zugrunde liegenden Signalweg in der retinalen und Tumor-Angiogenese.

10. REFERENCES

Adams, R.H., and Alitalo, K. (2007). Molecular regulation of angiogenesis and lymphangiogenesis. Nature reviews Molecular cell biology 8, 464-478.

Adams, R.H., and Eichmann, A. (2010). Axon guidance molecules in vascular patterning. Cold Spring Harbor perspectives in biology 2, a001875.

Alitalo, K. (2011). The lymphatic vasculature in disease. Nature medicine 17, 1371-1380.

Althoff, T.F., Juarez, J.A., Troidl, K., Tang, C., Wang, S., Wirth, A., Takefuji, M., Wettschureck, N., and Offermanns, S. (2012). Procontractile G protein-mediated signaling pathways antagonistically regulate smooth muscle differentiation in vascular remodeling. The Journal of experimental medicine 209, 2277-2290.

Arshavsky, V.Y., Lamb, T.D., and Pugh, E.N., Jr. (2002). G proteins and phototransduction. Annual review of physiology 64, 153-187.

Bastepe, M., Gunes, Y., Perez-Villamil, B., Hunzelman, J., Weinstein, L.S., and Juppner, H. (2002). Receptor-mediated adenylyl cyclase activation through XLalpha(s), the extra-large variant of the stimulatory G protein alpha-subunit. Molecular endocrinology 16, 1912-1919.

Bergers, G., and Hanahan, D. (2008). Modes of resistance to anti-angiogenic therapy. Nature reviews Cancer 8, 592-603.

Benedito, R., Rocha, S.F., Woeste, M., Zamykal, M., Radtke, F., Casanovas, O., Duarte, A., Pytowski, B., and Adams, R.H. (2012). Notch-dependent VEGFR3 upregulation allows angiogenesis without VEGF-VEGFR2 signalling. Nature 484, 110-114.

Bergers, G., and Benjamin, L.E. (2003). Tumorigenesis and the angiogenic switch. Nature reviews Cancer 3, 401-410.

Bjarnadottir, T.K., Gloriam, D.E., Hellstrand, S.H., Kristiansson, H., Fredriksson, R., and Schioth, H.B. (2006). Comprehensive repertoire and phylogenetic analysis of the G protein-coupled receptors in human and mouse. Genomics 88, 263-273.

Brown, J.H., Del Re, D.P., and Sussman, M.A. (2006). The Rac and Rho hall of fame: a decade of hypertrophic signaling hits. Circ Res 98, 730-742.

Carey, M.F., Peterson, C.L., and Smale, S.T. (2009). Chromatin immunoprecipitation (ChIP). Cold Spring Harb Protoc 2009, pdb prot5279.

Carmeliet, P. (2003). Angiogenesis in health and disease. Nature medicine 9, 653-660.

Carmeliet, P. (2005). Angiogenesis in life, disease and medicine. Nature 438, 932-936.

Carmeliet, P., Ferreira, V., Breier, G., Pollefeyt, S., Kieckens, L., Gertsenstein, M., Fahrig, M., Vandenhoeck, A., Harpal, K., Eberhardt, C., et al. (1996). Abnormal blood vessel development and lethality in embryos lacking a single VEGF allele. Nature 380, 435-439.

Carmeliet, P., Lampugnani, M.G., Moons, L., Breviario, F., Compernolle, V., Bono, F., Balconi, G., Spagnuolo, R., Oosthuyse, B., Dewerchin, M., et al. (1999). Targeted deficiency or cytosolic truncation of the VE-cadherin gene in mice impairs VEGF-mediated endothelial survival and angiogenesis. Cell 98, 147-157.

Cavallaro, U., and Dejana, E. (2011). Adhesion molecule signalling: not always a sticky business. Nature reviews Molecular cell biology 12, 189-197.

Chen, S., and Lechleider, R.J. (2004). Transforming growth factor-beta-induced differentiation of smooth muscle from a neural crest stem cell line. Circulation research 94, 1195-1202.

Clapham, D.E., and Neer, E.J. (1997). G protein beta gamma subunits. Annu Rev Pharmacol Toxicol 37, 167-203.

Claxton, S., Kostourou, V., Jadeja, S., Chambon, P., Hodivala-Dilke, K., and Fruttiger, M. (2008). Efficient, inducible Cre-recombinase activation in vascular endothelium. Genesis 46, 74-80.

Cleaver, O., and Melton, D.A. (2003). Endothelial signaling during development. Nature medicine 9, 661-668.

Connolly, A.J., Ishihara, H., Kahn, M.L., Farese, R.V., Jr., and Coughlin, S.R. (1996). Role of the thrombin receptor in development and evidence for a second receptor. Nature 381, 516-519.

Coultas, L., Chawengsaksophak, K., and Rossant, J. (2005). Endothelial cells and VEGF in vascular development. Nature 438, 937-945.

Dorsam, R.T., and Gutkind, J.S. (2007). G-protein-coupled receptors and cancer. Nature reviews Cancer 7, 79-94.

Downes, G.B., and Gautam, N. (1999). The G protein subunit gene families. Genomics 62, 544-552.

Dumont, D.J., Jussila, L., Taipale, J., Lymboussaki, A., Mustonen, T., Pajusola, K., Breitman, M., and Alitalo, K. (1998). Cardiovascular failure in mouse embryos deficient in VEGF receptor-3. Science 282, 946-949.

Eichmann, A., and Simons, M. (2012). VEGF signaling inside vascular endothelial cells and beyond. Current opinion in cell biology 24, 188-193.

Ferrara, N., Carver-Moore, K., Chen, H., Dowd, M., Lu, L., O'Shea, K.S., Powell-Braxton, L., Hillan, K.J., and Moore, M.W. (1996). Heterozygous embryonic lethality induced by targeted inactivation of the VEGF gene. Nature 380, 439-442.

Ferrara, N., and Kerbel, R.S. (2005). Angiogenesis as a therapeutic target. Nature 438, 967-974.

Fischer, C., Mazzone, M., Jonckx, B., and Carmeliet, P. (2008). FLT1 and its ligands VEGFB and PlGF: drug targets for anti-angiogenic therapy? Nature reviews Cancer 8, 942-956.

Folkman, J. (1971). Tumor angiogenesis: therapeutic implications. N Engl J Med 285, 1182-1186.

Folkman, J. (2007). Angiogenesis: an organizing principle for drug discovery? Nature reviews Drug discovery 6, 273-286.

Fromm, C., Coso, O.A., Montaner, S., Xu, N., and Gutkind, J.S. (1997). The small GTP-binding protein Rho links G protein-coupled receptors and Galpha12 to the serum response element and to cellular transformation. Proc Natl Acad Sci U S A 94, 10098-10103.

Fukuhara, S., Chikumi, H., and Gutkind, J.S. (2001). RGS-containing RhoGEFs: the missing link between transforming G proteins and Rho? Oncogene 20, 1661-1668.

Gaengel, K., and Betsholtz, C. (2013). Endocytosis regulates VEGF signalling during angiogenesis. Nature cell biology 15, 233-235.

Gaengel, K., Genove, G., Armulik, A., and Betsholtz, C. (2009). Endothelial-mural cell signaling in vascular development and angiogenesis. Arteriosclerosis, thrombosis, and vascular biology 29, 630-638.

Gariano, R.F., and Gardner, T.W. (2005). Retinal angiogenesis in development and disease. Nature 438, 960-966.

Gerhardt, H., Golding, M., Fruttiger, M., Ruhrberg, C., Lundkvist, A., Abramsson, A., Jeltsch, M., Mitchell, C., Alitalo, K., Shima, D., et al. (2003). VEGF guides angiogenic sprouting utilizing endothelial tip cell filopodia. The Journal of cell biology 161, 1163-1177.

Germain, S., Monnot, C., Muller, L., and Eichmann, A. (2010). Hypoxia-driven angiogenesis: role of tip cells and extracellular matrix scaffolding. Current opinion in hematology 17, 245-251.

Gitler, A.D., Lu, M.M., and Epstein, J.A. (2004). PlexinD1 and semaphorin signaling are required in endothelial cells for cardiovascular development. Developmental cell 7, 107-116.

Gohla, A., Offermanns, S., Wilkie, T.M., and Schultz, G. (1999). Differential involvement of Galpha12 and Galpha13 in receptor-mediated stress fiber formation. J Biol Chem 274, 17901-17907.

Gohla, A., Schultz, G., and Offermanns, S. (2000). Role for G(12)/G(13) in agonist-induced vascular smooth muscle cell contraction. Circ Res 87, 221-227.

Gong, H., Shen, B., Flevaris, P., Chow, C., Lam, S.C., Voyno-Yasenetskaya, T.A., Kozasa, T., and Du, X. (2010). G protein subunit Galpha13 binds to integrin alphaIIbbeta3 and mediates integrin "outside-in" signaling. Science 327, 340-343.

Greenberg, J.I., Shields, D.J., Barillas, S.G., Acevedo, L.M., Murphy, E., Huang, J., Scheppke, L., Stockmann, C., Johnson, R.S., Angle, N., et al. (2008). A role for VEGF as a negative regulator of pericyte function and vessel maturation. Nature 456, 809-813.

Griffin, C.T., Srinivasan, Y., Zheng, Y.W., Huang, W., and Coughlin, S.R. (2001). A role for thrombin receptor signaling in endothelial cells during embryonic development. Science 293, 1666-1670.

Gu, C., Yoshida, Y., Livet, J., Reimert, D.V., Mann, F., Merte, J., Henderson, C.E., Jessell, T.M., Kolodkin, A.L., and Ginty, D.D. (2005). Semaphorin 3E and plexin-D1 control vascular pattern independently of neuropilins. Science 307, 265-268.

Gu, J.L., Muller, S., Mancino, V., Offermanns, S., and Simon, M.I. (2002). Interaction of G alpha(12) with G alpha(13) and G alpha(q) signaling pathways. Proceedings of the National Academy of Sciences of the United States of America 99, 9352-9357.

Haigh, J.J., Morelli, P.I., Gerhardt, H., Haigh, K., Tsien, J., Damert, A., Miquerol, L., Muhlner, U., Klein, R., Ferrara, N., et al. (2003). Cortical and retinal defects caused by dosage-dependent reductions in VEGF-A paracrine signaling. Developmental biology 262, 225-241.

Hanahan, D., and Weinberg, R.A. (2000). The hallmarks of cancer. Cell 100, 57-70.

Harper, S.J., and Bates, D.O. (2008). VEGF-A splicing: the key to anti-angiogenic therapeutics? Nature reviews Cancer 8, 880-887.

Hayden, M.S., and Ghosh, S. (2008). Shared principles in NF-kappaB signaling. Cell 132, 344-362.

Herbert, S.P., and Stainier, D.Y. (2011). Molecular control of endothelial cell behaviour during blood vessel morphogenesis. Nature reviews Molecular cell biology 12, 551-564.

Herlitze, S., Garcia, D.E., Mackie, K., Hille, B., Scheuer, T., and Catterall, W.A. (1996). Modulation of Ca2+ channels by G-protein beta gamma subunits. Nature 380, 258-262.

Herroeder, S., Reichardt, P., Sassmann, A., Zimmermann, B., Jaeneke, D., Hoeckner, J., Hollmann, M.W., Fischer, K.D., Vogt, S., Grosse, R., et al. (2009). Guanine nucleotide-binding proteins of the G12 family shape immune functions by controlling CD4+ T cell adhesiveness and motility. Immunity 30, 708-720.

Illi, B., Puri, P., Morgante, L., Capogrossi, M.C., and Gaetano, C. (2000). Nuclear factor-kappaB and cAMP response element binding protein mediate opposite transcriptional effects on the Flk-1/KDR gene promoter. Circulation research 86, E110-117.

Jain, R.K. (2001). Normalizing tumor vasculature with anti-angiogenic therapy: a new paradigm for combination therapy. Nat Med 7, 987-989.

Jain, R.K. (2005). Normalization of tumor vasculature: an emerging concept in antiangiogenic therapy. Science 307, 58-62.

Jones, C.A., London, N.R., Chen, H., Park, K.W., Sauvaget, D., Stockton, R.A., Wythe, J.D., Suh, W., Larrieu-Lahargue, F., Mukouyama, Y.S., et al. (2008). Robo4 stabilizes the vascular network by inhibiting pathologic angiogenesis and endothelial hyperpermeability. Nature medicine 14, 448-453.

Katz, A., Wu, D., and Simon, M.I. (1992). Subunits beta gamma of heterotrimeric G protein activate beta 2 isoform of phospholipase C. Nature 360, 686-689.

Kelly, P., Moeller, B.J., Juneja, J., Booden, M.A., Der, C.J., Daaka, Y., Dewhirst, M.W., Fields, T.A., and Casey, P.J. (2006). The G12 family of heterotrimeric G proteins promotes breast cancer invasion and metastasis. Proceedings of the National Academy of Sciences of the United States of America 103, 8173-8178.

Kim, J., Oh, W.J., Gaiano, N., Yoshida, Y., and Gu, C. (2011). Semaphorin 3E-Plexin-D1 signaling regulates VEGF function in developmental angiogenesis via a feedback mechanism. Genes & development 25, 1399-1411.

Kim, Y.H., Hu, H., Guevara-Gallardo, S., Lam, M.T., Fong, S.Y., and Wang, R.A. (2008). Artery and vein size is balanced by Notch and ephrin B2/EphB4 during angiogenesis. Development 135, 3755-3764.

Klages, B., Brandt, U., Simon, M.I., Schultz, G., and Offermanns, S. (1999). Activation of G12/G13 results in shape change and Rho/Rho-kinase-mediated myosin light chain phosphorylation in mouse platelets. The Journal of cell biology 144, 745-754.

Klemke, M., Pasolli, H.A., Kehlenbach, R.H., Offermanns, S., Schultz, G., and Huttner, W.B. (2000). Characterization of the extra-large G protein alpha-subunit

XLalphas. II. Signal transduction properties. The Journal of biological chemistry 275, 33633-33640.

Kono, M., Mi, Y., Liu, Y., Sasaki, T., Allende, M.L., Wu, Y.P., Yamashita, T., and Proia, R.L. (2004). The sphingosine-1-phosphate receptors S1P1, S1P2, and S1P3 function coordinately during embryonic angiogenesis. The Journal of biological chemistry 279, 29367-29373.

Korhonen, H., Fisslthaler, B., Moers, A., Wirth, A., Habermehl, D., Wieland, T., Schutz, G., Wettschureck, N., Fleming, I., and Offermanns, S. (2009). Anaphylactic shock depends on endothelial Gq/G11. The Journal of experimental medicine 206, 411-420.

Krakstad, B.F., Ardawatia, V.V., and Aragay, A.M. (2004). A role for Galpha12/Galpha13 in p120ctn regulation. Proceedings of the National Academy of Sciences of the United States of America 101, 10314-10319.

Kuhnert, F., Mancuso, M.R., Shamloo, A., Wang, H.T., Choksi, V., Florek, M., Su, H., Fruttiger, M., Young, W.L., Heilshorn, S.C., et al. (2010). Essential regulation of CNS angiogenesis by the orphan G protein-coupled receptor GPR124. Science 330, 985-989.

Lappano, R., and Maggiolini, M. (2011). G protein-coupled receptors: novel targets for drug discovery in cancer. Nature reviews Drug discovery 10, 47-60.

Lawson, N.D., Scheer, N., Pham, V.N., Kim, C.H., Chitnis, A.B., Campos-Ortega, J.A., and Weinstein, B.M. (2001). Notch signaling is required for arterial-venous differentiation during embryonic vascular development. Development 128, 3675-3683.

Lee, S., Chen, T.T., Barber, C.L., Jordan, M.C., Murdock, J., Desai, S., Ferrara, N., Nagy, A., Roos, K.P., and Iruela-Arispe, M.L. (2007). Autocrine VEGF signaling is required for vascular homeostasis. Cell 130, 691-703.

Lindahl, P., Johansson, B.R., Leveen, P., and Betsholtz, C. (1997). Pericyte loss and microaneurysm formation in PDGF-B-deficient mice. Science 277, 242-245.

Liu, G., Han, J., Profirovic, J., Strekalova, E., and Voyno-Yasenetskaya, T.A. (2009). Galpha13 regulates MEF2-dependent gene transcription in endothelial cells: role in angiogenesis. Angiogenesis 12, 1-15.

Liu, Y., Wada, R., Yamashita, T., Mi, Y., Deng, C.X., Hobson, J.P., Rosenfeldt, H.M., Nava, V.E., Chae, S.S., Lee, M.J., et al. (2000). Edg-1, the G protein-coupled receptor for sphingosine-1-phosphate, is essential for vascular maturation. J Clin Invest 106, 951-961.

Logothetis, D.E., Kurachi, Y., Galper, J., Neer, E.J., and Clapham, D.E. (1987). The beta gamma subunits of GTP-binding proteins activate the muscarinic K+ channel in heart. Nature 325, 321-326.

Maisonpierre, P.C., Suri, C., Jones, P.F., Bartunkova, S., Wiegand, S.J., Radziejewski, C., Compton, D., McClain, J., Aldrich, T.H., Papadopoulos, N., et al. (1997). Angiopoietin-2, a natural antagonist for Tie2 that disrupts in vivo angiogenesis. Science 277, 55-60.

Mammoto, A., Connor, K.M., Mammoto, T., Yung, C.W., Huh, D., Aderman, C.M., Mostoslavsky, G., Smith, L.E., and Ingber, D.E. (2009). A mechanosensitive transcriptional mechanism that controls angiogenesis. Nature 457, 1103-1108.

Martin, C.B., Mahon, G.M., Klinger, M.B., Kay, R.J., Symons, M., Der, C.J., and Whitehead, I.P. (2001). The thrombin receptor, PAR-1, causes transformation by activation of Rho-mediated signaling pathways. Oncogene 20, 1953-1963.

Meigs, T.E., Fedor-Chaiken, M., Kaplan, D.D., Brackenbury, R., and Casey, P.J. (2002). Galpha12 and Galpha13 negatively regulate the adhesive functions of cadherin. The Journal of biological chemistry 277, 24594-24600.

Meigs, T.E., Fields, T.A., McKee, D.D., and Casey, P.J. (2001). Interaction of Galpha 12 and Galpha 13 with the cytoplasmic domain of cadherin provides a mechanism for beta -catenin release. Proceedings of the National Academy of Sciences of the United States of America 98, 519-524.

Mikelis, C.M., Palmby, T.R., Simaan, M., Li, W., Szabo, R., Lyons, R., Martin, D., Yagi, H., Fukuhara, S., Chikumi, H., et al. (2013). PDZ-RhoGEF and LARG are essential for embryo development, and provide a link between thrombin and LPA receptors and Rho activation. The Journal of biological chemistry.

Millauer, B., Shawver, L.K., Plate, K.H., Risau, W., and Ullrich, A. (1994). Glioblastoma growth inhibited in vivo by a dominant-negative Flk-1 mutant. Nature 367, 576-579.

Millauer, B., Wizigmann-Voos, S., Schnurch, H., Martinez, R., Moller, N.P., Risau, W., and Ullrich, A. (1993). High affinity VEGF binding and developmental expression suggest Flk-1 as a major regulator of vasculogenesis and angiogenesis. Cell 72, 835-846.

Moers, A., Nieswandt, B., Massberg, S., Wettschureck, N., Gruner, S., Konrad, I., Schulte, V., Aktas, B., Gratacap, M.P., Simon, M.I., et al. (2003). G13 is an essential mediator of platelet activation in hemostasis and thrombosis. Nature medicine 9, 1418-1422.

Murakami, M., Nguyen, L.T., Hatanaka, K., Schachterle, W., Chen, P.Y., Zhuang, Z.W., Black, B.L., and Simons, M. (2011). FGF-dependent regulation of VEGF receptor 2 expression in mice. J Clin Invest 121, 2668-2678.

Muzumdar, M.D., Tasic, B., Miyamichi, K., Li, L., and Luo, L. (2007). A global double-fluorescent Cre reporter mouse. Genesis 45, 593-605.

Nakayama, M., Nakayama, A., van Lessen, M., Yamamoto, H., Hoffmann, S., Drexler, H.C., Itoh, N., Hirose, T., Breier, G., Vestweber, D., et al. (2013). Spatial regulation of VEGF receptor endocytosis in angiogenesis. Nature cell biology 15, 249-260.

Neves, S.R., Ram, P.T., and Iyengar, R. (2002). G protein pathways. Science 296, 1636-1639.

Nierodzik, M.L., and Karpatkin, S. (2006). Thrombin induces tumor growth, metastasis, and angiogenesis: Evidence for a thrombin-regulated dormant tumor phenotype. Cancer cell 10, 355-362.

Oelrichs, R.B., Reid, H.H., Bernard, O., Ziemiecki, A., and Wilks, A.F. (1993). NYK/FLK-1: a putative receptor protein tyrosine kinase isolated from E10 embryonic neuroepithelium is expressed in endothelial cells of the developing embryo. Oncogene 8, 11-18.

Offermanns, S., Mancino, V., Revel, J.P., and Simon, M.I. (1997a). Vascular system defects and impaired cell chemokinesis as a result of Galpha13 deficiency. Science 275, 533-536.

Offermanns, S., Toombs, C.F., Hu, Y.H., and Simon, M.I. (1997b). Defective platelet activation in G alpha(q)-deficient mice. Nature 389, 183-186.

Offermanns, S., Hashimoto, K., Watanabe, M., Sun, W., Kurihara, H., Thompson, R.F., Inoue, Y., Kano, M., and Simon, M.I. (1997c). Impaired motor coordination and persistent multiple climbing fiber innervation of cerebellar Purkinje cells in mice lacking Galphaq. Proceedings of the National Academy of Sciences of the United States of America 94, 14089-14094.

Oldham, W.M., and Hamm, H.E. (2006). Structural basis of function in heterotrimeric G proteins. Q Rev Biophys 39, 117-166.

Olsson, A.K., Dimberg, A., Kreuger, J., and Claesson-Welsh, L. (2006). VEGF receptor signalling - in control of vascular function. Nature reviews Molecular cell biology 7, 359-371.

Pasolli, H.A., Klemke, M., Kehlenbach, R.H., Wang, Y., and Huttner, W.B. (2000). Characterization of the extra-large G protein alpha-subunit XLalphas. I. Tissue distribution and subcellular localization. The Journal of biological chemistry 275, 33622-33632.

Patterson, C., Perrella, M.A., Hsieh, C.M., Yoshizumi, M., Lee, M.E., and Haber, E. (1995). Cloning and functional analysis of the promoter for KDR/flk-1, a receptor for vascular endothelial growth factor. The Journal of biological chemistry 270, 23111-23118.

Perkins, N.D. (2007). Integrating cell-signalling pathways with NF-kappaB and IKK function. Nature reviews Molecular cell biology 8, 49-62.

Perona, R., Montaner, S., Saniger, L., Sanchez-Perez, I., Bravo, R., and Lacal, J.C. (1997). Activation of the nuclear factor-kappaB by Rho, CDC42, and Rac-1 proteins. Genes & development 11, 463-475.

Pierce, K.L., Premont, R.T., and Lefkowitz, R.J. (2002). Seven-transmembrane receptors. Nature reviews Molecular cell biology 3, 639-650.

Pitulescu, M.E., Schmidt, I., Benedito, R., and Adams, R.H. (2010). Inducible gene targeting in the neonatal vasculature and analysis of retinal angiogenesis in mice. Nature protocols 5, 1518-1534.

Plate, K.H., Breier, G., Millauer, B., Ullrich, A., and Risau, W. (1993). Up-regulation of vascular endothelial growth factor and its cognate receptors in a rat glioma model of tumor angiogenesis. Cancer research 53, 5822-5827.

Potente, M., Gerhardt, H., and Carmeliet, P. (2011). Basic and therapeutic aspects of angiogenesis. Cell 146, 873-887.

Profirovic, J., Gorovoy, M., Niu, J., Pavlovic, S., and Voyno-Yasenetskaya, T. (2005). A novel mechanism of G protein-dependent phosphorylation of vasodilator-stimulated phosphoprotein. J Biol Chem 280, 32866-32876.

Pugh, C.W., and Ratcliffe, P.J. (2003). Regulation of angiogenesis by hypoxia: role of the HIF system. Nature medicine 9, 677-684.

Quinn, T.P., Peters, K.G., De Vries, C., Ferrara, N., and Williams, L.T. (1993). Fetal liver kinase 1 is a receptor for vascular endothelial growth factor and is selectively expressed in vascular endothelium. Proceedings of the National Academy of Sciences of the United States of America 90, 7533-7537.

Rahman, A., Anwar, K.N., Uddin, S., Xu, N., Ye, R.D., Platanias, L.C., and Malik, A.B. (2001). Protein kinase C-delta regulates thrombin-induced ICAM-1 gene expression in endothelial cells via activation of p38 mitogen-activated protein kinase. Molecular and cellular biology 21, 5554-5565.

Reynolds, A.R., Hart, I.R., Watson, A.R., Welti, J.C., Silva, R.G., Robinson, S.D., Da Violante, G., Gourlaouen, M., Salih, M., Jones, M.C., et al. (2009). Stimulation of tumor growth and angiogenesis by low concentrations of RGD-mimetic integrin inhibitors. Nat Med 15, 392-400.

Rhee, S.G. (2001). Regulation of phosphoinositide-specific phospholipase C. Annu Rev Biochem 70, 281-312.

Richard, D.E., Vouret-Craviari, V., and Pouyssegur, J. (2001). Angiogenesis and G-protein-coupled receptors: signals that bridge the gap. Oncogene 20, 1556-1562.

Rieken, S., Sassmann, A., Herroeder, S., Wallenwein, B., Moers, A., Offermanns, S., and Wettschureck, N. (2006). G12/G13 family G proteins regulate marginal zone B cell maturation, migration, and polarization. Journal of immunology 177, 2985-2993.

Ritter, S.L., and Hall, R.A. (2009). Fine-tuning of GPCR activity by receptor-interacting proteins. Nature reviews Molecular cell biology 10, 819-830.

Roca, C., and Adams, R.H. (2007). Regulation of vascular morphogenesis by Notch signaling. Genes & development 21, 2511-2524.

Rocha, S.F., and Adams, R.H. (2009). Molecular differentiation and specialization of vascular beds. Angiogenesis 12, 139-147.

Ruppel, K.M., Willison, D., Kataoka, H., Wang, A., Zheng, Y.W., Cornelissen, I., Yin, L., Xu, S.M., and Coughlin, S.R. (2005). Essential role for Galpha13 in endothelial cells during embryonic development. Proceedings of the National Academy of Sciences of the United States of America 102, 8281-8286.

Sainson, R.C., Johnston, D.A., Chu, H.C., Holderfield, M.T., Nakatsu, M.N., Crampton, S.P., Davis, J., Conn, E., and Hughes, C.C. (2008). TNF primes endothelial cells for angiogenic sprouting by inducing a tip cell phenotype. Blood 111, 4997-5007.

Sawamiphak, S., Seidel, S., Essmann, C.L., Wilkinson, G.A., Pitulescu, M.E., Acker, T., and Acker-Palmer, A. (2010). Ephrin-B2 regulates VEGFR2 function in developmental and tumour angiogenesis. Nature 465, 487-491.

Shalaby, F., Rossant, J., Yamaguchi, T.P., Gertsenstein, M., Wu, X.F., Breitman, M.L., and Schuh, A.C. (1995). Failure of blood-island formation and vasculogenesis in Flk-1-deficient mice. Nature 376, 62-66.

Shan, D., Chen, L., Wang, D., Tan, Y.C., Gu, J.L., and Huang, X.Y. (2006). The G protein G alpha(13) is required for growth factor-induced cell migration. Developmental cell 10, 707-718.

Siekmann, A.F., and Lawson, N.D. (2007). Notch signalling and the regulation of angiogenesis. Cell adhesion & migration 1, 104-106.

Simon, M.I., Strathmann, M.P., and Gautam, N. (1991). Diversity of G proteins in signal transduction. Science 252, 802-808.

Sivaraj, K.K., Takefuji, M., Schmidt, I., Adams, R.H., Offermanns, S., and Wettschureck, N. (2013). G13 Controls Angiogenesis through Regulation of VEGFR-2 Expression. Developmental cell 25, 427-434.

Solnica-Krezel, L. (2006). Gastrulation in zebrafish -- all just about adhesion? Curr Opin Genet Dev 16, 433-441.

Spiegel, S., and Milstien, S. (2003). Sphingosine-1-phosphate: an enigmatic signalling lipid. Nature reviews Molecular cell biology 4, 397-407.

Sunahara, R.K., Dessauer, C.W., and Gilman, A.G. (1996). Complexity and diversity of mammalian adenylyl cyclases. Annu Rev Pharmacol Toxicol 36, 461-480.

Suri, C., Jones, P.F., Patan, S., Bartunkova, S., Maisonpierre, P.C., Davis, S., Sato, T.N., and Yancopoulos, G.D. (1996). Requisite role of angiopoietin-1, a ligand for the TIE2 receptor, during embryonic angiogenesis. Cell 87, 1171-1180.

Taddei, A., Giampietro, C., Conti, A., Orsenigo, F., Breviario, F., Pirazzoli, V., Potente, M., Daly, C., Dimmeler, S., and Dejana, E. (2008). Endothelial adherens junctions control tight junctions by VE-cadherin-mediated upregulation of claudin-5. Nature cell biology 10, 923-934.

Takefuji, M., Wirth, A., Lukasova, M., Takefuji, S., Boettger, T., Braun, T., Althoff, T., Offermanns, S., and Wettschureck, N. (2012). G(13)-mediated signaling pathway is required for pressure overload-induced cardiac remodeling and heart failure. Circulation 126, 1972-1982.

Tammela, T., and Alitalo, K. (2010). Lymphangiogenesis: Molecular mechanisms and future promise. Cell 140, 460-476.

Tammela, T., Zarkada, G., Wallgard, E., Murtomaki, A., Suchting, S., Wirzenius, M., Waltari, M., Hellstrom, M., Schomber, T., Peltonen, R., et al. (2008). Blocking VEGFR-3 suppresses angiogenic sprouting and vascular network formation. Nature 454, 656-660.

Tang, W.J., and Gilman, A.G. (1991). Type-specific regulation of adenylyl cyclase by G protein beta gamma subunits. Science 254, 1500-1503.

Tong, R.T., Boucher, Y., Kozin, S.V., Winkler, F., Hicklin, D.J., and Jain, R.K. (2004). Vascular normalization by vascular endothelial growth factor receptor 2 blockade induces a pressure gradient across the vasculature and improves drug penetration in tumors. Cancer research 64, 3731-3736.

Tsopanoglou, N.E., and Maragoudakis, M.E. (1999). On the mechanism of thrombin-induced angiogenesis. Potentiation of vascular endothelial growth factor activity on endothelial cells by up-regulation of its receptors. The Journal of biological chemistry 274, 23969-23976.

Urbich, C., Stein, M., Reisinger, K., Kaufmann, R., Dimmeler, S., and Gille, J. (2003). Fluid shear stress-induced transcriptional activation of the vascular endothelial growth factor receptor-2 gene requires Sp1-dependent DNA binding. FEBS letters 535, 87-93.

van Nieuw Amerongen, G.P., Koolwijk, P., Versteilen, A., and van Hinsbergh, V.W. (2003). Involvement of RhoA/Rho kinase signaling in VEGF-induced endothelial cell migration and angiogenesis in vitro. Arteriosclerosis, thrombosis, and vascular biology 23, 211-217.

Wang, Y., Nakayama, M., Pitulescu, M.E., Schmidt, T.S., Bochenek, M.L., Sakakibara, A., Adams, S., Davy, A., Deutsch, U., Luthi, U., et al. (2010). Ephrin-B2 controls VEGF-induced angiogenesis and lymphangiogenesis. Nature 465, 483-486.

Weis, S.M., and Cheresh, D.A. (2005). Pathophysiological consequences of VEGF-induced vascular permeability. Nature 437, 497-504.

Wettschureck, N., and Offermanns, S. (2005). Mammalian G proteins and their cell type specific functions. Physiol Rev 85, 1159-1204.

Wild, R., Ramakrishnan, S., Sedgewick, J., and Griffioen, A.W. (2000). Quantitative assessment of angiogenesis and tumor vessel architecture by computer-assisted digital image analysis: effects of VEGF-toxin conjugate on tumor microvessel density. Microvascular research 59, 368-376.

Worzfeld, T., Wettschureck, N., and Offermanns, S. (2008). G(12)/G(13)-mediated signalling in mammalian physiology and disease. Trends Pharmacol Sci 29, 582-589.

Xue, J., Thippegowda, P.B., Hu, G., Bachmaier, K., Christman, J.W., Malik, A.B., and Tiruppathi, C. (2009). NF-kappaB regulates thrombin-induced ICAM-1 gene expression in cooperation with NFAT by binding to the intronic NF-kappaB site in the ICAM-1 gene. Physiological genomics 38, 42-53.

Zovein, A.C., Luque, A., Turlo, K.A., Hofmann, J.J., Yee, K.M., Becker, M.S., Fassler, R., Mellman, I., Lane, T.F., and Iruela-Arispe, M.L. (2010). Beta1 integrin establishes endothelial cell polarity and arteriolar lumen formation via a Par3-dependent mechanism. Dev Cell 18, 39-51.

11. CURRICULUM VITAE

Kishor Kumar Sivaraj

Department of Pharmacology
Max-Planck-Institute for Heart and Lung Research
Ludwigstraße 43
61231 Bad Nauheim
Tel.: +49(6032)705-1208
Fax: +49(6032)705-1204

E-mail: kishor.sivaraj@mpi-bn.mpg.de

EDUCATION

Since, 2009	PhD student	Dept. of Pharmacology Max-Planck-Institute for Heart and Lung Research. Bad Nauheim. Germany.
2006 – 2008	Junior Research Fellow	Centre for Cellular and Molecular Biology , Hyderabad. INDIA
2004 –2006	MSc in Biotechnology	Bharathidasan University. INDIA
2003 –2004	Diploma in Bioinformatics	PSG collage, Coimbatore, TN. INDIA
2000 –2003	BSc in Biochemistry	Bharathiar University, INDIA.

PUBLICATIONS

Sivaraj KK, Takefuji M, Schmidt I, Adams R, Offermanns S, Wettschureck N (2013) G_{13} controls angiogenesis through regulation of VEGFR-2 expression. **Dev Cel**l 25, 427-34

Schuhmacher D, Strilic B, **Sivaraj KK**, Wettschureck N, Offermanns S (2013) Platelet-derived nucleoides promote tumor-cell transendothelial migration and metastasis via $P2Y_2$ receptor. **Cancer Cell** 24, 1-8

Takefuji M Krüger M, **Sivaraj KK**, Kaibuchi K, Offermanns S, Wettschureck N. RhoGEF12 controls cardiac remodeling by integrating G-protein- and integrin-dependent signaling cascades. **J Exp Med** 210:665-73

Worzfeld T, Swiercz JM, Looso M, Straub BK, **Sivaraj KK**, Offermanns S (2012) ErbB-2 signals through Plexin-B1 to promote breast cancer metastasis. **J Clin Invest** 122, 3296-2305

Sivaraj KK and Kumar MJ (2008) Antiestrogen therapy for Breast Cancer: An Overview. **Cancer Therapy** Vol.6:B.655-664

Mahesh Kumar MJ, Ponvijay KS, Nagaraj RS, Nandhini R, Jose J, Srinivas G, **Sivaraj KK** and S.Shingh (2007) A mouse model for lumina epithelial like ER positive subtype of human breast cancer. **BMC Cancer**, 7:180 3.

POSTER PRESENTATION:

27-01/01/2013-	Gordon Research Conference on "Vascular Cell Biology" Ventura, California, USA.
06-05/06/2012 -	17th International Vascular Biology Meeting (IVBM). Wiesbaden, Germany.
29-30/09/2011-	IIed International Vascular Biology -SFB/TR23 Meeting. Mannheim, Germany
23-24/02/2008-	12th ADNAT convention**"** The Biology of Embryonic and Adult stem cells". CCMB, Hyderabad. India.

HONORS AND AWARDS

27/01/2013 - 01/02/2013	Travel Scholarship to attend the Vascular Cell Biology 2013 Gordon Research Conferences, Ventura, California, United states.
2010 – 2013	Endothelial Signaling and Vascular Repair (SFB834) – Student of Graduate programme. Goethe University, Germany.
10/ 2010 -10/2013	International Max Planck Research School for Heart and Lung Research (IMPRS-HLR) Scholar, Goethe University, Germany.
2011 & 2012	IMPRS- PhD student representative.
2011 &2 012	IMPRS –HLR, Annual retreat - Organizers and PhD – Committee member

PERSONAL INFORMATION

Surname/ name: Sivaraj Kishor Kumar
Date of Birth : 30/09/1983
Marital status : Single
Nationality : INDIAN